UNIVERSITÀ DEGLI STUDI
DI MILANO

DOTTORATO DI MEDICINA MOLECOLARE E TRASLAZIONALE

CICLO XXXII

Anno Accademico 2018/2019

TESI DI DOTTORATO DI RICERCA

BIO/12

Impact of vitamin D deficiency, dyslipidemia and obesity on serum lipidomic profile. Search for new biomarkers as early predictors of obesity-associated comorbidities.

Dottorando: Pietro BARBACINI
Matricola N°: R11750

TUTORE: Ch.ma Prof.ssa Cecilia GELFI

COORDINATORE DEL DOTTORATO: Ch.mo Prof. Michele SAMAJA

SOMMARIO

I dati scientifici suggeriscono che entro il 2030, fino al 58% della popolazione adulta mondiale sarà sovrappeso o obesa [1]. L'insorgenza di questa patologia [2] non è solo dovuta alla mera componente alimentare, infatti, una serie di elementi che spaziano dallo stile di vita alla genetica contribuiscono al suo sviluppo [3–5]. L'obesità è di frequente associata al deficit della vitamina D (Vit. D) [6,7] e la genetica è spesso stata invocata per fornire una spiegazione a questa associazione [8], tuttavia, differenze nell'esposizione solare e nel metabolismo della vitamina D sono ugualmente responsabili [9]. Recentemente, i lipidi ed in particolare gli sfingolipidi, come le ceramidi (Cers) e le sfingomieline (SMs), vengono sempre più spesso indicati come responsabili, non solo dell'aumento dell'attività infiammatoria [10,11], ma anche dello sviluppo di patologie cardiovascolari e diabete di tipo 2 [12–14], due condizioni comunemente osservate nei soggetti obesi. Il nostro studio è stato motivato dal ruolo cruciale che gli sfingolipidi (SLs) svolgono nelle patologie associate all'obesità e dall'associazione esistente tra obesità, dislipidemia e deficit della Vit. D. Il nostro progetto è stato quindi focalizzato alla definizione dei profili degli sfingolipidi circolanti nell'uomo, caratterizzato dalla presenza di questa triade di condizioni, in modo tale da fornire suggerimenti per l'identificazione di nuovi biomarker che potessero essere introdotti nella pratica clinica.

Per definire il profilo sfingolipidico durante l'obesità, la dislipidemia ed il deficit associato di Vit. D, i sieri di 23 soggetti normopeso normolipidemici (NWNL), 46 soggetti normopeso dislipidemici con deficit della Vit. D (NWDL) e 60 soggetti obesi dislipidemici con deficit della Vit. D (ODL) sono stati analizzati tramite un duplice approccio, caratterizzato dall'utilizzo di due tecniche complementari, l'HPTLC-Primuline profiling e l'analisi LC-MS. Inoltre per definire i profili sfingolipidici nel contesto dell'adattamento

differenziale ad alta quota, i sieri di 59 bambini dislipidemici, con deficit della Vit. D e provenienti da un altipiano Argentino (3775 mt s.l.m) sono stati analizzati tramite LC-MS. I soggetti sono stati divisi, in base al percentile del loro BMI, in quattro gruppi: 7 sottopeso (UW), 30 normo peso (NW), 13 sovrappeso (OW) e 9 obesi (O).

Le differenze nei profili sfingolipidici identificate nei soggetti NWNL e ODL provenienti dall'Arabia Saudita sono causate non solo dall'obesità ma anche dall'associazione con la dislipidemia e con il deficit di Vit. D. Le differenze di genere determinano invece alterazioni dei profili sfingolipidici che sono indipendenti dalla dislipidemia e dal deficit della Vit. D. Nel confronto NWDL vs. ODL sono state identificate delle alterazioni nei profili di specifiche catene di SMs, Cers e diidrosfingomieline (dhSMs) strettamente associate alla sola obesità, le quali si ritiene possano essere correlate ad un aumento del rischio di sviluppare patologie legate all'obesità.

Le alterazioni osservate nei soggetti che vivono ad alta quota, dislipidemici e con deficit della Vit. D hanno permesso di confermare i risultati relativi all'associazione tra SLs, dislipidemia e deficit della Vit. D ottenuti nei soggetti provenienti dall'Arabia Saudita. L'analisi di questi soggetti ha inoltre permesso di identificare profili sfingolipidici caratteristici, associati al BMI e dipendenti dall'adattamento all'ipossia.

ABSTRACT

Research studies indicate that up to 58% of the world adult population will be overweight or obese by 2030 [1]. Obesity is not only related to food intake, but factors such as lifestyle and genetic background contribute to its onset [3–5]. This disease [2] is commonly associated with vitamin D (Vit. D) deficiency [6,7], and genetic associations have been identified to explain this link [8]; however, differences in dietary intake, sun exposure, or Vit. D metabolism are also involved [9]. Moreover, along with Vit. D deficiency, lipids, and particularly sphingolipids (SLs) as ceramides (Cers) and sphingomyelins (SMs) have been described as involved, not only in increasing inflammation [10,11], but also in the development of cardiovascular disease and type two diabetes [12–14], two common conditions observed in obese subjects. Given the pivotal role of SLs in obesity associated co-morbidities and the association of Vit. D, dyslipidemia and obesity, our study was aimed at profiling circulating SLs in human subjects under these conditions, in order to provide hints for the identification of new biomarkers to be introduced in clinical settings.

To define human SLs profile in obesity, dyslipidemia, and Vit. D associated deficiency, sera from 23 normal-weight normolipidemic (NWNL), 46 normal-weight, dyslipidemic, Vit. D deficient (NWDL) and 60 obese dyslipidemic, Vit. D deficient (ODL) Saudi Arabian subjects were analyzed with a dual approach, characterized by the use of two complementary techniques: the HPTLC-Primuline profiling and the LC-MS analysis. Furthermore, to define SLs profiles in the context of human adaptation to high altitude hypoxia, sera from 59 Vit. D deficient dyslipidemic children living at high altitude were analyzed by LC-MS. Children were grouped based on their BMI percentiles in 7 underweight (UW), 30 normal-weight (NW), 13 overweight (OW) and 9 obese (O).

SLs profile analysis of NWNL and ODL Saudi Arabian subjects displayed differences in total Cer and total SM caused by dyslipidemia and vitamin D deficiency, whereas specific Cers, and SMs acyl chains characterize obese subjects, only. Gender differences were found in SLs profiles independently from dyslipidemia and Vit. D status. Obesity-associated Cers, SMs, and dihydrosphingomyelins (dhSMs) specific acyl chains were identified in the NWDL vs. ODL comparison independently from dyslipidemia and Vit D status, and are thought to be drivers of increased risk of developing obesity-associated morbidities.

The analysis of SLs profiles from dyslipidemic children with Vit. D deficiency allowed to confirm the results of Saudi Arabian subjects regarding SLs association with dyslipidemia and associated Vit. D deficiency. Furthermore, SLs profile analysis led to the identification of a characteristic SLs portraits associated with BMI and related to hypoxia metabolic adaptation.

INDEX

RESEARCH INTEGRITY

Results reported in this work comply with the four fundamental principles of research integrity of The European Code of Conduct for Research Integrity (ALLEA, Berlin, 2018):

- Reliability in ensuring the quality of research, reflected in the design, the methodology, the analysis and the use of resources;
- Honesty in developing, undertaking, reviewing, reporting and communicating research in a transparent, fair, full and unbiased way;
- Respect for colleagues, research participants, society, ecosystems, cultural heritage and the environment;
- Accountability for the research from idea to publication, for its management and organization, for training, supervision and mentoring, and for its wider impacts.

List of abbreviations

Vitamin D	Vit. D
Sphingolipids	SLs
Ceramides	Cers
Sphingomyelins	SMs
Dihydrosphingomyelins	dhSMs
Interleukin 6	IL-6
Tumor necrosis factor-α	TNF-α
Sphingomyelinases	SMases
Toll-like receptor 4	TLR-4
Free fatty acids	FFA
Serine C-Palmitoyltransferase	SPT
Sphingosine-1-phosphate	S1P
Phosphoinositide 3-kinases	PI3K
Protein Kinase B	AKT
Protein phosphatase	PP2A
Glucose transporter type 4	GLUT-4
Low-density lipoprotein-cholesterol	LDL-C
Very low-density lipoprotein cholesterol	VLDL-C
High-density lipoprotein cholesterol	HDL-C
Non-alcoholic fatty liver disease	NAFLD
Body mass index	BMI
World Health Organization	WHO
Waist circumference	WC
Cardiovascular diseases	CVD
US Center for Disease Control and Prevention	CDC
Underweight	UW
Normal weight	NW
Overweight	OW
Obese	O
Type 2 diabetes mellitus	T2DM
Melanocortin receptor 4	MC4R
Fat mass and obesity-associated gene	FTO
Short-chain fatty acids	SCFA
Triglycerides	TG
25-hydroxyvitamin D	25-D
1,25-dihydroxyvitamin D	1,25-D
24,25-dihydroxyvitamin D	24,25-D
Vitamin D receptor	VDR
Parathyroid hormone	PTH
Total cholesterol	TC
Apolipoprotein B	ApoB
Normal weight normolipidemic	NWNL
Normal weight dyslipidemic	NWDL
Obese dyslipidemic	ODL
Sphingosine	Sph
Saturated fatty acids	SFA

Acid Sphingomyelinase	aSMase
Neutral Sphingomyelinase	nSMase
High fat diet	HFD
Dihydroceramides	DhCers
Sphingosine	Sph
Dihydrosphingosine-1-phosphate	DhS1P
Glycosphingolipids	GSLs
Dihydroceramide desaturase	DEGS
Ceramide synthase	CerS
Ceramide-1-phosphate	C1P
Galactosylceramides	GalCer
Glucosylceramides	GlcCer
Ceramidases	Cdases
HexosylCeramides	HexCer
Dihexosylceramides	DiHexCer
Fatty acid	FA
Ceramide transfer protein	CERT
Thin layer chromatography	TLC
Retention factors	Rfs
Gas chromatography	GC
High performance thin layer Chromatography	HPTLC
Lipopolysaccharides	LPS
Nuclear factor NF-κB	NF-κB
C-Jun N-terminal kinases	JNK
Suppressor of cytokine signaling proteins	SOCS
Diacylglicerol	DAG
Triacylglycerol	TAG
Antisense oligonucleotide	ASO
Sphingomyelin synthase 2	SMS2
Lysophosphatidylcholine	LPC
sphingosine kinases	SphK
Peroxisome proliferator-activated receptor-α	PPAR-α
Sphingosine-1-phosphate receptor 1	S1PR1
Homeostatic model assessment of insulin resistance	HOMA-IR
Peroxisome proliferator activated receptor γ	PPAR γ
3,5-Di-tert-4-butylhydroxytoluene	BHT
Sulfatides	SLF
Cardiolipin	CL
Dipalmitoyl-sn-Glycero-3-Phosphocholine	DPPC
Dipalmitoyl-sn-Glycero-3-Phosphoethanolamine	DPPE
Fluorescence detection by intensity changes	FDIC
Dihydrosphingosine	dhSPh
Fatty-acid-binding proteins	FABP
Hypoxia-inducible factors	HIFs
Sialidase-3	NEU3
Monosialodihexosylganglioside	GM3
2,3-Bisphosphoglyceric acid	2,3-BPG

1. OBESITY

The debate over the term obesity and its implications engaged physicians and general public information during the last three decades. It has been so challenging to decide whether it was only a condition or an illness that only in 2013 the American Medical Association recognized it as a disease [15], a decision already been made by the National Institute of Health since 1998 [16]. This peculiar pathology is a growing-worldwide emergency, estimated to affect more than 58% of adults by 2030 [1], so crucial that its burden and impact over the worldwide population generated the term “globesity” [17].

Nowadays, obesity and overweight are defined by the World Health Organization (WHO) as the excessive or abnormal deposition of fat with a risk for health [18].

Obesity can be measured using anthropometrical parameters such as skinfold thickness, waist circumference (WC), waist to hip ratio and BMI, or can be assessed employing technical methods as X-ray absorptiometry or densitometry.

Skinfold thickness measures subcutaneous adipose tissue in the triceps and subscapular area and is used in addition to BMI to evaluate obesity providing a more accurate assessment of body fat [19,20]. The waist circumference measurement (WC) is the easiest way to determine central obesity, and some reports identified WC as a significant predictor of obesity-related diseases, particularly of cardiovascular diseases (CVD) [21,22]. The waist to hip ratio is another parameter used to assess and predict cardiovascular risk in obese patients because it is a surrogate marker of visceral obesity, and it has been shown to perform better in risk prediction than BMI alone [23,24].

From the technical point of view, dual-energy X-ray absorptiometry provides measurements that permit to infer the body composition in humans [25], while densitometry, based on Archimedes’ principle of water

displacement, provides an estimation of total body fat and lean tissues content [26]. Methods based on anthropometrical parameters are commonly used to assess the risk of developing obesity-associated diseases, however, the technical measurements based on densitometry and X-ray absorptiometry are more focused on the “quantification” of adipose tissue and are therefore a better indication of obesity *per se*. Independently from their utility in the classification of obese patients, the two techniques are challenging to perform, time-consuming, expensive, and require sophisticated instrumentation. As a result, due to its simplicity and effectiveness in classifying subjects, BMI is the most employed system for the screening of overweight and obesity.

Current guidelines from WHO [18] and the Center for Disease Control and Prevention (CDC) [27] define obesity using BMI, obtained as the ratio between the weight (Kg) and the square of the height (m). This simple measure permits to classify adults population into four main different classes: underweight (UW) (BMI< 18.5 kg/m^2), normal weight (NW) (18.5-24.9 kg/m^2), overweight (OW) (25-29.9 kg/m^2) and obese (O) (BMI> 30 kg/m^2). In turn, obesity can be further organized in five main classes: type 1 obesity (30-35 kg/m^2), type 2 (35-40 kg/m^2), type 3 (BMI> 40kg/m^2), type 4 (BMI> 50kg/m^2) and type 5 (BMI> 60 kg/m^2). Asian population usually have lower BMI cut-off for obesity and overweight [28]. For children, the definition of obesity relies not only on their intrinsic BMI but also on their age, gender, and their corresponding percentile in the population growth chart. Children whose BMI falls in the 5th percentile are considered UW, NW if BMI falls in the 5th to the 85th, OW if BMI falls from the 85th to the 95th, and O if their BMI is located above the 95th percentile [29].

Following this classification in 2016, the WHO concluded that since 1975, the global prevalence of obesity and overweight has tripled, affecting more

than 1.9 billion adults, more than 340 million children aged 5-10 and more than 41 million children under the age of five [18].

The increase in adiposity and specifically, its excess is an established risk factor associated with several causes of mortality [30]. During obesity, the whole organism develops an altered metabolism causing an increased risk of developing CVD, type 2 diabetes mellitus (T2DM) and many types of cancer.

Basically and historically, obesity is the result of an imbalance between caloric intake and energy expenditure, and thus the increase in food intake and the reduction in physical activity are to blame for the increase in weight gain [31–33].

Diet

Human experimental studies regarding food consumption and energy intake demonstrated that an increase in the amount of available food resulted directly into voluntary increased energy intake [34]. Consistently, a meta-analytic review found that doubling food portions results in a 35% increase in energy intake in humans [35].

In the last forty years, diet composition and food availability have changed worldwide. These changes reflect the pro-capita food availability. As an example, caloric intake in the U.S. from 1971 to 2004 increased respectively of 335 calories per day for women and 168 calories per day for men [36]. The idea that an increased energy intake overcoming energy expenditure could be the driver of obesity led to the creation of a model to predict body weight gain [37]. This model predicts that and increase in 100 kJoule per day (23.9 cal) will lead to an increase of 1kg of body weight in approximately three years. A recent study conducted in 2015, analyzing the food energy supply from 69 different countries, demonstrated that in 56 nations, the increment in body weight is associated with an increase in food

energy supply [38]. Studies have confirmed that this trend towards global caloric intake increase positively correlates with the increase in weight gain observed in different populations worldwide [39,40].

These studies confirmed that the availability of more food and specifically of more caloric food result in increased food energy intake, that is a driver of obesity.

As previously stated, the cause of obesity seems to be simple: it is the result of a prolonged period of caloric energy intake, overcoming the energy requirements of the organism.

Nevertheless, this direct association has been revised by several studies, suggesting that genetics, gut microbiota, and other associated illness are also involved in the increased risk of developing obesity.

Genetic causes

People exposed to similar habits (sedentary life) and diets (western diet) does not develop the same response in term of weight gain, suggesting that genetic background contribute to regulate obesity. Studies involving monozygotic and dizygotic twins initially approached hereditability of BMI. Those studies concluded that body fat-mass had a vast concordance in monozygotic twins (70-90%), while a lower concordance was identified for dizygotic twins (35-45%) [41,42]. Other studies conducted on adoptive families confirmed the correlation of adoptees' BMI with biological parents' BMI, but not with BMI from adoptive parents [43].

Furthermore, the observation that BMI is, to some extent inheritable [44] supported the idea of genetics drivers behind obesity.

Nowadays, only a few rare genes have been identified as causative for the increase in BMI. These genes control the coding of different components of the leptin, proopiomelanocortin and melanocortin signaling [45,46].

The signaling of leptin takes place in the hypothalamus, the "nutrient-sensing" organ, in which leptin derived from adipose tissue stimulates

neurons in the arcuate nucleus, inhibiting hunger and stimulating satiety [47]. Similarly, melanocortins (a group of peptide hormones) acts in the arcuate nucleus of the hypothalamus by binding melanocortin receptor 4 (MC4R) in the food intake regulation [48]. Despite these interesting results, it is believed that the “genetics of obesity” does not rely only on monogenic cases, but rather is based on the interaction of a multitude of different genes with smaller effect sizes.

Genome-wide association studies provided useful information regarding the association between single-nucleotide polymorphisms and obesity-associated traits. Specifically, more than 140 genetic chromosomal regions are related to obesity, and gene expression related to adiposity is highly enriched in the central nervous system [49]. More recently, another genome-wide association studies identified 227 genetic variants related to different biological pathways (food sensing, adipocyte differentiation, insulin signaling, lipid metabolism, muscle and liver, gut microbiota) as relevant for the development of polygenic obesity [50]. The first and most interesting identified variants were related to fat mass and obesity-associated gene (FTO), for which several studies showed increased heterozygotes and homozygotes risk for developing obesity and T2DM [51,52].

Gut microbiota

The human gastrointestinal tract and specifically the colon is highly populated in bacteria, viruses and fungi [53]. The resulting ecosystem, commonly called gut microbiota, is exposed since birth to several factors influencing its development (type of birth, diet, use of antibiotics) [54]. Several evidences highlighted the importance of gut microbiota in supporting different processes in the gastrointestinal tract, ranging from digestive process [55], vitamin synthesis [56] protection from pathogens [57] to modulation of the immune system [58]. Gut microbiota contributes to human health, and changes in its composition, called dysbiosis, can

contribute not only to the development of diseases but also to the development of obesity. As an example, germ-free obesity-resistant mice develop obesity if they are transplanted with microbiota from a healthy donor, increasing the overall energy intake from diet [59]. Qualitative variations also account for obesity gut microbiota profile. Obese subjects are characterized by reduced diversity in the components of their gut microbiota, and moreover, they present increased Firmicutes/Bacteroides ratio [60,61]. Data indicating an increased prevalence of Firmicutes at the expense of Bacteroides were further confirmed in feces from obese mice [62].

One of the explanations proposed to understand the role of gut microbiota in obesity development relies on the capacity of bacteria to ferment polysaccharides coming from the diet that generally would not be digested by humans [63]. As a result of dietary fiber fermentation, short-chain fatty acids (SCFA) [63] are produced, quickly uptaken from enterocytes, and transported into circulation. The increased absorption of SCFA due to altered fermentation results in both an increase of triglycerides (TG) synthesis and an increase in energy uptake from the diet [64]. The gut microbiota influences not only nutrient uptake but also trigger metabolic inflammation, exacerbating the chronic low-grade inflammation and insulin resistance seen in obese patients [65]. Lipopolysaccharides from gram-negative bacteria, commonly found in the gastrointestinal tract, are known to be activators of Toll-like receptor 4 (TLR-4) [66]. In turn, TLRs are known to upregulate inflammatory response stimulating the production of cytokines and chemokines.

Associated illness

Physical and mental illnesses, as well as medications that are used to treat them, are also known to increase the risk of developing obesity. In this context: hypothyroidism [67], Cushing's syndrome [68] the use of

antidepressant [69], corticosteroids [70], and eating disorders [71] have commonly been linked to obesity.

2. VITAMIN D

Vitamin D is a group of fat-soluble steroids mainly represented in plants by vitamin D2 (ergocalciferol) and in animals by vitamin D3 (cholecalciferol) [72]. Their active forms are responsible for multiple biological processes, of which the most prevalent is the intestinal uptake of calcium [73] and phosphate [74]. Natural sources of Vit. D in humans are related to both sun exposure and diet intake, with the first accounting as the primary source and the second covering up to 20% of the required daily Vit. D intake [75].

During sun exposure, the 7-diidrocholesterol present in the skin, between *stratum basale* and *stratum spinosum*, is converted by UVB radiation (290-315 nm) into pre-vitamin D [76].

Pre-vitamin D in the skin it is not active and requires two subsequent hydroxylations steps to develop the fully active form. Hydroxylation of Vit. D is provided by two distinct hydroxylase (CYP2R1 and CYP27B1) [77]. The first, located in the liver, hydroxylates Vit. D in position 25 and produces the 25-hydroxyvitamin D (25-D), whereas the latter is present in the proximal renal tubule of kidneys and produces the biologically active form 1,25-dihydroxyvitamin D (1,25-D). Vit. D degradation takes place in the kidneys as a result of another hydroxylation (hydroxylase CYP24A1) acting on both 25-D and 1,25-D, causing the formation of 24,25-dihydroxyvitamin D (24,25-D) [78]. Vit. D levels in serum are generally estimated through the quantification of its more abundant and inactive form 25-D [79].

The biological effects of Vit. D (e.g., mineral homeostasis, cell differentiation/proliferation) [80] are mediated by its binding to nuclear Vit. D receptor (VDR), a ligand-activated transcription factor that controls gene expression. After being activated by its ligand, VDR heterodimerizes with the retinoid X receptor and in turn, recruits coregulatory complexes to modify gene expression [81]. Even though responses are tissue-specific and biological effects range from growth control to immune system and

functional control of cellular activity, the main biological effect undertaken by Vit. D is the regulation of calcium homeostasis, specifically obtained by increasing calcium absorption in the small intestine and calcium resorption from bones [82]. Calcium absorption in the small intestine is finely regulated by increasing gene expression of several calcium-associated molecules: TRPV6 (enterocytes membrane calcium transporter), calbindin-D_{9K} (facilitates calcium transport through the enterocytes and buffers high levels of calcium-induced cytotoxicity), CaATPase and PMCA1b (mediating the extrusion of calcium from the basolateral membrane of enterocytes). Furthermore, when normal calcium levels are not reached, Vit. D acts synergically with parathyroid hormone (PTH) to stimulate both osteoclast differentiation in bones for calcium resorption [83,84] and calcium reabsorption from the distal renal tubule (increase expression of genes controlling calcium transporter TRPV5 and calbindin-D_{9K}) [85].

2.1. Vitamin D deficiency

The paramount role of Vit. D in the regulation of calcium homeostasis and bone remodeling results in the maintenance of correct Vit. D levels not only during human development but also in adults for the preservation of bone health and cellular homeostasis. The role of Vit. D deficiency in bone homeostasis was at first uncovered in children with rickets [86], nevertheless several other associated illnesses have been linked to this status and in particular, infectious diseases [87], autoimmune disorders [88], cancer [89], cardiovascular diseases [90] and obesity [7,91,92] are thought to be affected by Vit. D deficiency.

There is not a worldwide consensus on correct Vit. D levels, and even though there is a general agreement in defining Vit. D severe deficiency as serum levels of 25-D are below 10-12 ng/ml (25/30 nmol/l), several differences emerge between guidelines from different groups and nations in

the definition of Vit. D insufficiency or sufficiency. Vitamin D Council denotes as sufficient for humans, a level of Vit. D superior to 100nmol/l or 40ng/ml. On the contrary, the Scientific Advisory Committee on Nutrition starts to consider Vit. D sufficiency at lower levels (30nmol/l or 12ng/ml). For the Endocrine Society, the International Osteoporosis Foundation and the American Geriatrics Society serum 25-D sufficiency sits over the cut-off of 75nmol (30ng/ml), while for the Institute of Medicine and American Academy of Pediatrics the adequacy of Vit. D comes from levels higher than 50nmol (20ng/ml). The definition of Vit. D sufficiency is, even more, complicate in children. Where the European food safety authority draws a line for sufficiency at levels of at least 50nmol/l (20ng/ml), the Scientific Advisory Committee on Nutrition reports lower lever of sufficiency (30nmol/l or 12ng/ml).

The only standard global-accepted level for Vit. D deficiency is, therefore, the cut off identifying the Vit. D severe deficiency (Vit. D levels lower than 10-12 ng/ml). The lack of harmony in the definition of Vit. D sufficiency or insufficiency between different guidelines significantly affects the prevalence reported from different studies conducted in different locations. Additionally, the fragmentation of reviews coming from different countries, the use of different cohorts, and the incomplete picture of Vit. D determinants (UVB exposure, dietary intake) severely hamper the recognition of a global Vit. D prevalence.

Nowadays, data coming from reviews on global Vit. D status indicates widespread Vit. D deficiency, and even though data were produced ten years ago; some consistent results are showing a higher prevalence of deficiency in Asia, Middle East and Africa in both children and adults [93]. A systematic review [94] from 2014 describes the best picture for Vit. D deficiency worldwide. However in this case, authors, analyzing 103 national reports, indicate a widespread lack of data from several countries, the use

of different Vit. D detection method and different cohorts, suggesting that the definition of a global prevalence for Vit. D deficiency is far to be defined. Vit. D deficiency arise from a multitude of causes, including inadequate food intake and sun exposure, liver and kidney chronic diseases [95,96], obesity [97,98], pathologies resulting from malabsorption (celiac disease, inflammatory bowel diseases) [99] and treatment with medication that induce hepatic P450 in degrading Vit. D (carbamazepine, dexamethasone, nifedipine) [100].

In the last 20 years and more precisely from 2000, Vit. D deficiency and its relation with obesity become more interesting for the scientific community. Published papers regarding obesity and Vit. D, in fact, increased significantly from 14 in 2000 to 565 in 2018, suggesting a strict association between the two phenomena but also an increased concern over the global effects of these two pandemics.

2.2. Vitamin D deficiency and obesity

Researchers have found a consistent association between low serum vit.D concentration and obesity [101–104]. To our knowledge, the first study identifying a link between obesity and Vit. D was conducted in 1977 by Teitelbaum *et al*. [105]. The authors noticed that obese patients who underwent small intestine bypass for the treatment of obesity had low levels of Vit. D and concluded that the treatment resulted in a transient deficiency of circulating Vit. D. Apart from the interest of the study, the link between obesity and Vit. D deficiency was a result of the effects of surgery, and it was only in 1981 that Compston and colleagues were able to demonstrate that obese subjects have a higher risk of developing Vit. D deficiency than normal-weight subjects [106].

Several other studies have been conducted over the years, in 1985 Bell *et al*. [107], confirmed the reduction of 25-D seen in obese patients by

Compston but identified in the same patients an increase in 1,25-D, the active form of Vit. D. In 1988 a work from Liel *et al*. [108] identified the same reduction in 25-D in obese patients but not the increase in 1,25-D. More recently, other studies identified the same dependency between obesity and Vit. D. In 2010, a work by Herranz Antolín S [109] and colleagues found that morbidly obese patients have lower mean levels of Vit. D (16.6 ng/ml vs. 21.9 ng/ml) and higher prevalence of Vit. D deficiency (80% during obesity, 40% in non-obese) when compared to normal-weight subjects. Further supporting these results, a bi-directional genetic study by Karani S. Vimaleswaran and colleagues identified, in 21 adult cohorts (42,024 participants), an association between serum Vit. D levels and BMI. Their study indicated that for every increase in one BMI point (1kg/m^2), a 1.15 % decrease in Vit. D levels is seen, confirming in a large cohort the detrimental effects of obesity on Vit. D status.

Multiple hypotheses have been formulated to explain the decrement of Vit. D in obese subjects, specifically regarding dietary intake, reduce bio-synthesis, altered metabolism/catabolism/intestinal absorption, or adipose tissue distribution.

Vitamin D dietary intake was shown to be lower in obese men compared to normal-weight but not in obese women [110]. In obese children aged 1-3 compared to normal-weight age-matched controls, a two-fold decrease (although not statistically significant) in dietary intake of Vit. D was seen [111]. Similarly, a decrement in dietary intake was also seen in obese children and normal-weight children aged 1-5, resulting in an 80% of Vit. D deficiency prevalence for the obese group and 70% for the normal-weight [112]. Nevertheless, lower Vit. D status have been identified in obese women compared with normal-weight despite higher Vit. D intake [113], suggesting that other underlying factors also need to be taken into account for Vit. D deficiency.

Reduced synthesis from reduced skin exposure or altered skin biosynthetic capacity have also been proposed as causes for obesity-related Vit. D deficiency. In the first case, differences in sun exposure have been proposed to explain differences in Vit. D biosynthesis. Authors found that people with a BMI> 30kg/m^2 were less willing to expose their bodies to the sun when compared to people whose body mass index (BMI) was lower than 30 kg/m^2 [114]. In the second case, altered skin biosynthetic capacity was supposed to be causative in the reduction of levels of Vit. D during obesity, nevertheless, 7-dihydrocholesterol was found to have similar levels in obese and normal-weight patients as well as its conversion to Vit. D [115], suggesting that Vit. D deficiency is not caused by reduced biosynthesis.

Both the altered metabolism and catabolism of Vit. D were proposed as causative in obesity-associated Vit. D deficiency. Subcutaneous human adipose tissue expresses the three hydroxylases required for the formation of 25-D (precursor form), 1,25-D (active form) and 24,25-D (degradation), respectively. Moreover, both the 25-hydroxylase (CYP2J2) and the 1α-hydroxylase (CYP27B1) show reduced expression in obese adipose tissue [116], supporting the idea that altered metabolism for Vit. D is present in adipose tissue of obese patients. Furthermore, the presence of the hydroxylase CYP24A1, responsible for the inactivation and sequent degradation of 25-D, has been documented in human adipocytes [117], and the expression of its mRNA is strongly induced *in vitro* by incubation with 1,25-D, suggesting that adipose tissue can actively metabolize Vit. D.

Altered intestinal absorption was also indicated as a possible explanation for Vit. D deficiency during obesity. As demonstrated by Teitelbaum *et al*. [105] in 1977, low levels of 25-D were present in obese patients after small-intestine bypass, suggesting decreased intestinal Vit. D assimilation. This article paved the way for intensive studies regarding bariatric surgery, Vit. D

levels and risk of bone diseases [118–121] — however, the procedure induced the resulting 25-D deficiency, and today there is no evidence in Vit. D malabsorption during obesity.

By being fat-soluble, when Vit. D (radiolabeled) is administered to mice, it quickly accumulates in the adipose tissue, and it has been observed that one month after radiolabeled treatment, Vit. D is still present in the same tissue, indicating that its release is slow and prolonged [122]. Blum M *et al*. identified a positive correlation between human serum Vit. D levels and adipose tissue, suggesting the storage of Vit. D in adipose tissue [123].

In 2012, a work by Drincic AT and colleagues provided an alternative explanation by demonstrating that when 25-D levels of obese subjects were corrected by body size, the difference in Vit. D levels with normal-weight were in such a way abolished. Their model, called volumetric dilution, asserted that any increase in Vit. D has to be distributed not only in serum but also in total body fat. As an example, if the whole body fat mass is doubled as in obese compared to a normal-weight subject, the increase, due to any input, in serum Vit. D levels of obese subjects would be half of the size [124].

Even though the association between these phenomena is today acknowledged, and several possible explanations have been identified, a causal relationship is still lacking, and further studies are mandatory not only to identify the pathogenesis of this relationship but also to assess its associated risk.

2.3. Vitamin D deficiency and dyslipidemia

Vitamin D deficiency does not only correlate with obesity-specific criteria like BMI, adiposity, or subcutaneous adipose tissue, but also with other obesity-related parameters commonly identified in obese subjects as changes in lipidic serum profile, called dyslipidemias.

In the context of abnormal serum lipid profiles, dyslipidemias are usually observed in the 60-70% of obese subjects [125]. These subjects are characterized by increased serum levels of TG, total cholesterol (TC), VLDL, slightly increased LDL-C, and decreased levels of HDL-C [126].

In a small cohort of 150 Indian subjects, Chaudhuri and colleagues [127] were able to identify high levels of TC, LDL, TG, and low levels of HDL-C in Vit. D deficient subjects. Consistently, in 2012, a work by Ponda and colleagues [128], found that, when compared to Vit. D deficient patients, those with correct levels had lower TG, TC, LDL-C, and higher HDL-C levels. However, the authors found that when Vit. D levels are raised in Vit. D deficient subjects, there is an increase in HDL-C levels and total TC while LDL-C levels remain stationary, suggesting that Vit. D supplementation may not result in an improvement of all serum lipid parameters.

Similarly, while working on Vit. D and CVD risk factors, Jiang *et al.* [129] confirmed data for Vit. D deficiency from Chaudhuri and Ponda, showing that Vit. D levels negatively correlate with LDL-C and TG and positively with HDL-C, furthermore confirming that Vit. D deficiency results in a poorer lipid profile. Accordingly to previous reports, Wang *et al*. [130] identified a negative association between Vit. D level, TG and LDL-C and recently, a work by Sun X [131] showed that serum Vit. D levels are inversely associated with triglycerides, Apolipoprotein B (ApoB), with the ratio of LDL cholesterol/HDL cholesterol, and ApoB/ApoA-1.

Vit. D affects serum lipid profiles through mechanisms that are not fully understood and includes: the suppression of parathyroid hormone secretion [132], the intestinal absorption of calcium [133], the modulation of beta cells activity and insulin resistance [134], the regulatory effect of Vit. D on adipose tissue differentiation and Vit. D suppression of lipoprotein lipase [135,136].

Regardless of the causes that are not clear and will require further studies, increasing evidences indicate that high serum Vit. D levels are associated with a more favorable serum lipid profile [136–138].

Data from literature raise the point that Vit. D deficiency is pandemic and acts detrimentally on both obesity and obesity-associated dyslipidemia. Studies should, therefore, address this triad of disorders together in order to asses and fully entangle this intricate metabolic flux.

3. SPHINGOLIPIDS

3.1. Sphingolipid synthesis

Sphingolipids are molecular components of membranes responsible for their homeostasis. Changes in lipid composition can influence not only membrane structure but also receptors organization and function. Ceramide, sphingosine (Sph), and sphingosine-1-phosphate (S1P) are known to act as signaling molecules and are involved in the regulation of cell growth, differentiation, senescence, and apoptosis [139–142].

The SLs metabolic pathway is an intricate structure that envelopes simple molecules like Cers and a multitude of complex glycosphingolipids in which Cers represents the molecular core of the biosynthesis and catabolism of SLs. Ceramide levels in cells can be associated with *de novo* synthesis or hydrolysis of complex sphingolipids resulting from degradation of glycosphingolipids (GSLs) or hydrolysis of sphingomyelins [143,144]. In the *de novo* pathway, serine and palmitoyl-CoA are condensed by serine palmitoyltransferase (SPT) to produce 3-ketodihydrosphingosine, which in turn is reduced to dihydrosphingosine (sphinganine) [145]. Cer synthases (CerS1-6), N-acylate the sphinganine to produce dihydroceramide (dhCer) that undergo desaturation by dihydroceramide desaturase (DEGS) to finally generate Cers. By this pathway, several Cers with different acyl chain lengths can be produced, depending on the different CerS isoforms, from 1 to 6, that have specific preference for different chain length fatty acyl-CoAs [146]. The biological role of products from different Cers isoforms generating Cers with different acyl moiety remains so far undisclosed. The produced Cer can undergo three different pathways: it can be phosphorylated to Ceramide-1-phosphate (C1P) [147], converted to GSLs [148,149], or can be used to synthesize sphingomyelins [150]. Cer is also produced from the breakdown of complex glycosphingolipids through the

sequential removal of the hydrophilic portions of GSLs by specific hydrolases producing galactosylceramides (GalCer) or glucosylceramides (GlcCer), which in turn can be hydrolyzed by specific galactosidase or glucosidases to produce ceramide [151].

At variance, the SM hydrolysis is controlled by five main types of sphingomyelinases (SMases): lysosomal acid SMase, neutral SMase (Mg^{2+} dependent), alkaline SMase or zinc-dependent SMase with different subcellular localization and pH. Their action on SMs determines the release of Cer and phosphocholine [152].

Once released, Cer can undergo degradation as a result of acid, alkaline, and neutral alkaline ceramidases (CDases) regulated by pH and subcellular localization. Those enzymes remove the fatty acid (FA) from Cer, producing free sphingosine (Sph). The latter can return to the SLs pathway or be phosphorylated by the action of specific kinases (Sphingosine kinases 1-2) to S1P [153]. S1P can be dephosphorylated to Sph by specific S1P phosphatases or can be metabolized by S1P lyase, resulting in the release of ethanolamine phosphate and hexadecenal [154]. The precise compartmentalization of these molecules regulates SLs synthesis: the initial step occurs at the cytosolic side of the ER but also on ER perinuclear membranes or mitochondrial associated membranes (Figure 1). The second and third steps occur in the Golgi, in which more complex molecules are synthesized and transported to the plasma membrane through vesicular trafficking. From the plasma membrane, SLs can be recirculated through the endosomal pathway. SM and GlcCer are metabolized to Cer in the lysosomal compartment by SMases and glucosidases, while Cer is degraded by acid CDase to form Sph. The latter, thanks to its positive charge, can leave the lysosome and move in the cytosol between membranes becoming available for recycling. This precise compartmentalization reinforce the concept that those molecules are not

merely structural component but actively participate to biological processes [155–157] and their dysregulation can impact not only on membrane structure dynamics but also on signaling pathways involved in metabolic diseases.

Figure 1. Sphingolipids biosynthesis and intracellular trafficking.

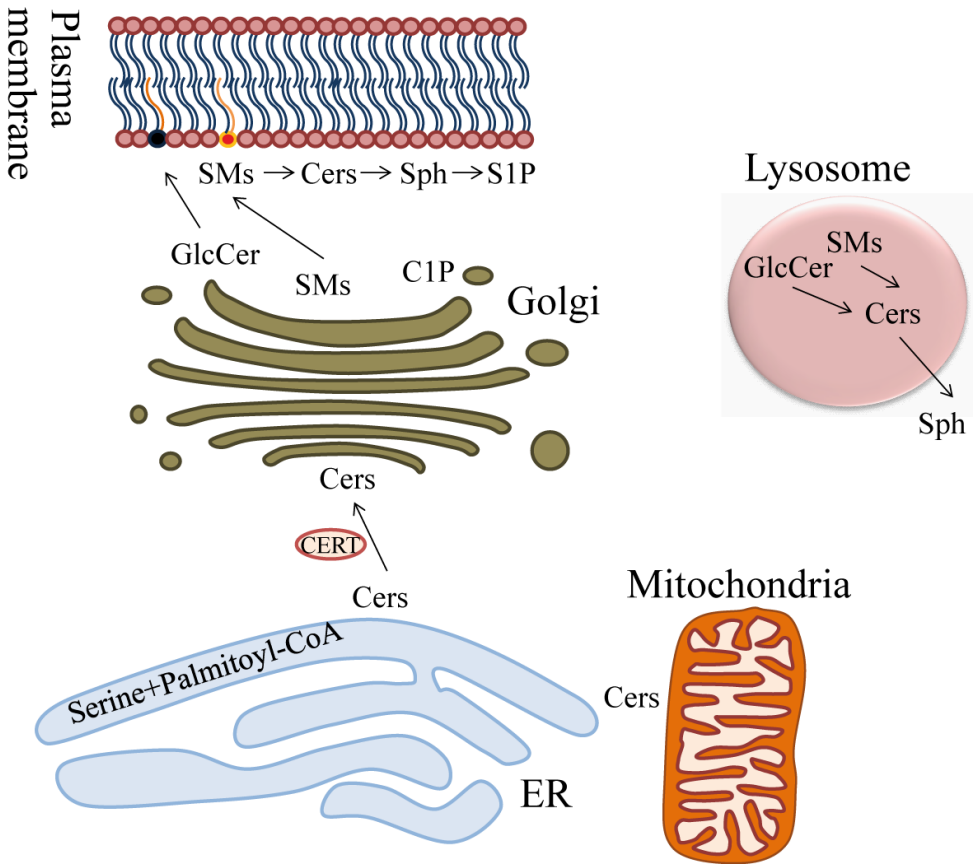

3.2. Sphingolipid analysis

Sphingolipids have been traditionally analyzed by thin layer chromatography (TLC), which allows the separation and characterization of SLs by retention factors (Rfs) comparison with known standards [158]. More recently, SLs-specific ELISA immunoassays have been developed

[159]. However, this methodology allows to determine the SLs total content leaving unspecified the contribution of the saturated or unsaturated acyl chains.

Furthermore, the wide dynamic range affecting sphingolipid composition in tissues and biological fluids requires sensitive technologies able to detect high and low abundant species; coupling a separative step with a precise detection of the chemical composition of molecules. The goal was achieved when mass spectrometry was introduced, and different ionization methods [160,161] and analyzers [162–164] were used successfully. Furthermore, the high homology among similar sphingolipids and the consequent mismatch [165] was overcome by coupling liquid chromatography [166], gas chromatography (GC) [167] and TLC or High-Performance Thin Layer Chromatography (HPTLC) [168–170] prior mass spectrometry analyses. LC-ESI MS/MS is nowadays the most utilized method [171,172], but other on-line hyphenated techniques have also been applied to sphingolipid research, such as LC-NMR [173], CE-MS [174] and TLC/HPTLC-MS [175–178]. Despite cutting edge technologies, there are still some concerns about sphingolipid analysis connected to the profiling of SLs species in a single high-throughput analytical step. The last generation mass spectrometers have the possibility to get better inside into the sphingolipidome. However, the dynamic range is still far to be entirely resolved, and the complexity of the number and the structure of sphingolipids further complicate analyses.

3.3. Sphingolipids and obesity

The neologism “Globesity” perfectly defines the escalation of the pandemic of obesity, a complicated status in which the increase in nutrient intake, adipocyte dysfunction, insulin resistance, ectopic fat accumulation and inflammation act in synergy. Obese subjects are characterized by chronic

inflammatory status (pro-inflammatory cytokines) [179], availability of free fatty acids (FFA) [180] and oxidative stress [181]; all these features are connected with co-morbidities associated with obesity. A profound alteration of systemic metabolism induced by obesity and by obesity-related co-morbidities severely affect SLs homeostasis, generating unbalance targeting adipose tissue, liver, and skeletal muscle [182–184]. In physiological conditions, FFA are used as an energy source/storage, nevertheless, their pathological increment leads to apoptosis, insulin resistance, and to several alterations referred as “lipotoxicity” [185]. In obese subjects, sphingolipid metabolism is affected by increased bio-availability of FFA, which induce increment of palmitoyl-CoA, thus increasing ceramide production via *de novo* pathway [186].

Studies on rodents show that saturated fatty acids (SFA) can stimulate the TLR-4, activating SMases converting SMs to Cers, contributing to increasing Cer levels [187,188]. Furthermore, the increment of pro-inflammatory cytokines like IL-6 and TNF-α observed in obese subjects can play a central role in SLs modulation. In C57BL/6J mice the intraperitoneal administration of TNF-α induces upregulation of acid SMase (aSMase), neutral SMase (nSMase) and SPT suggesting that Cers level can be increased not only through *de novo* synthesis associated to higher availability of palmitoyl-CoA precursors but also to the indirect activity of TLR-4 and pro-inflammatory cytokines [189].

It is well known that obesity is connected to inflammatory response, however, the precise mechanisms that trigger this response are not completely clear, nonetheless activation of TLR-4 by lipopolysaccharides (LPS) [190], or by FFA [191], macrophage infiltration [192], adipose tissue expansion [191] and hypoxia [193] have been proposed as causative effects, leading to release of several pro-inflammatory cytokines, also known as adipokines [194,195]. The suggestion that saturated fatty acids

could be potential activators of TLR-4 [191] links ceramides increase to inflammation. William L. Holland [187] by using *in vivo* and *in vitro* models, induced TLR-4 activation, demonstrating that saturated fatty acid leads to ceramide-biosynthesis by activating TLR-4 and that increased Cers are required for TLR-4 dependent insulin resistance. TLR-4 is known to be responsible for initiating signals that activate NF-κB, JNK, and SOCS pathways [196,197], all factors involved in the regulation of inflammation. In 1992 it was demonstrated by Dressler *et al*. [198] that the increment of TNF-α was able to reduce membrane sphingomyelin levels, increasing ceramide, suggesting that SMase was activated by TNF-α. This idea was further confirmed in 1994 by Schütze *et al*. [199], which showed an independent activation of aSMase and nSMase by TNF-α, resulting in an increased ceramide production and activation of NF-Kβ by aSmase. In 2001 Teruel *et al*. [200] demonstrated increased levels of Cers in brown adipocytes treated with TNF-α and glucose and that the relocation of glucose transporter type 4 (GLUT-4) to the plasma membrane was inhibited by treating the same cell with a short-chain ceramide analog (C2-ceramide).

Furthermore, C2-Ceramide was indicated as activator of Protein phosphatase 2 (PP2A), leading to Protein Kinase B (AKT) dephosphorylation. Kolak *et al*. [201], confirmed that increased levels of ceramide and increased expression of SMases (SMPD1 and 2) characterized the subcutaneous adipose tissue of obese women with high levels of fat in the liver. Nevertheless, TNF-α increase was not statistically changed whereas other markers of inflammation (i.e., macrophage marker CD68, chemokines monocyte chemoattractant protein-1 and macrophage inflammatory protein-1alpha) were found at variance in a group of patients with high fat liver (NAFLD), supporting the hypothesis that an increased inflammatory status is associated with ceramide in obesity.

Despite increasing evidence supporting the role of ceramides in obesity-induced metabolic disorders, a clear portrait for different ceramide sub-species and their biological role still lacks; thus, the characterization of their actions in obesity and related-comorbidity is warranted,

3.4. Ceramides and obesity

Ceramide represents the central node of SLs, it is the keystone of sphingolipid molecules, and it is localized in the middle of the sphingolipid pathway. Even though it is not the most abundant SL in the human blood (accounting for 3% of the total SLs in serum) [202], it is the most studied. In the cell, Cers exert several actions [203], ranging from induction of apoptosis [204] and insulin resistance [205] to alteration of vascular tone [206].

The first study linking obesity, ceramides, and insulin resistance was conducted in 1990 by Turinsky J *et al*. [207] on Zucker diabetic fa/fa rats. In lean animals, 1,2-Diacylglycerol and ceramide levels were lower in muscle than in liver, whereas in Zucker diabetic fa/fa rats, both liver and muscle ceramide levels were high, suggesting a connection between ceramide and insulin resistance.

In vivo, high fat diet (HFD) or *in vitro* FFA administrations have been widely adopted as tools to stimulate weight gain on animal and cell models to mimic fat accumulation that precedes obesity [208–210]. Those type of induced-obesity allow to decipher the role of molecules without other confounding factors. Cell lines from murine myotubes [211] treated with radioactive palmitate, or human female myotubes supplemented with palmitate [212] show increased palmitate incorporation into ceramide and increased ceramide production, further supporting the idea that exogenous (dietary) oversupply of fatty acids, and specifically palmitate, is utilized to produce ceramide but also contribute to the increment of its levels.

Moreover, attention was focused on the acyl chain length of different ceramide species rather than total Cers, associating specific acyl chain activities to chain length. Murine models, fed with HFD or treated with palmitate, have shown increased ceramide C16:0 and C18:0 levels independently from tissue or cell type [213–220]. However, discrepancies after HFD treatment were noticed in the amount of some long-chain Cers in metabolic tissues as liver, skeletal muscle and adipose tissue (Table 1).

Nevertheless, quantitative results were contradictory, Cer C24:0 has been shown to decrease in liver [213,216] and increase [214], as well as C24:1, that was decreased in [216], but increased in [214,215,221]. C24:1 gave conflicting results also in skeletal muscle, resulting decreased in [222] but increased in [214]. Conversely, Cer C22:0 decreased in adipose tissue according to [223] but increased in [216]. Total Cers increased in a study from Lyn-Cook *et al*. [224], which also demonstrated that HFD increased the expression of ceramide synthase, SPT and SMase in the liver. Ceramide was measured by dot blot in the liver and by ELISA in serum and resulted increased in HFD fed rats compared to LFD fed animals [225]. Ussher *et al*. [226], determined Cers levels derivatizing the molecule to an o-Phthalaldehyde to generate a fluorescent compound that was separated by HPLC and quantified by fluorescence spectrometry. In gastrocnemius, ceramide was doubled in HFD fed animals, whereas hepatic ceramide levels were unaffected, in countertrend to Lyn-Cook data [224], that utilized the same quantification method on the same animal model. Other discrepancies were described for sphingosine, in one work by LC-MS, sphingosine increased [227,228], whereas, with fluorescence, no changes were detected [229] (Table 1).

These results suggest that, before considering data as absolute, a careful evaluation of the efficiency of the methods adopted for quantitation have to be carefully considered.

Levels of ceramide, insulin resistance and glucose intolerance observed in HFD mice were completely reversed by treatment with myriocin (a *de novo* Cer biosynthesis inhibitor). Utilizing C57BL/6J mice, Boini KM *et al*. [230] discovered a significant increase in plasma ceramide levels in mice on an HFD and that the treatment with amitriptyline (an inhibitor of both SMases and CDases) was able to reduce plasma ceramide levels. By studying non-alcoholic fatty liver disease on Long-Evan rats, Longato *et al*. [225] confirmed previous results, highlighting the detrimental role of HFD. In particular, HFD compared to low-fat diet (LFD) led to NALFD, peripheral insulin resistance, increased expression of pro-ceramides gene in liver and increased levels of serum ceramides. Kurek *et al*. [229], confirmed in Wistar rats that HFD by itself was able to determine NAFLD and induce insulin resistance; nevertheless, treatment with myriocin was able to reduce DAG, TAG and Cer levels in liver, leading to a reduction on NAFLD severity.

The use of leptin-deficient *ob/ob* mice models partially confirmed these data, even if Samad *et al*. [189] detected a decrement of total Cers in adipose tissue, other authors investigating the same HFD fed animals indicated increase of most of acyl chain Cers in the same tissue [216,217,223] (Table 2). In human subjects, Haus JM *et al*. [231] found that obese T2DM patients had higher plasma concentration of total, C18:0, C20:0, C24:0 and C24:1 Cer compared to control and the same Cer chains were inversely correlated with insulin sensitivity. However, the same Cer C18:0, C20:0 and C24:1 were not detected as changed in serum of obese subjects by [232] (Table 3). Concerning the quantitative assessment of different acyl chains Cers, several discrepant data characterized both animal models and human subjects, thus data have to be considered cautiously.

Turpin SM *et al*. [223] demonstrated that CerS6 mRNA expression and Cer C14:0, C16:0, C16:1, C18:0, C18:1 and C22:1 were elevated in obese

adipose tissue from mice and that an increase in CerS6 positively correlated with insulin resistance in humans. These data were further confirmed by CerS6 deficient mice, which were protected from HFD and showed reduced obesity, glucose intolerance and low levels of Cer C16:0. Recently, Raichur S *et al*. [233] demonstrated using antisense oligonucleotide (ASO) in leptin-deficient *ob/ob* and HFD mice models that CerS6 ASO treatment determined a reduction in the CerS6 expression in liver and decrement of subcutaneous and visceral fat. Furthermore, this treatment induced a reduction of C16:0 ceramides plasma levels, resulting in improved glucose tolerance and insulin sensitivity, confirming the strict correlation between ceramide, obesity, and insulin resistance again. A recent study by Turpin SM *et al*. [234] revealed increased levels of C18:0 ceramide and Cers1 overexpression in skeletal muscle of HFD fed mice, while in mice lacking Cers1, a reduction in levels of Cer18:0 is observed, and it is accompanied by the improvement of glucose homeostasis. However, the muscle-specific deficiency of CerS5/6 failed to protect mice from obesity-induced insulin resistance [234], highlighting the relationship among acyl chain length and isoforms of Cers (1-6) enzymes.

Table 1. Discrepancies in sphingolipid's species alteration in HFD animal models.

Tissue	Sphingolipid	Variation	References	Experimental model	Quantification method
Liver	Cer C24:0	Decreased	[213,216]	C57BL/6 mice HFD (60%fat)	LC-MS/MS
		Increased	[214]	C57BL/6 mice HFD (42%fat)	LC-MS/MS
	Cer C24:1	Decreased	[216]	C57BL/6 mice HFD (42%fat)	LC-MS/MS
		Increased	[214,215,221]	C57BL/6 mice HFD (42%fat)	LC-MS/MS
	Total Cers	Increased	[224,225]	C57BL/6 mice HFD (60%fat)	Nile Red fluorescence-based assay
		No change	[226]	C57BL/6 mice HFD (60%fat)	Derivatizion to O-Phthalaldehyde
	Sphingosine	Increased	[227,228]	Syrian hamsters HFD (30% fat)	LC-MS/MS
		No change	[229]	Wistar rats HFD (60% fat)	Scraped off TLC+GC-LC
Skeletal muscle	Cer C24:1	Decreased	[222]	C57BL/6 mice HFD (42%fat)	LC-MS/MS
		Increased	[214]	C57BL/6 mice HFD (42%fat)	LC-MS/MS
Adipose tissue	Cer C22:0	Decreased	[223]	C57BL/6 mice HFD (55.2%fat)	LC-MS/MS
		Increased	[216]	C57BL/6 mice HFD (42%fat)	LC-MS/MS

Table 2. Discrepancies of sphingolipid species alteration between ob/ob mice and HFD fed animals.

Tissue	Sphingolipid	Variation	References	Experimental model	Quantification method
ADIPOSE TISSUE	Total ceramide	Decreased	[189]	C57BL-ob/ob mice	LC-MS/MS
	Cer C16:0, C18:0, C18:1, C20:0, C22:0	Increased	[216,217,223]	C57BL/6 mice HFD (42%fat)	LC-MS/MS
				C57BL/6 mice HFD (60%fat)	LC-MS/MS
				C57BL/6 mice HFD (55.2%fat)	LC-MS/MS
	Total SM and C20:0, C20:1, C22:1, C24:0, C24:1	Decreased	[189]	C57BL-ob/ob mice	LC-MS/MS
	SM C14:0, C16:0, C16:1, C18:0, C18:1	Increased	[216]	C57BL/6 mice HFD (42%fat)	LC-MS/MS

Table 3. Discrepancies of sphingolipid species between plasma and serum in obese human subjects.

Biological fluid	Sphingolipid	References	Variation	Subjects	Quantification method
Plasma	S1P	[240]	Increased	Obese adults	LC-MS/MS
Plasma	S1P	[241]	Increased	Obese adults	ELISA
Serum	S1P	[232]	No change	Overweight adolescent	LC-MS/MS
Plasma	Cer C18:0, C20:0, C24:1	[231]	Increased	Obese T2D adults	LC-MS/MS
Serum	Cer C18:0, C20:0, C24:1	[232]	No change	Overweight adolescent	LC-MS/MS

3.5. Dihydroceramides and obesity

Dhcers were considered for long time inactive precursors of ceramides, generated during the *de novo* synthesis, since the short-chain (C2-C6) ceramides, and not their saturated counterpart were able to stop cell proliferation and to induce apoptosis [235–237]. Only in 2006, a bioactive role for dhCers was first acknowledged by Zheng *et al*., during a lipidomic screening of cultured cells treated with fenretinide, an anticancer drug supposed to induce cell death through ceramide-mediated action. After treatment, dhCers levels increased, whereas the expected increase of ceramide was not observed [238].

In 2013 Brozizick *et al*. [239] revealed that monkeys under a long period of HFD showed increased plasma levels of Cer and dhCer, exacerbated when animals developed diabetes. In 2013, Lopez *et al*. [240] discovered that, among dhCers, only C24:1 were increased in plasma of obese children and adolescent females with T2DM. Mamtani *et al*. [241] performing an analysis of the human lipidomic profile, discovered in Mexican Americans a peculiar association between plasma levels of dhCers 18:0, 20:0, 22:0 and 24:1 and

waist circumference. Bergman *et al*. [242] investigating the effects of exercise in relation to the sphingolipid metabolism in human subjects, linked dhCer and insulin resistance and found that total dhCer together with C16:0 ceramide and C18:0 sphingomyelin were higher in T2DM subjects and positively correlated with insulin resistance. More recently, a work by Wigger and colleagues [243] identified a specific group of sphingolipids that correlate with glucose intolerance and insulin secretion in mice. Notably, dhCer C22:0 could be used in humans as biomarkers of T2DM disease progression. Several studies described correlations among insulin and obesity, metabolic parameters and dhCers linking them to the development of metabolic disorders, although the pathophysiological mechanisms associated with these molecules are still unknown [244].

Most of the studies in the context of dhCer alterations rely on Des1, the enzyme that introduces the double bond in dhCers producing Cers. Mice Des1−/− resulted in an incomplete penetrance lethality phenotype characterized by increased levels of dhCer and decreased levels of Cer [245].

Another study [246] described the increment of arterial ceramide-induced by HFD in Des1+/+ but not in Des1+/− mice, although Des1+/− HFD animals developed a severe increase of fat mass, decreased lean mass and impaired glucose tolerance than Des1+/+. Nevertheless, Des1+/- mice from [246], develop a more severe metabolic alteration compared to Des1+/- mice, described by Holland and colleagues [245]. Both papers pointed out that the causative role for the metabolic alterations leading to insulin resistance and vascular dysfunction has to be ascribed to the rate of conversion of dhCer to Cer more than dhCer itself.

Conversely, Barbarroja *et al*. [247], indicated that, both *in vivo* and *in vitro* Des1 reduction, impairs adipogenesis and lipogenesis, and that adipocyte treatment with dhCers resulted in metabolic dysregulation.

It can be concluded that Des1 is a crucial enzyme in sphingolipid generation, and its activation or impairment is crucial for sphingolipids homeostasis. Nevertheless, it is still not completely clear if its role in metabolic alterations is due to its increment or due to the decrement of its product. Further investigation will be required to precisely define pathophysiological mechanisms regulated by this enzyme, which is pivotal in obesity.

3.6. Sphingomyelins and obesity

Sphingomyelin is one of the most abundant sphingolipids in body fluids and tissues, accounting for 87% of total plasma sphingolipids [202]. Correlations have been found among high levels of SMs and cholesterol, coronary artery disease in humans and HFD and insulin sensitivity in mice [216,248,249]. Conversely, in the adipose tissue of *ob/ob* mice, reduced levels of SMs and increased SMases (both neutral and acidic) mRNA expression were observed, and the more significant decrease was observed in long-chain SMs (20:0, 20:1, 22:1, 24:0, 24:1) (Table 2). Interestingly, serum levels of SMs increased in *ob/ob* mice, suggesting an intriguing SLs flux from tissue to body fluids [189]. Norris and colleagues, utilizing a C57BL/6J mice fed with HFD for ten week, found that mice fed with HFD and supplemented with SMs displayed reduced hepatic steatosis, lower cholesterol, lower liver TG accumulation and tissue macrophage infiltration, suggesting that SMs dietary supplementation could ameliorate metabolic complications induced by HFD [250]. The question is if the exogenous sphingomyelin acts differently compared to the endogenous one, or if these differences are related to adopted quantitative methodologies (enzymatic methods and TLC) is still opened.

Localization of SMs plays a vital role in overweight and obesity. Hints on this direction were provided by Mitsutake and colleagues investigating the

sphingomyelin synthase 2 (SMS2) KO mice [251]. These mice exhibited a reduced number of large and mature lipid droplets in the liver, caused by lack of SM and by the association of SMS2 with the fatty acid transporter CD36/FAT and caveolin 1. Also, SMS2 KO mice did not increase their body weight by HFD, suggesting SMS2 as a target to prevent high fat diet-induced obesity and insulin resistance.

Studies on human subjects by Hanamatsu *et al* demonstrated that, in obese, SMs saturated acyl chain (C18:0, 20:0, 22:0, and 24:0) were increased compared to control group and positively correlated with serum biochemical (TC, TG and LDL-C) and insulin resistance parameters (Homeostatic model assessment of insulin resistance (HOMA-IR), AST and ALT) [252].

Recent metabolomic studies identified correlations between lysophosphatidylcholine (LPC) (lysoPC C17:0, 18:1, and 18:2) and obesity, whereas sphingomyelins (C18:1) and dhCers were associated to pre-diabetic insulin state [253].

Bagheri and colleagues, at variance, found a negative association between LPC and obesity (C18:1 and C18:2) in obese Iranian adults without any correlation among SMs and obesity [254].

Hellmuth *et al*. [255], on the other hand, by investigating metabolomics profiles and insulin resistance in European children, found that SMs C32:2 was strongly associated with BMI z-score, whereas the association with HDL and body weight was absent. Recently, Im and colleagues [256] found that SM concentration correlated positively with cholesteryl esters and waist to hip ratio, and that sphingomyelin levels are higher in pre-diabetic men with abdominal obesity.

The effects of SMs in obesity or the obesity-induced generation of SMs are slightly disregarded compared to Cers, even though their levels in obesity or HFD increased in serum [189], liver [215], adipose tissue [216]

erythrocyte and heart [257]. Altogether these studies suggest that sphingomyelin and its different acyl chains can play a causative effect in the onset and development of obesity. However, results are, to some extent, contradictory. To define the precise role of SMs in obesity will require a strict control of sampling, the use of defined standards and the identification of standardized analytical procedure to overcome the lack of reproducibility that in sphingolipid research remain a central node.

3.7. S1P and obesity

Sphingosine is produced by ceramide breakdown, and the sphingosine-1-phosphate represents its phosphorylated counterpart. Both molecules are key signaling bioactive elements in liver [258], muscle [259], blood [260], and adipose tissue [261]. Despite their consistent signaling activities, studies investigating their role in obesity are limited compared to other SLs.
Kowalsky and colleagues [262] investigated S1P plasma levels by a commercially available ELISA, indicating an increase of S1P in mice characterized by genetically and HFD induced obesity. The study was extended to humans identifying a positive correlation among S1P and BMI, total body fat percentage and HOMA-IR. Notably, S1P levels increased in mice after 12 h fasting, suggesting that the S1P pool is quickly modified and S1P can exert potentially positive effects contributing to recovery/surviving of pancreatic B-cells during the compensatory hyperinsulinemia status in insulin-resistant and obese subjects.
Revising the literature, studies on human subjects as well as on animal models provided different results even by using the same quantitative methodology. Majumdar *et al*. described no differences in S1P levels in obese adolescents [232], whereas Ito *et al*. [263] confirmed the S1P increase in obese in line with Kowalsky.

The S1P increment in mice was confirmed by Fayyaz [264], which identified increased levels of hepatic S1P in HFD fed New Zealand obese mice. An increase in S1P was also seen in primary culture of rat and human hepatocytes supplemented with palmitate. Furthermore, the S1P increment decreased insulin stimulation of the PI3K/AKT signaling through the sphingosine-1-phosphate receptor 2, proposing a negative regulatory effect of S1P on insulin signaling in hepatocytes. These observations were not confirmed by Kurek *et al*., who identified increased levels of Cers and SMs nor of S1P in the liver of male Wistar rats fed with an HFD, neither after 7-day treatment with myriocin [217].

In a recent paper, the group of Kleuser [265] was able to clarify in-vivo the apparent discrepancy between the pro-survival effect of pancreatic β-cell suggested by Kowalsky and increased hepatocyte insulin resistance mediated by S1P. Analyzing New Zealand obese mice (that develops β-cell loss under HFD), they identified an increase in T2D prevalence, paralleled by increased levels of S1P in plasma. Mice treated with a specific sphingosine-1-phosphate receptor 2 antagonist (JTE-013) by counteracting the binding of S1P. This action induces disruption of insulin signaling and β-cell dysfunction, suggesting that S1P can act on pancreatic β-cell by increasing its levels or by binding to different receptors; thus, it can both lead to a negative or positive outcome.

In 2012, Moon *et al*. [266] identified on C57B/6J mice and 3T3-L1 cells the central role of the sphingosine-1-phosphate analog (FTY720) in the regulation of adipogenesis and lipolysis. This molecule was able to down-regulate adipogenesis and enhance lipolysis, both *in vivo* and *in vitro*, opening a new avenue in the treatment of obesity.

Interestingly, the same group [267] demonstrated that S1P was able to reduce TG accumulation and to inhibit differentiation in 3T3-L1 preadipocytes, resulting in the downregulation of markers of adipogenic

differentiation like peroxisome proliferator activated receptor γ (PPAR γ), CCAAT/enhancer binding protein and adiponectin. Surprisingly, it has been reported that the action of S1P and FTY720 toward the SphK receptor 1 is different, it is based on the recycling of the ligand in the former and degradation in the latter [268].

A positive role for S1P in obesity was also observed by Silva *et al*. [269] that, in 2014, identified the S1P/sphingosine kinase receptor1 axis as a central node in energy homeostasis. S1P intracerebroventricular injection was able to reduce food intake, increasing rat energy expenditure, arising the questions of differences between exogenous and endogenous sphingolipids.

Levels of S1P and sphingosine are finely tuned inside cells, tissue, and in body fluids and are regulated by sphingosine kinases 1-2 (SphK1-2) and sphingosine phosphatases [154]. The administration of exogenous palmitate to C2C12 myotubes was able to increase levels of S1P and activity of SphK1 [211]. Notably, this was not observed when myotubes were treated with oleate, suggesting that Sphk1 is activated in the presence of palmitate, only. In 2013, the same group was able to dissect the mechanism through which palmitate was able to induce SphK1 increase in muscle [270]. Sphk1 overexpression was linked to the interaction between peroxisome proliferator-activated receptor-α (PPAR-α) and SphK1 promoter. However, it remains unclarified if SphK promoter induction was in response to direct PPAR-α interaction or due to PPAR-α downstream signaling.

In 2018 Nagahashi *et al*. [271], investigating the link among obesity, inflammation and cancer, confirmed that in breast cancer patients and animal models the HFD alone was able to induce the axis SphK1/S1P/S1PR1 and to stimulate in obesity a cancer-associated pro-inflammatory cytokines (IL-6 and TNF-α). Treatment with FTY720 was able

to reduce activation of the S1P axis and levels of cytokines, resulting in prolonged survival of HFD-administered tumor-bearing mice.

Not only SphK1 but also SphK2 contribute to the action of S1P. Notably, SphK2 -/- mice are protected from diet-induced obesity and develop a lean phenotype and improved glucose tolerance [272] and are characterized by a two-fold increase of S1P in plasma suggesting that the inhibition of SphK2 contributes to the maintenance of high levels of S1P, potentially positive in the treatment of obesity. Through these studies, it can be hypothesized that the S1P increase follows two possible mechanisms: upregulation of SphK1, already seen in other animal models lacking SphK2 [273], or inhibition of the SphK2 gene [274,275].

Collectively this data indicate that S1P is an essential player in obesity and obesity-related comorbidities, through its pleiotropic intracellular and extracellular activities target different pathways, even if its role remains so far unclear. The outcomes of S1P increment is at variance in human and animal models, being protective in obese subjects and detrimental in animal models leaving opened the question in obesity if animal models can recapitulate the human conditions.

4. AIM OF THE STUDY

The World Health Organization defines obesity as abnormal or excessive deposition of fat that contribute to put your health at risk [276]. This frequent status is not due to food intake only, but other contributing factors like genetic background, inactivity and hypercaloric food intake [3–5] play a role.

This condition is also associated with vitamin D deficiency involved in obesity-associated morbidities [6]. Two recent studies assessing serum proteomic alterations in obese Saudi Arabian Vit. D deficient subjects identified differentially expressed proteins related to Vit. D function, inflammation/immunity and lipid metabolism [277,278]. Along with Vit. D deficiency, a peculiar class of lipids called sphingolipids have been identified as contributors to the chronic low-grade inflammation status [10,11] observed in obese subjects and also in obesity-associated comorbidities [12–14]. Sphingolipids metabolism is profoundly interconnected with inflammation, the increase in pro-inflammatory cytokines (IL-6, TNF-a) observed in obese subjects, results in the activation of sphingomyelinases (SMases), both directly and via toll-like Receptor-4 (TLR-4), [279] that hydrolyzes SMs to Cers. Furthermore, increased plasma free fatty acids levels of obese subjects, stimulate Cers *de novo* biosynthesis by providing increased substrate for serin-palmitoyl transferase (SPT) [280].

SLs levels are pretty well described in tissues, but a precise knowledge of their flux in biological fluids and their relative effect over different target tissues is still lacking. Recent data show that SLs travel in body fluids mainly in association with albumin, low-density lipoprotein-cholesterol (LDL-C), very low-density lipoprotein cholesterol (VLDL-C) and high-density lipoprotein cholesterol (HDL-C) particles; and that the level of different SLs

associated to a particular lipoprotein correlate with obesity-related comorbidities as, the increased risk of developing non-alcoholic fatty liver disease (NAFLD) or the increase in cardiovascular risk [186,281].

This study approached the role of sphingolipids in obesity, assessing sphingolipids flux in biological fluids in the presence of Vit. D deficiency and dyslipidemia. The general aim of this study was to precisely characterize SLs profiles in two different population. The first, from Saudi Arabia, was defined by a high prevalence of obesity, Vit. D deficiency and dyslipidemia, while the latter, from the Andean region of Argentina, was characterized by a low prevalence of obesity but high levels of Vit D. deficiency and dyslipidemia.

The aim of the first study was to analyze SLs profiles of normal-weight subjects in presence/absence of dyslipidemia to decipher the contribution of dyslipidemia on SLs profiles and furthermore to assess SLs profiles in Vit. D deficient dyslipidemic obese and lean subjects to identify SLs patterns not related to dyslipidemia, therefore potentially attributable to weight gain. The second study was aimed at profiling sphingolipids in groups characterized by different BMIs but similar Vit D. deficiency and dyslipidemic traits, in order to provide a molecular signature not only of obesity but also of possible different phenotype adaptation to high altitude hypoxia.

5. MATERIALS AND METHODS

5.1. Participants and Sample Collection (Arabian subjects)

Men and women adult Saudis were enrolled from the Vitamin D School Project Database of the Prince Mutaib Chair for Biomarkers of Osteoporosis, College of Science, King Saud University, Riyadh, Kingdom of Saudi Arabia [282]. The study was approved by the Ethics Committee of the College of Science, King Saud University in Riyadh, Saudi Arabia (Ref No. 15/0502/IRB). Enrolled subjects provided their full informed consent. All subjects were grouped according to the BMI into normal weight (BMI <25kg/m^2) and obese (BMI ≥30kg/m^2). Serum samples were collected from 23 normolipidemic normal weight (NWNL) controls, 46 vitamin D deficient dyslipidemic (HDL-C <40 mg/dL; TG >200mg/dL) normal weight (NWDL) and from 60 vitamin D deficient obese (ODL) subjects, and stored at -80°C until use. Adult Saudis parameters for: age, gender, weight (Kg), height (Cm), BMI, total cholesterol (mg/dL), HDL-C (mg/dL), LDL-C (mg/dL) and Vitamin D (ng/mL) can be found in Table 4. BMI was calculated as weight (Kg) divided by height squared (m). TC, HDL–C, and TG were obtained using a chemical analyzer (Konelab, Espoo, Finland), while LDL-C levels were calculated using the Friedewald's formula. Vit. D levels were obtained by electrochemiluminescence immunoassay on Roche Elecsys Cobas e411 analyzer (Roche Diagnostics, GmbH, Mannheim, Germany).

5.2. Participants and Sample Collection (Andean subjects)

Fifty-nine children (age 5–13 years) from San Antonio de Los Cobres (3775 m a.s.l.), who were previously enrolled [283], were classified as UW (<5th percentile), NW (5th to < 85th percentile), OW (85th to < 95th percentile), or O (≥95th percentile) on the basis of their body mass percentiles, accordingly to the US Centers for Disease Control and Prevention (CDC) norms [29]. Children's anthropometry—age, gender, weight (kg) and height (cm)—are indicated in Table 6. TC (mg/dL), HDL-C (mg/dL), LDL-C (mg/dL), Vit. D, ng/mL), fasting glucose (Glycaemia, mg/dL), fasting insulin (Insulin, µU/mL), and triglycerides TG, mg/dL) were assessed, while BMI, TC/HDL-C ratio, and HOMA-IR were calculated as follows: BMI was calculated as weight (kg) divided by height squared (m); TC/HDL-C ratio was calculated as TC(mg/dL)/HDL-C(mg/dL); while HOMA-IR was calculated as Glycaemia (mg/dL) × Insulin/405. Blood samples were collected after 10-h fasting. Fasting glucose was measured by glucose oxidase, while serum lipids were assessed with Architect c 16000 instrument (Toshiba, Kanagawa, Japan). Chemiluminescent was utilized for the detection of fasting insulin levels and serum Vitamin D (Abbott Laboratories, Chicago, IL, USA).

The study was carried out following the rules of the Declaration of Helsinki and was approved by the Human Rights Committee of the Salta Health Ministry (project number: 4518; date of approval: 8 November 2010). Each caregiver and child gave written informed consent after an explanation of the study and before its initiation.

5.3. Reagents and Chemicals

Methanol, Propan-2-one, 1-butanol LC-MS grade water, 3,5-Di-tert-4-butylhydroxytoluene (BHT), primuline yellow dye, and ammonium formate were from Sigma-Aldrich (Saint Louis, MO, USA). Ethanol and HPLC analytical grade chloroform were, respectively, from J.T. Baker (Center Valley, PA, USA) and Carlo Erba (Cornaredo, MI, Italy). Potassium hydroxide was from Merk Millipore (Burlington, Massachusetts, USA). Acetic and formic acid were from Fluka-Analytical (Honeywell, Morris Plains, NJ, USA). N-lignoceroyl-D-erythro-sphingosine (Cer C24:0) 1,2-Dipalmitoyl-sn-Glycero-3-Phosphocholine (DPPC), Cardiolipin (CL), 1,2-Dipalmitoyl-sn-Glycero-3-Phosphoethanolamine (DPPE), D-glucosyl-ß-1,1'-N-stearoyl-D-erythro-sphingosine-d5 (GlcCer), N-lauroyl-D-erythro-sphingosine , N-lauroyl-D-erythro-sphinganine, N-lauroyl-D-erythro-sphingosylphosphorylcholine N-lauroyl-D-erythro-sphinganylphosphorylcholine, D-glucosyl-ß-1,1'-N-lauroyl-D-erythro-sphingosine, D-lactosyl-ß-1,1' N-lauroyl-D-erythro-sphingosine and C17 d-erythro-dihydrosphingosine-1-phosphate lipids standards. Sphinganine (d17:0), sphinganine-1-phosphate (d17:0), C12 Ceramide, Sphingomyelin (d18:1/12:0), Glucosyl (β) C12 Ceramide, d-31 phosphatidylcholine, Lyso-phosphatidylcholine (C17:0), d-31 phosphatidylethanolamine, d5-diglyceride (17:0/17:0), d5-triglyceride (17:0/17:0/17:0) and cholesteryl ester (17:0) were from were from Avanti Polar Lipids (Alabaster, AL, USA). Sphingolipids standard mixture containing Sphingomyelin (SM) and Sulfatides (SLF) was from Matreya LLC (Pleasant Gap, PA, USA).

5.4. HPTLC-profiling (Arabian subjects)

5.4.1. HPTLC lipid Extraction

Serum samples from 129 adult subjects were analyzed. Briefly, serum aliquots of 100µL were mixed with 1 ml of methanol/butanol 1:1 (v/v) containing ammonium formate 5mM. Mixtures were vortexed for 10 seconds, sonicated for 1 hour in a sonic water bath (20°C) and centrifuged for 10 minutes at 16000g (20°C). Liquid phases were collected and transferred in borosilicate glass vials with Teflon-lined caps (VWR, Radnor, PA) and, after nitrogen-flux drying, re-suspended in 150µL of chloroform/methanol 2:1 (v/v) containing BHT 0.01% (w/v) and stored at -20°C.

5.4.2. HPTLC-Primuline profiling

Aluminium backed HPTLC silica plates 200x100mm (Merck, Billerica, Massachusetts), were washed in chloroform/methanol 1:1 (v/v), and dried at 120°C for 20 minutes. A volume corresponding to 100µg of total protein was loaded in duplicate on HPTLC plates using Linomat 5 semiautomatic TLC spotter (CAMAG, Switzerland) (lane width: 6 mm, dosage speed: 150nL/s). Two different standard mixtures were loaded on HPTLC plates' lateral edges. The first mixture consisted of SM, SLF, GlcCer, and C24:0 standards; the second one was made of CL, DPPE, and DPPC.

Loaded HPTLC plates were developed in a solution of chloroform/methanol/water 55:20:3 (v/v/v), using Camag Automatic Developing Chamber 2 (CAMAG, Switzerland). Developed plates were sprayed with a solution of primuline yellow dye, 5mg/100ml in propan-2-one/water 80:20 (v/v). Images were acquired using Ettan DIGE Imager (GE Healthcare, Chicago, IL, USA). Imager settings were: pixel size 100µm, excitation filter 480/30, emission filter 592/25. Acquired images were

analyzed using ImageQuant software v.8.1 (GE Healthcare, Chicago, IL, USA).

5.5. UPLC-MS/MS (Arabian and Andean subjects)

5.5.1. UPLC-MS Sphingolipid Extraction

Sphingolipids were extracted from sera, following minor modification, according to a previous study [284]. 0.1 mL of serum was mixed with 0.1 mL of ultrapure water and 1.5 mL of methanol/chloroform 2:1 (0.01% BHT), fortified with internal standards 200 pmol: Sphinganine (d17:0), sphinganine-1-phosphate (d17:0), C12 Ceramide (d18:1/12:0), C12 Sphingomyelin (d18:1/12:0), and Glucosyl (β) C12 Ceramide. After a brief sonication, samples were heated at 48 °C overnight. 0.15 mL of KOH 1 M in methanol was added, and after 2-h incubation at 37 °C, the solution was neutralized with 0.15 mL of acetic acid 1 M and dried. After resuspension in 0.5 mL of methanol, solutions were transferred to a clean Eppendorf tube. Samples were dried again, resuspended in 0.15 mL of methanol, and centrifuged for 3 min at 10,000 *g*. Liquid phases were collected in UPLC glass vials and stored at −80 °C.

5.5.2. UPLC-MS quantification

For sphingolipid analysis of Saudi Arabian subjects, 72 sera were randomly sub-pooled into 24 pools (8sub-pool for NWNL, 8 for NWDL and 8 for ODL). The pooling was adopted as a method to reduce the variance among biological groups increasing the power to detect changes when few samples are available, and the variance is high [285,286].

The sphingolipid analyses of Andean subjects were conducted on 59 sera samples.

Liquid chromatography-mass spectrometer configuration included a Waters Acquity UPLC system linked to a Waters LCT Premier Orthogonal Accelerated Time of Flight Mass Spectrometer (Waters, Millford, MA, USA).

The instrument operated in positive or negative electrospray ionization mode. Full scans were obtained in a window, ranging from 50 to 1500 Da. Accuracy and reproducibility were maintained employing an independent reference spray via LockSpray. First, 10 µL of sphingolipid extract were injected and separated on an analytical column, kept at 30 °C, 100 mm × 2.1 mm id, 1.7 µm C8 Acquity UPLC BEH (Waters), using the following linear gradient: 0.0 min: 80% B; 3 min: 90% B; 6 min: 90% B; 15 min: 99% B; 18 min: 99% B; 20 min: 80% B, at 0.3 mL/min flow rate. Phase B consisted of 1 mM ammonium formate in methanol, 0.05 mM formic acid, while phase A was 2 mM ammonium formate in H_2O, with 0.05 mM formic acid. Sphingolipids quantification was carried out using the ion chromatogram obtained for each compound using 50 mDa windows. The linear dynamic range was determined by injection of standard mixtures. Identification of compounds was based on the accurate mass measurement, with an error <5 ppm and its retention time, compared to that of a standard (± 2%). Mass spectra were analyzed by MassLynx™ 4.1 Software (Waters, Millford, MA, USA), and lipids were annotated as lipid subclasses as follows (sphingosine backbone/number of carbon atoms of the fatty acid: number of unsaturation of the fatty acid). A paragraph explaining which sphingolipid species were identified and quantified and the single lipid species added to obtain total class levels can be found in supplementary file 1.

5.5.3. MRM Analysis

S1P was quantified in 59 specimens from Andean subjects and on 24 pool from Saudi Arabian subjects using a Xevo TQ-MS mass spectrometer (Waters, Millford, MA, USA). Briefly, 10 µl of sphingolipid extracts were injected and separated on an analytical column, kept at 30 °C, 100 mm × 2.1 mm id, 1.7 µm C8 Acquity UPLC BEH (Waters). The following gradient was used: 0.0 min: 80% B; 3 min: 90% B; 6 min: 90% B; 9 min: 99% B; 12

min: 99% B; 14 min: 80% B, at 0.3 mL/min flow rate. Phase B consisted of 1 mM ammonium formate in methanol, 0.05 mM formic acid, while phase A was 2 mM ammonium formate in H_2O, with 0.05 mM formic acid. An electrospray interface operating in positive ion mode was employed to obtain MS/MS spectra by acquiring MRM transitions of: C17 sphinganine-1-phosphate, 368.4–252.4, collision energy 18 eV; Sph 300.4-264.4 Da, collision energy 16eV; dhS1P, 382.4- 284.4, collision energy 16 eV and S1P, 380.4–264.4 Da, collision energy 16 eV. Mass spectra were analyzed by MassLynx™ 4.1 Software.

5.6. Statistical Analysis

5.6.1. Arabian subjects

Participants were grouped according to sex, obesity, and dyslipidemia status, and their characteristics were described using median and interquartile range, if continuous, and percentages, if categorical. Comparison of biochemical parameters like age, weight, height, BMI, TC, HDL-C, LDL-C, Vitamin D, and TG were investigated between groups using One way ANOVA with Bonferroni's correction if data were normally distributed, otherwise the Kruskal-Wallis' with Dunn's correction was adopted. Circulating levels of Cers and SMs were transformed as logarithm and were compared by sex, weight group and dyslipidemia status using a generalized linear model (GLM) adjusted for BMI and age. Retro transformed least-square means from the GLM models were reported along with their standard errors, and comparisons were performed using the Tukey adjustment to control for inequalities of group size [287]. All statistical analyses were performed using the SAS software version 9.4, SigmaPlot software version 12.0, and Prism software version 7.0.

5.6.2. Andean subjects

Participants were grouped according to their BMI percentiles, and their characteristics were described using median and interquartile range (if continuous) or counts and percentages (if categorical). Comparison biochemical parameters like age, weight, height, BMI, TC, HDL-C, CT/HDL, LDL-C, Vitamin D, glycaemia, HOMA-IR, insulin, and TG were investigated between groups using One way ANOVA with Bonferroni's correction if data were normally distributed, otherwise the Kruskal-Wallis' with Dunn's correction was adopted. Correlation tables for sphingolipids and biochemical parameters were obtained using Pearson's or Spearman's correlation, when data were parametrically or not distributed, respectively. Differences in Cers, dhCers, SMs, dhSMs, HexCers, diHexCers, and S1P from LC-MS and LC-MS/MS quantitative data were assessed among groups. Statistical analyses were performed using SigmaPlot software version 12.0 and Prism software version 7.0.

6. RESULTS AND DISCUSSION

6.1. Arabian Subjects

6.1.1. Biochemical and anthropometric results

Obesity and overweight prevalence in Saudi Arabia is increasing at an alarming rate. The last report from the WHO indicates that 44% of women and 28% of men are obese but also, that 71% of women and 66% of men are overweight [288], these data are confirmed by [289] and [290]. Furthermore, dyslipidemia represents also a significant health problem independently from BMI. A study by Al-Nozha MM and colleagues in a cohort of 16,819 patients identified hypercholesterolemia in 54% and hypertriglyceridemia in 40.3% of adult subjects, independently from their urban/rural origin [291]. These data were further confirmed by a more recent work by Hamam [292] that found an overall prevalence of dyslipidemia (around 60%) in a smaller group of University students and by Al-Kaabba *et al*. [293] that identified a prevalence of 44% for hypertriglyceridemia in a cohort of 4490 subjects [293]. Surprisingly, Vitamin D deficiency is another health concern, with reports indicating a prevalence of over 60% in the general population [294] and around 80% considering age and BMI [295]. Anthropometrical and biochemical data from 129 subjects enrolled in this study are summarized in Table 4. NWDL subjects were characterized by mean levels of LDL-C and TG classified as borderline or high, ODL subjects showed high levels of TG and slightly lower LDL-C levels compared to NWDL [296]. Conversely, NWNL subjects were characterized by acceptable mean levels of LDL-C and TG. Regarding HDL-C, NWNL subjects showed ideal levels, while ODL and NWDL showed levels lower than 40 mg/dL [297]. TC levels were borderline for both ODL and NWDL [297]. Levels of vitamin D, assessed in NWDL and

ODL groups, were low, being lower than the recommended level of 30ng/mL [298], whereas NWNL subjects had normal levels of vitamin D.

Table 4. Saudi Arabian subjects assessment of anthropometrical and biochemical parameters. Data are described by median and interquartile range (if continuous) or counts and percentages (if categorical).

	NWNL	NWDL	ODL
N.	23	46	60
Age	39 (33/46)	45 (32/55)	42 (35/49)
Weight (Kg)	68 (60/73)	64 (60/68)	98 (91/107)
Height (Cm)	171 (168/177)	162 (159/167)	160 (154/165)
BMI	23 (21/23)	24 (23/25)	38 (36/41)
SEX (% of females)	34.7	50	58.3
TC (mg/dL)	172 (163/184)	208 (180/235)	209 (183/230)
HDL-C(mg/dL)	64 (56/69)	25 (21/31)	29 (26/32)
LDL-C (mg/dL)	97 (82/108)	149 (123/173)	125 (90/138)
Vit. D (ng/mL)	30 (26/34)	12 (7/15)	12 (9/16)
TG(mg/dL)	69 (63/111)	302 (265/359)	267 (243/303)

The prevalence of obesity, Vit. D deficiency and dyslipidemia in subjects enrolled in this study was 46%, 82%, and 82%, respectively. Therefore the analyzed groups show a prevalence consistent with Saudi Arabian general population for obesity and Vit. D deficiency. Conversely, the investigated subjects showed a higher rate of dyslipidemia (82% vs. 60% in Saudi Arabia) compared to Saudi Arabian general population. This study was focused on blood sphingolipids profiling to identify putative biomarkers to be used in clinical practice to reduce the risk of developing obesity-associated morbidities.

Differences between groups obtained from comparison of anthropometry and biochemical parameters are summarized in Table 5, while p-value from ANOVA one-way can be found in supplementary table 1.

NWNL, NWDL and O group were homogeneous for age distribution, having a median between 39 and 45 years. The weight showed no statistically

significant differences between NWNL and NWDL, whereas ODL had higher BMI compared to NWNL and NWDL groups (p-value< 0.001 in both comparisons).

NWLN group had a higher mean height than NWDL and ODL groups (p-value< 0.001 in both comparisons). No difference was observed between NWNL and NWDL in BMI values, while both groups were statistically significantly different from ODL (p-value< 0.001 in both comparisons). Total cholesterol was higher in ODL and NWDL compared to NWNL (p-value< 0.01 and p-value< 0.001 respectively). Furthermore, HDL-C levels were statistically significantly higher in NWNL than in ODL and NWDL (p-value< 0.001 in both comparisons). NWDL showed high levels of LDL-C, higher than NWNL and ODL (p-value 0.001 in both comparisons), whereas ODL showed higher levels of LDL-C compared to NWNL (p-value< 0.01). TG levels were high in NWDL and ODL compared to NWNL (p-value< 0.001 in both comparisons)

Table 5. Anthropometry and biochemical parameters comparison between different BMI/lipidic profile groups. One-way ANOVA with Bonferroni's correction was employed if data were normally distributed, otherwise Kruskal-Wallis' with Dunn's correction was adopted. (*p-value < 0.05, **p-value < 0.01, ***p-value < 0.001)**.**

	NWNL vs. NWDL	NWNL vs. ODL	NWDL vs. ODL
Age			
Weight (Kg)		↑ ODL***	↑ ODL***
Height (Cm)	↑ NWNL***	↑ NWNL***	
BMI		↑ ODL***	↑ ODL***
TC (mg/dL)	↑ NWDL***	↑ ODL**	
HDL-C (mg/dL)	↓ NWDL***	↓ ODL***	
LDL-C (mg/dL)	↑ NWDL***	↑ ODL**	↑ NWDL***
Vit. D (ng/mL)	↓ NWDL***	↓ ODL***	
TG (mg/dL)	↑ NWDL***	↑ ODL***	

Results from anthropometrical and biochemical comparison among BMI/lipemia pointed out differences in weight and lipid composition,

clustering subjects in three different groups. Specifically, NWNL group was characterized by statistically significant differences in Vit. D, lipid profile and BMI compared to ODL. Conversely, NWDL and ODL were characterized by similar Vit. D deficiency and lipid composition, being divided only by their BMIs. No other parameters, except for height, were found to be at variance between groups, resulting in the absence of confounding biochemical/anthropometrical factors that could influence this investigation. These comparisons demonstrate that the three groups can be effectively clustered and that the comparison with their sphingolipidic profiles can be possible.

6.1.2. Variations in sphingolipid profiles

Circulating ceramide and sphingomyelin levels, from normolipidemic normal-weight individuals, were compared to dyslipidemic, vitamin D deficient, normal-weight or obese subjects, in order to identify variation in sphingolipid profiles.

HPTLC-primuline profiling was the first technique of choice to semi-quantify SMs and Cers levels in our samples. Sphingolipid, obtained from 23 NWNL (15 men and 8 women) control subjects, 46 NWDL (23 men and 23 women) and 60 ODL (25 men and 35 women) were extracted from sera, and the sphingolipid species were separated by HPTLC. After primuline staining, HPTLC-densitometry and FDIC (fluorescence detection by intensity changes) emission, detected SLs bands generating SLs profiles (supplementary figure 1).

HPTLC-primuline profiling revealed six different bands in the HPTLC plate, but only bands corresponding to Cers and SMs could be identified by Rf comparison with standards. Both ceramides and SMs showed a clear separation in two distinct bands over the HPTLC plate. Bands showing Rf=0.176, Rf=0.152, Rf=0.923 and Rf=0.858, were attributed to SMs (C20-C24), SMs (C14-C18), Cers (C20-C24) and Cers (C14-C18).

Results for Cers and SMs from HPTLC/primuline profiles comparisons and LC-MS data can be found in Figure 2.

The LC-MS analysis was performed to precisely quantify variation over different acyl chain. The analysis was conducted on 8 sub-pools per group. The primuline profiling indicated a Cer C14-C18 decrease in NWNL compared to NWDL and ODL (p-value< 0.001 in both comparisons) (Figure 2 A). Conversely, “short-chain” SMs (C14-18) were higher in NWNL subject compared to NWDL and ODL groups (p-value<0.001 in both comparisons) (Figure 2 C). Non-statistically significant results from Cers (C20-C24) and SMs (C20-C24) are reported in Supplementary figure 2. Long-chain SMs and cers from HPTLC-Primuline profiling did not provide significant results; nevertheless, the statistically significant trend identified for short chains (C14-18) was confirmed for long chains (C20-24), both SMs and cers (supplementary Figure 2).

Figure 2. A: HPTLC/primuline profiling of Cers C14-C18 in sera of NWNL (n=23), NWDL (n=46) and ODL (n=60) subjects. B: LC-MS analysis of total Cers and dhCers in sub-pooled sera from NWNL, NWDL and ODL subjects. C: HPTLC/densitometry profiling of SMs C14-C18 in sera of NWNL (n=23), NWDL (n=46) and ODL (n=60) subjects. D: LC-MS analysis of total SMs and dhSMs in sub-pooled sera from NWNL, NWDL and ODL subjects. Tukey's correction was employed after one-way ANOVA statistical analysis. Data are expressed in log scale and reported as mean ± SD. (*p-value < 0.05, **p-value < 0.01, ***p-value < 0.001).

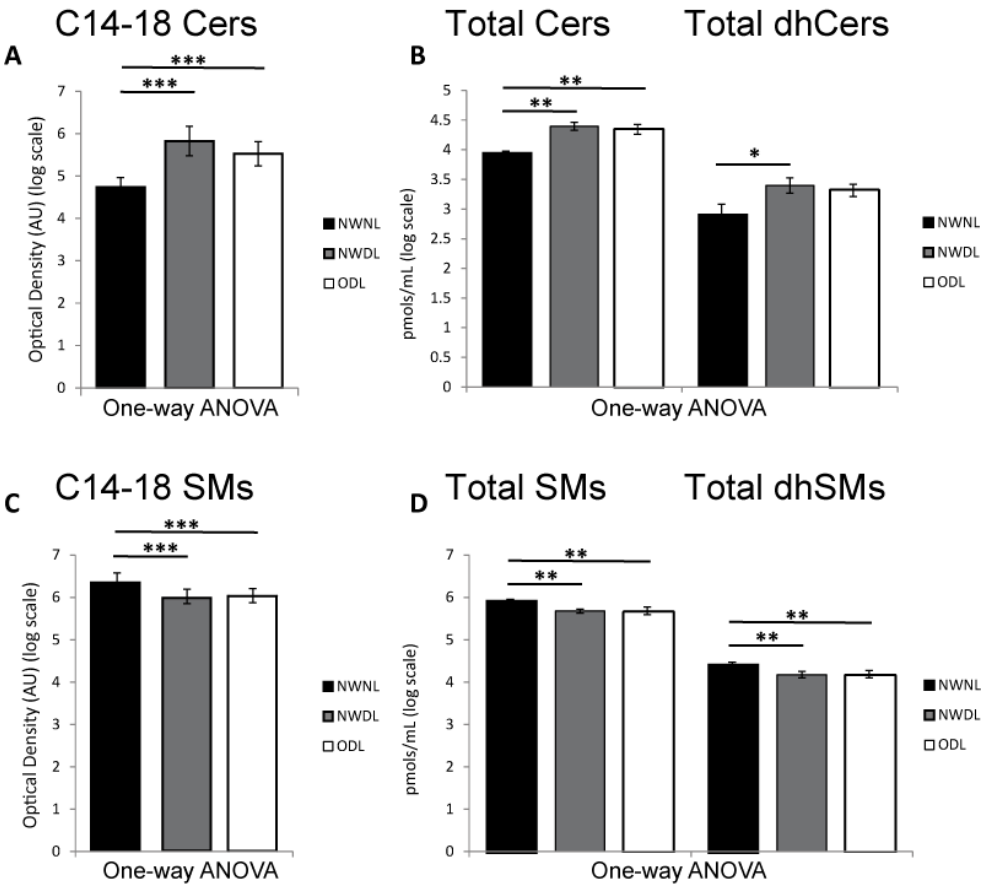

LC-MS data confirmed variation highlighted by primuline profiling, in particular, total levels of Ceramide were found to be increased in NWDL and ODL subjects compared to NWNL (Figure 2B) and furthermore specific acyl chain C16:0, C20:0, C22:0, C22:1, C24:0, C24:1, and C24:2 were also found increased in the same comparison by LC-MS (supplementary figure 3A and B). The analysis of sphingolipid profiles using two different

techniques allowed us to validate our results, being the adopted technique independent. HPTLC primuline profiling and LC-MS provided similar results for cers SMs and dhSMs. It should be noted that HPTLC-primuline profiling is a semi-quantitative method, while LC-MS is a precise quantification tool, so the latter is commonly preferred for quantifying sphingolipids [171,172]. Nevertheless, the results presented here show high levels of similarity between the two techniques, suggesting that the inexpensive HPTLC-primuline profiling method could be adopted routinely for profiling and semi-quantify sphingolipids in sera. NWDL and ODL comparison was otherwise characterized by the decrease of Cer C20:0, C24:1 and C24:2 in the ODL group. Total dhCers were found to be increased in the NWDL group only compared to NWNL, and a precise quantification of the acyl chain revealed that dhCer C16:0, C18:0, C20:0 and C22:0 had the same statistically significant trend. Moreover, acyl chain C18:0, C20:0 and C22:0 of dhCer were also found to be increased in ODL compared to NWNL (supplementary figure 3 C and D).

Regarding Sphingomyelins, the trend compared to Cers was reversed. NWNL showed higher levels of SMs (C14-18) (Figure 2 C) compared to NWDL and ODL (p-value< 0.001 in both comparisons) and also total dhSMs were decreased in NWDL and ODL (Figure 2 D). More specifically, SMs acyl chains C16:0, C16:1, C18:0, C18:1, C20:1, C22:1 (Supplementary figure 3 E and F) and dhSMs C14:0 and 16:0 (Supplementary figure 3 G and H) were decreased in NWDL and ODL groups.

The increase in cers and the decrease in SMs observed in ODL subjects could be the result of *de novo* SLs synthesis activation and of sphingomyelinase pathway. Ceramide generation, during HFD-induced obesity, is stimulated by the continuous and excessive supply of FFA from diet and adipose tissue, providing substrate for SPT and cerS(1-6)

[211,299], resulting in increased levels of plasmatic cers during obesity. The increased dhCer levels similar to Cers, in ODL subjects compared to NWNL further confirms the idea that *de novo* synthesis was altered in the obese group.

In animal models, HFD administration stimulates the expression and the activity of both aSMase and nSMAse [215,225], while the pharmacological inhibition of aSMase by amitriptyline reduces HFD-stimulated ceramide release in blood [230], suggesting activation of the sphingomyelinase pathway during HFD-induced obesity.

Regarding specific acyl chains influenced by obesity, we found peculiar chains of Cers, namely Cers C20:0 and C24:2 decreased in obese men compared to NWDL men, while cer C24:1 was decreased in ODL women compared to NWDL women (Supplementary Figure 3 A and B). Other chains were directly influenced by obesity in ODL men like dhSM C18:0, which was found increased compared to NWDL men (Supplementary Figure 3 G). In ODL women SM C16:0 was increased compared to NWDL women (Supplementary Figure 3 F). The fact that specific acyl chains of Cers were found at variance in obesity, rather than the total Cers, highlights the role of different Cer synthase isoforms in the regulation of SLs production during obesity.

Little is known regarding SLs behavior during dyslipidemia and Vit. D deficiency. In plasma, sphingolipids, thanks to their hydrophilicity, circulate, bound to albumin and lipoproteins [186]. Particularly, cers are present and equally distributed in HDL-C, LDL-C and VLDL-C [202], while SMs travels for the 70% on LDL/VLDL-C and the 30% in HDL-C [202]. Interestingly, NWDL showed higher levels of total cers, dhCers and lower levels of SMs and dhSMs, compared to NWNL. Previous studies compared sphingolipids abundance in the obese group and lean healthy [231,262,300] or lean

normoglycemic [232] controls, without taking into account dyslipidemia as a confounding parameter.

The increase of Cers and the decrease if SMs in obese subjects are well documented and the pathomechanisms almost known [301,302]. Our work confirms these data in obese subjects and expands the knowledge on sphingolipid profiling, suggesting that NWDL subjects, presenting Vit. D deficiency and dyslipidemia independently from obesity develop a sphingolipid plasma profile that is profoundly influenced by lipemia with dysregulated LDL-C, HDL-C and TG.

It is possible to speculate that normal-weight subjects, presenting Vit. D deficiency and dyslipidemia, develop altered plasma SLs profiles because of the differential “transport” capacity of lipoprotein in their plasma, while the alterations observed during obesity are related to changes in SLs biosynthesis (e.g., *de novo* biosynthesis and sphingomyelinase pathway).

6.1.3. Sphingolipid profiles and sex-related variations

The study of obesity have to consider differences characterizing men and women, resulting not only in different phenotypes but also in a different risk for obesity-associated co-morbidities. Sexual dimorphism in body fat composition and distribution is not visible at infancy, starts at puberty and become present in adulthood [303]. These differences are so clear that results in the identification of different body shapes associated to gender, producing an android shape in men, characterized by accumulation of body mass above the waist [304], and a gynoid shape in women associated to a higher percentage of body mass below the waist [305]. In this context, women tend to accumulate more adipose tissue in the gluteofemoral area, whereas men develop mainly abdominal adipose tissue. Sex does not only influence adipose tissue distribution but also its localization; a predominant deposition of subcutaneous fat characterizes women while in men, visceral

fat is preferred [306]. Visceral adipose tissue and subcutaneous accumulation also differ for the type of adipocyte (which can present hyperplasia/hypertrophy) [307]. While in the subcutaneous fat, the hyperplasia is preferred, resulting in a more vascularized, more insulin-sensitive and less inflamed tissue, visceral depots usually develop hypertrophic adipocytes; less vascularized, less effective in TG storage and prone to release inflammatory cytokines [308].

The adipose tissue expansion, type, and localization are central modulators in the development of different metabolic risk between men and women. Subcutaneous adipose tissue is correlated to some extent to a metabolic protection from metabolic syndrome, insulin resistance and CVD, while visceral depots are associated with an increased risk of developing CVD and obesity-related co-morbidities [309].

From primuline profiling of “long chain” Cers and SMs, a trend, suggesting gender-specific differences was seen (Supplementary figure 2).

To understand the impact of sex-related alteration, a direct comparison of the sphingolipid pattern for NWNL, NWDL, and ODL men and women was undertaken. NWNL men showed higher levels of cers C20:0, C24:1, C24:2 (figure 3 A) and of total SMs, C18:0, C20:0, C22:1, and C24:1 (Figure 3B) when compared to NWNL women. Furthermore, NWNL women showed higher C18:0 diHexCer when compared to NWNL men (figure 3 F). On the contrary, in the NWDL group, women were characterized by higher SMs C22:0 when compared to men (Figure 3C). In the ODL comparison, men showed lower SMs C14:1 (Figure 3 D), higher dhSMs C18:0 (Figure 3 E) when compared to women and also lower total HexCer and C16:0 HexCer when compared to women (Figure 3 G)

Figure 3. UPLC-MS analysis of sex-related glyco/sphingolipid alteration in sub-pooled sera samples from NWNL men and women (**A, B** and **F**), NWDL men and women (**C**) and ODL men and women (**D, E,** and **G**).Unpaired t-test was employed. Data are expressed in log scale and reported as mean ± SD. (*p-value < 0.05, **p-value < 0.01, ***p-value < 0.001).

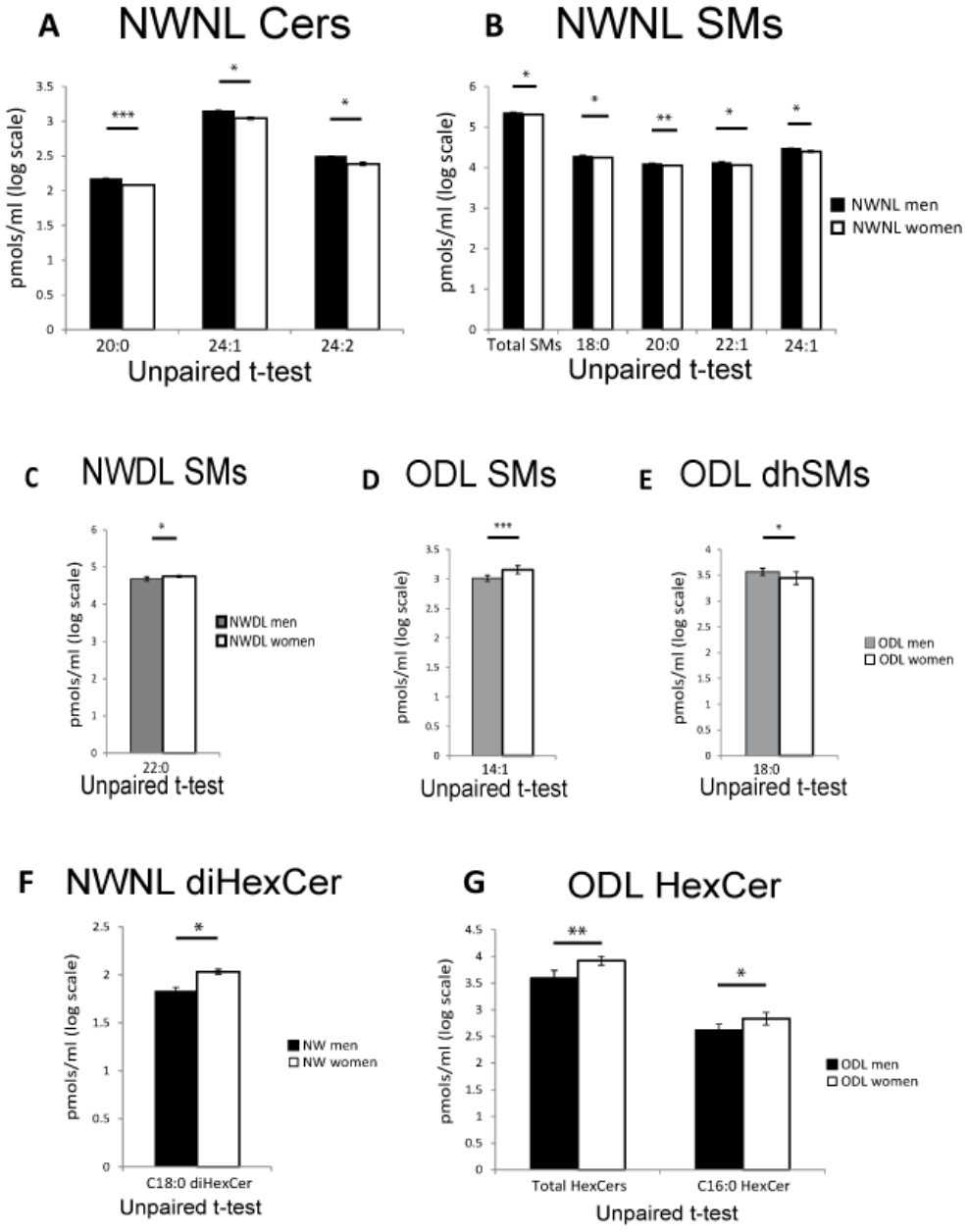

By this study, we were able to acknowledge the influence of gender, in modifying circulating SLs levels, independently from serum lipids and vitamin D status.

Our data highlights the increase in Cer C20:0, C24:1 and C24:2 observed in normolipidemic normal-weight men compared to women; Weir *et al*. partially confirmed these data, in a cohort of 1431 Mexican Americans, where they found increased levels of ceramide C22:0, C24:0 and C24:1 in men compared to women [310], suggesting that an increase in cerS-2 could be responsible for the increase in long-chain ceramides.

In our study, total SMs, SM C18:0, C20:0, C22:1 and C24:1 increased in normolipidemic normal-weight men compared to women, while these data contrast with results published in other studies [311–313] that found higher levels of SMs in women's. We found that in dyslipidemic normal-weight and obese women, the expected increase in SMs [312] was observed, and particularly SM C22:0 and C14:1 were increased compared to dyslipidemic normal-weight and obese men, respectively.

The idea that gender could affect sphingolipid profiles led to further assessment of differences by analyzing different BMI groups, excluding the gender as a confounding factor.

LC-MS data analysis from NWNL, NWDL and ODL men and women can be found in Figure 4. Men did not show particular alterations regarding sphingolipid, except for total diHexCers that were found to be statistically decreased in NWDL and ODL men compared to NW (Figure 4, panel A). On the contrary, women were found to be more subjected to variations in the sphingolipid profile, in fact, total HexCer was found increased in ODL compared to NWDL women (Figure 4, panel B) and more specifically, HexCer C16:0 was increased in NWNL and ODL compared to NWDL while diHexCer C24:1 was decreased in ODL and NWDL when compared to NW.

HexCer levels do not appear to have effects on insulin resistance in skeletal muscle; however, in adipocytes, glucosylceramide-synthase overexpression stimulates the suppression of insulin signaling [314]. The increase in plasma Hexcer levels of obese women compared to NWDL women can, therefore, be related to the overexpression of glucosylceramide-synthase in adipocytes and release of HexCers in the circulation. Moreover, hexosylceramide has been described as a possible inducer of plaque inflammation and instability [315]. Therefore its increment in obese women could underline the importance of this class of molecules for risk assessment of obesity-related morbidities and particularly of CVD. It must be stated that due to the similarity in the hydrophobic moiety and mass identity, Hexosylceramides (glucosylceramides and galactosylceramides) are not easily separated and quantified using a standard reverse-phase chromatography [316]. HexCers are represented in this work as the sum of detected glucosylceramides and galactosylceramides. Therefore observed changes are related to both molecules, and further studies will be needed to precisely identify the contribution of single glycosphingolipids to the total pool and the relative effect of different glycosphingolipids.

Figure 4. UPLC-MS analysis of sphingolipid alteration in sub-pooled sera samples from NWNL, NWDL and ODL men (**Panel A**); NWNL, NWDL and ODL women (**Panel B**). Tukey's correction was employed after one-way ANOVA statistical analysis. Data are expressed in log scale and reported as mean ± SD. (*p-value < 0.05, **p-value < 0.01, ***p-value < 0.001).

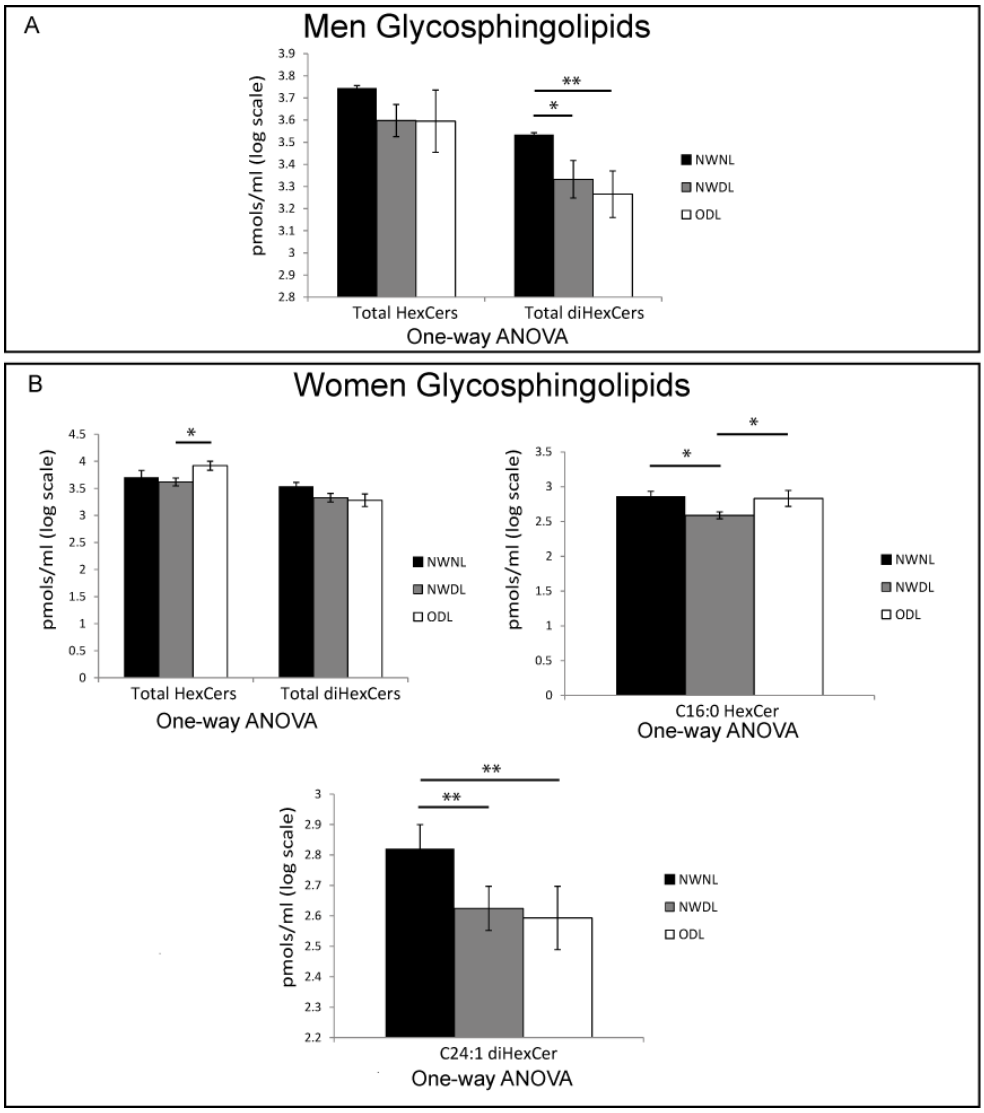

Both NWDL and ODL men and women showed decreased levels of dihexcer, total and C24:1 compared to NWNL, respectively. These data suggest a protective role exerted by dihexCer that decrease in parallel in

obesity and dyslipidemia. Plasmatic dihexosylceramide was, in fact, found to be positively associated with anti-inflammatory cytokine IL-10 before and after adjustments for age, body fat and sex [317]. DihexCer levels were also found to be negatively associated with BMI in [310] and negatively associated with T2DM and prediabetic condition in both the San Antonio Family Heart Study and the Australian Diabetes, Obesity, and Lifestyle Study [318], confirming our results.

To additionally increase the coverage of the sphingolipid profile of serum, S1P, and dhS1P levels, two sphingolipid newly associated with obesity [262] and usually not detected by standard LC-MS analysis, were investigated by LC-MS/MS following an MRM approach.

In this case, Sph and S1P resulted unchanged in NWNL, NWDL and ODL, both men and women (Figure 5, A), while, on the other hand, dhS1P was significantly decreased in NWNL compared to both ODL and NWDL (figure 5B). Data resulting from other sphingolipid classes compared in men and women are shown in Supplementary Figure 4.

In obese and dyslipidemic normal-weight women, it can be postulated that increased levels of dhS1P (Figure 5, B), can be driven by the overexpression of SK1 and the following deviation of metabolic flux through the formation of dhS1P from dhSPh [319]. It is known that dhSPh is used for the production of more complex sphingolipids that it could be used for the catabolic generation of S1P.

Figure 5. MRM analysis of sphingoid bases alteration in sub-pooled sera samples from NWNL, NWDL and ODL men (**A)** and NWNL, NWDL and ODL women (**B)**. Tukey's correction was employed after one-way ANOVA statistical analysis. Data are expressed in log scale and reported as mean ± SD. (*p-value < 0.05, **p-value < 0.01, ***p-value < 0.001).

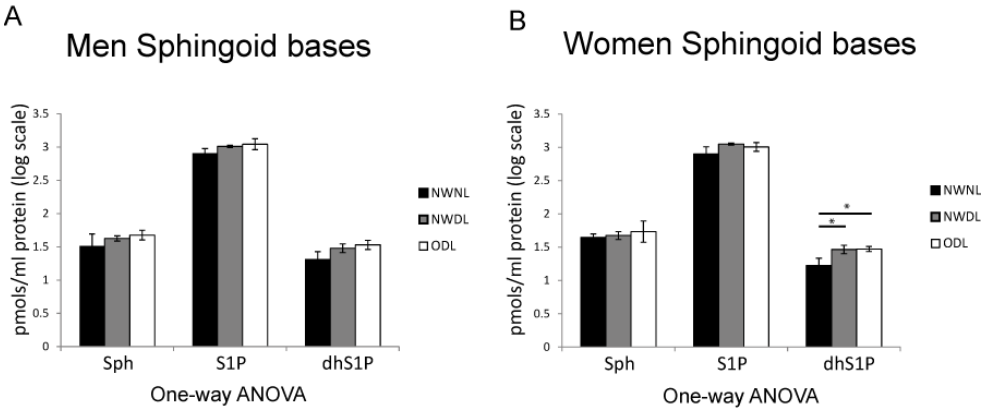

The precise biological functions of these dimorphic changes need to be further investigated to figure out if these data could provide a biological explanation and become a hint for personalized medicine. Also, in this case, there is a profound need for standardized methodologies and sampling to determine variation in this only apparently chemically simple class of molecules.

6.2. Andean subjects

6.2.1. Biochemical and anthropometrical results

Studies on Andean children born and living at San Antonio the Los Cobres, an Andean plateau located at 3775 mt above the sea level (a.s.l.), indicate a prevalence of dyslipidemia and hypertension compared to dwellers at lower altitudes, suggesting that despite similar food intake and daily activities, they undergo different metabolic adaptations [320]. This group of children is characterized by a prevalence of obesity and overweight of 8.1% [321] compared to the global population, in which the prevalence is 18% in children and adolescents [18] and Argentinean with a prevalence of 28.7% [322]. A report on children (aged 9.5±2 years) living in Buenos Aires indicates a prevalence of 29.7% for obesity and overweight [321]. The unexpected low prevalence of obesity and hypoxia are not the only characteristics of this group of subjects. Andean children show a peculiar dyslipidemic trait characterized by higher levels of TG (28% vs. 3.5%) and lower levels of HDL-C (30.0% vs. 5.5%) compared to children living in Buenos Aires [321]. Another study from San Pedro de Cajas (Peru) at 4100m a.s.l. showed lower rates of HDL-C and high levels of TG in native populations [323], further confirming that dyslipidemic alterations are a characteristic trait in high altitude dwellers. Although in San Antonio de Los Cobres, the weather is generally sunny both in summer and winter [324], two recent studies identified Vit. D insufficiency or severe deficiency [325] [326], with levels of Vit. D lower than 7.94 ng/ml and with a Vit. D deficiency prevalence of 67.7% [327].

The biochemical and anthropometrical parameters of the investigated group are summarized in Table 6, while p-values from biochemical and anthropometrical comparison can be found in supplementary Table 2. UW and OW groups showed acceptable mean levels of TC as indicated by the

National Cholesterol Educational Program [328], whereas borderline levels for total cholesterol (TC) were seen in NW and O. Mean levels of HDL-C were acceptable only in NW subjects. At variance, other groups were characterized by lower levels of HDL-C, classifying them as borderline [328]. Acceptable mean levels of LDL-C (lower than the 110 mg/dL cut-off), were detected in all groups. Conversely, borderline levels of mean triglycerides (TG) were seen in all groups except for O subjects that presented high levels [329]. Vitamin D was assessed, and the deficiency was present in all groups [298,327]. Blood sugar levels were beneath alert limits for all groups [329].

Table 6. Participant's assessment of anthropometry and biochemical parameters. Characteristics are, if continuous, described using median and interquartile range or, if categorical, with counts and percentages. normally distributed data were analyzed by One way ANOVA with Bonferroni's correction, otherwise Kruskal-Wallis' with Dunn's correction was adopted. (*t *p*-value for UW, $^{+}$ *p*-value for NW $^{+}$, ^{x} *p*-value for OW, ^{y} *p*-value for O) **p*-value < 0.05, ***p*-value < 0.01, ****p*-value < 0.001, $^{+}$*p*-value< 0.05, $^{++}$*p*-value< 0.01**,** $^{+++}$*p*-value< 0.001, ^{yy}*p*-value < 0.01.

	UW	NW	OW	O
N.	7 (43.7 %)	30 (44.1 %)	13 (65 %)	9 (50%)
Age	11 (8.5/11)	9 (8/11)	11 (10/11)	9 (8/9)
Weight (Kg)	25.2 (21.8/27.1)	27.2 (22.6/32.6)	45 (37.3/49.5)***,$^{+++}$	38.6 (37.6/42)**,$^{++}$
Height (Cm)	134 (124/138.5)	129.5 (121.7/140.7)	145 (134/149)	130 (124/137)
BMI	14 (13.7/14.3)	15.765 (14.9/16.9)	20.9 (18.6/22)***,$^{++}$	23.9 (22.5/25.6)***,$^{+++}$
Gender (M)	4 (57,1 %)	15 (50 %)	7 (53,8 %)	4 (44,4 %)
TC (mg/dL)	148 (128.5/163)	170 (166/180.5)	159 (140/170)	174 (148/193)
HDL-C (mg/dL)	43 (41/53)	50.5 (45/59.5)^{xx}	45 (40/50)	42 (32/46)
TC/HDL-C	3.1 (2.8/3.3)	3.35 (2.9/3.7)	3.7 (3.2/3.9)	4.1 (3.7/4.8)*,$^{++}$
LDL-C (mg/dL)	81 (74/90.5)	99.5 (94.2/104.7)	85 (81/100)	101 (89/104)
Vit. D (ng/mL)	14.2 (14/16.1)	17.2 (14.6/21.2)	16.2 (12.7/18.8)	15.8 (14.3/18.3)
Glycaemia (mg/dL)	88 (82/92)	83.5 (79.5/87.7)	85 (81/88)	84 (81/88)
HOMA-IR	1 (0.9/1.2)	0.9 (0.6/1.1)	1.7 (1.1/1.7)$^{+}$	1.5 (1.3/2)$^{++}$
Insulin (µU/mL)	5.1 (3.9/5.6)	4.4 (3/5.6)	7.7 (5.5/8.7)$^{+}$	7.2 (6.4/9.3)$^{++}$
TG (mg/dL)	83 (72.5/95.5)	97 (78.2/113.7)	90 (86/122)	129 (97/143)

HDL-C was higher comparing NW vs. O (*p*-value < 0.01), instead the TC/HDL-C ratio was higher in O participants compared to UW and NW (*p*-value < 0.05 and 0.01, respectively). HOMA-IR and insulin levels were

higher in O and OW subjects compared to NW (*p*-value < 0.01 and 0.05, respectively, in both comparisons).

From the anthropometrical point of view, groups were homogeneous for age and sex. BMI was higher in OW and O group compared to UW and NW; thus, subjects were clustered in four main BMI groups. From the biochemical point of view, normal HDL levels were observed in NW only, whereas discrepant HOMA-IR parameters and insulin levels characterized OW and O, even though HOMA-IR and insulin values were beneath alert limits. All groups are characterized by a Vit.D deficiency and by a peculiar dyslipidemic trait with low levels of HDL-C or high levels of TG and TC.

The investigated children have a higher prevalence of obesity and overweight (22% and 15.25% respectively) and a higher prevalence of Vit. D deficiency (100%) compared to previous reports [321]. The aim of the present study is to profile sphingolipids in different BMIs groups, independently from Vit. D. deficiency and dyslipidemic traits, to provide a molecular signature not only for obesity but also to identify molecules influencing their adaptation to high altitude hypoxia.

6.2.2. Biochemical and lipidomic correlations

Scatter plots for total Cers, total SMs, S1P levels and biochemical parameters are shown in Figure 6. The correlation table is shown in Supplementary Table 3.

In UW subjects, the only correlation found was a between SMs levels and HDL-C (r = 0.854, p-value = 0.015). Regardless of the low number of correlation in the UW group, the association between HDL-C and SMs levels has already been described [330] [331] and is thought to be involved in reverse cholesterol transport. Several studies showed that increasing the content of SMs in HDL-C particle improved the import of cholesterol from erythrocyte membranes [332] and from non-cholesterol-loaded human skin

fibroblasts [333] to HDL-C. These data suggest that the overall relationship existing between SMs and HDL-C can contribute to explain, at least partially, the inverse correlation among HDL-C levels and risk of CVD development [331].

NW subjects are characterized by a higher number of correlations. Cers showed positive correlations with HOMA-IR (r = 0.389, p-value= 0.036), insulin (r = 0.418, p-value = 0.021), and TG (r = 0.379, p-value= 0.039). In the same group, a negative correlation with Vitamin D was also found (r = −0.4, p-value = 0.028). No correlation was found between SMs and biochemical parameters; nevertheless, a negative correlation (r = −0.375, p-value = 0.041) was identified between S1P and HDL-C. Particularly in normal-weight patients, ceramides correlate with several biochemical parameters strictly related to insulin resistance and T2DM. Even if insulin levels, glycaemia, and HOMA-IR parameters cannot be associated with T2DM and/or pre-diabetes, cers increase in parallel with insulin and HOMA-IR. The positive correlation between Cers and increasing levels of insulin-resistance could be associated with detrimental effects exerted by ceramides in insulin singling [200] and on β-cell survival [334], increasing the risk of developing T2DM.

In OW subjects correlations with biochemical parameters were positive for all sphingolipid species. Total Cers had a strong positive correlation with TC (r = 0.721, p-value = 0.005), LDL-C (r = 0.691, p-value = 0.024), as well as total SMs that strongly correlate with TC (r = 0.726, p-value = 0.005), LDL-C (r = 0.655,p-value = 0.015), and HDL-C (r = 0.603, p-value = 0.029), at last, S1P negatively correlated with LDL-C levels (r = −0.691, p-value = 0.011).

In overweight subjects, sphingolipids correlate with plasma lipid parameters, both for ceramides and SMs, confirming the relation between these two classes of lipids.

In O subjects, a single positive correlation links Cers and Glycaemia (r = 0.683, p-value = 0.043).

Our data did not allow us to figure out the causes behind these associations, that would have required, the assessment of enzymatic activity of several biological pathways as well as levels of SLs from tissue; nevertheless, results highlighted the strict association of sphingolipids not only with lipid parameters as TC, LDL-C HDL-C and TG but also with Vit. D and other biochemical parameters as HOMA-IR, insulin and glycaemia.

Figure 6. Scatter plots for total Ceramide **A**, total sphingomyelin **B**, and total S1P **C**. X-Data for Cers, SMs, and S1P are in pmol/mL (log scale); Y-data for Vitamin D are in ng/mL, and Y-data for insulin are in µU/mL; Y-data for TG, TC, LDL-C are in mg/dL; r-value (Pearson's correlation) p-values (two-tailed test).

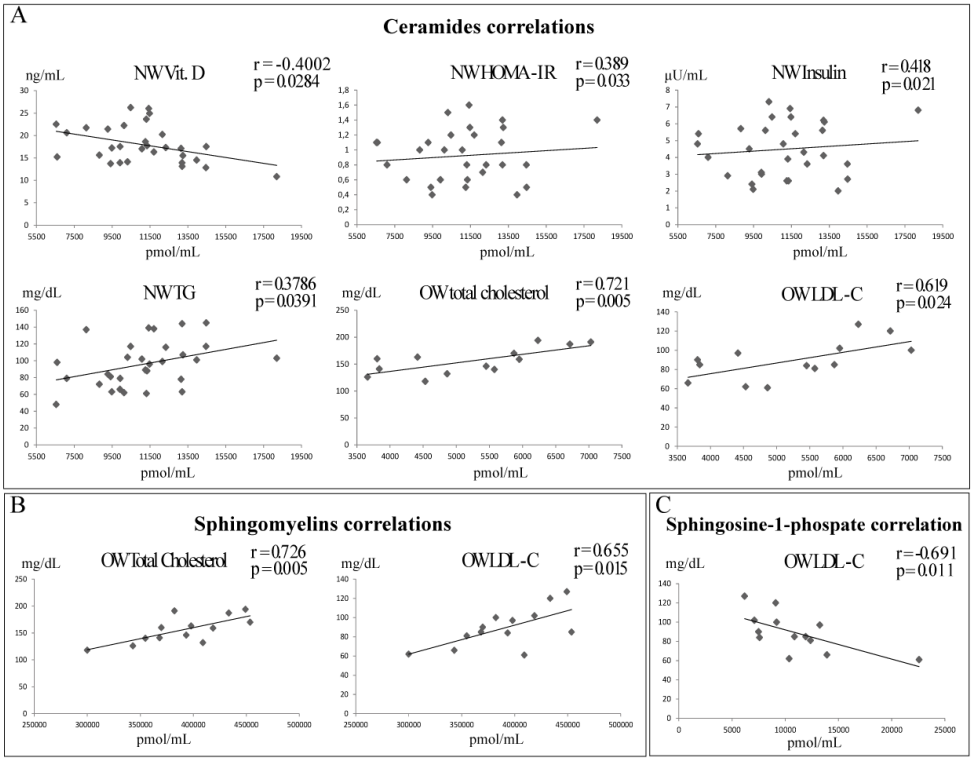

6.2.3. UPLC-MS sphingolipid results

In order to obtain complete information regarding differences on sphingolipid profiles, Cers (Figure 7), SMs (Figure 8), total dihydroceramides (dhCers), total hexosylceramides (HexCer), total dihexosylceramides (diHexCer), total monosialodihexosylganglioside (GM3), and total S1P levels (Figure 9) were assessed and compared between groups characterized by different BMIs. Cers acyl chains: d18:1/16:0, d18:1/22:0, and d18:1/24:0 (Figure 7), and SMs d18:1/18:0, d18:1/20:0, and d18:1/22:0 (Figure 8) were also investigated.

Total Ceramides were found to be higher in NW compared to both UW and OW (*p*-value, < 0.01 and 0.001) subjects, and in O and UW compared to OW (*p*-value < 0.001 and 0.05). Cers acyl chains (d18:1/16:0, d18:1/22:0, and d18:1/24:0) presented a similar trend as total Cers.

Specifically, Cer (d18:1/16:0) was higher in UW, NW, and O subjects compared to OW (*p*-value < 0.05, *p*-value <0.001 and *p*-value < 0.001). Cer (d18:1/22:0) interestingly followed the same pattern as Cer (d18:1/16:0) in NW (*p*-value < 0.001) and O (*p*-value < 0.001) compared to OW, but UW subjects in this case were characterized by lower levels of Cer (d18:1/22:0) compared to NW (*p*-value < 0.01). Ceramide (d18:1/24:0) levels resulted in a trend identical to the one obtained from total Cers, showing higher levels in NW subjects compared to UW and OW (*p*-value < 0.05 and *p*-value < 0.001). O and UW had higher levels of Cer (d18:1/24:0) in the OW comparison (*p*-value < 0.001 and *p*-value < 0.05).

Figure 7. UPLC-MS results for total ceramides **A**, Cer (d18:1/16:0) **B**, Cer (d18:1/22:0) **C**, and Cer (d18:1/24:0) **D**. Results are in pmol/mL in Log scale; *p* values are expressed as * *p*-value < 0.05, ** *p*-value < 0.01, and *** *p*-value < 0.001.

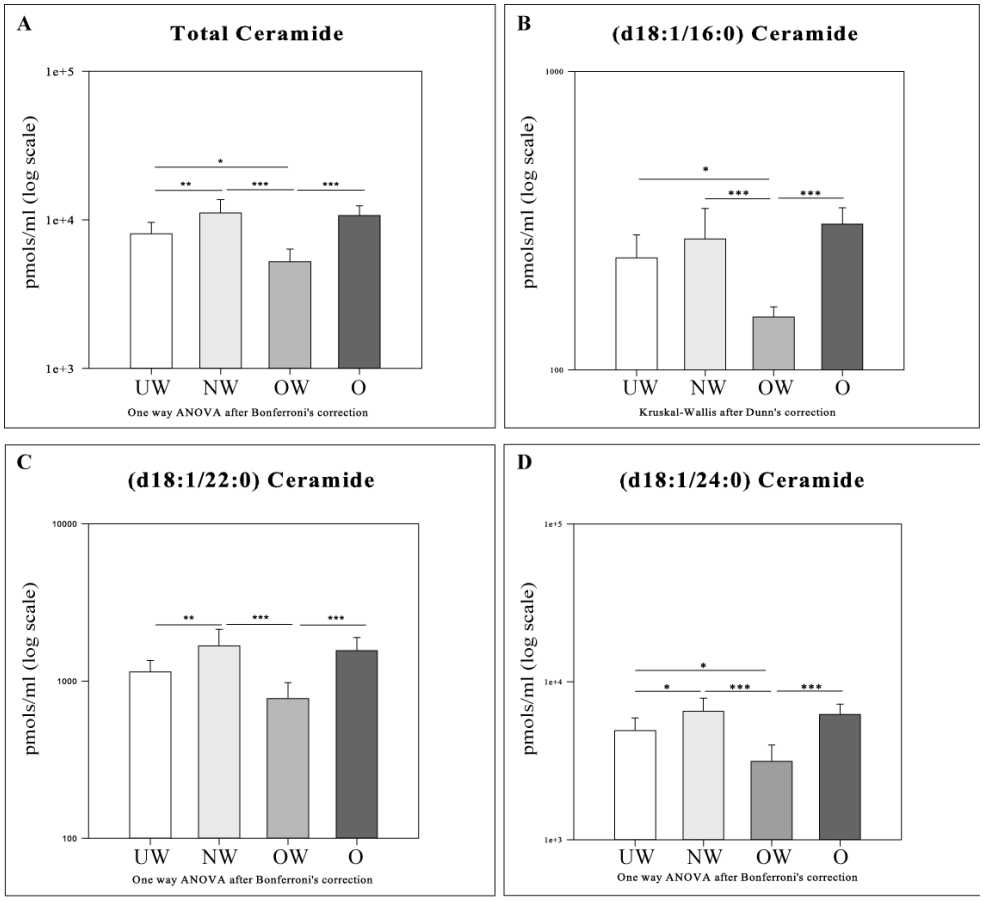

The comparison between dyslipidemic Vit. D deficient NW subjects and their O counterparts, confirmed data from Saudi Arabian subjects, showing that NW and O dyslipidemic subjects, independently from their BMI, develop similar levels of cers. However, it must be acknowledged the fact that comparisons or parallelisms among different populations must be undertaken with caution because of the profound differences present in terms of genetics, age, and environmental characteristics.

The pattern seen for Ceramides was reversed in sphingomyelins, in fact, total SMs (Figure 8) showed higher levels in OW compared to both O and

NW subjects (*p*-value < 0.01 and *p*-value < 0.001), and lower levels in NW compared to UW (*p*-value < 0.01).

As for Cers acyl chains, SMs acyl moiety followed the same trend seen for total SMs. SM (d18:1/18:0) was found to be higher in OW subjects compared to both NW (p-value < 0.001) and O (p < 0.01). NW and O group showed for SM (d18:1/20:0) decreased level when compared to OW (p-value <0.001 and p-value <0.001, respectively). SM (18:1/22:0) behaving as SM (d18:1/20:0) for the NW and O comparison with OW (p-value <0.001 and p-value <0.001, respectively), highlighted differences also in the UW vs. NW comparison, where higher levels were present in the UW group (p-value < 0.001). The UW group was also characterized by lower levels of this acyl chain when compared to OW (p-value <0.001).

Figure 8. UPLC-MS results for total sphingomyelins **A**, SMs (d18:1/18:0) **B**, Cer (d18:1/20:0) **C**, and Cer (d18:1/22:0) **D**. Results are in pmol/mL in Log scale; *p* values are expressed as ** *p*-value < 0.01, and *** *p*-value < 0.001.

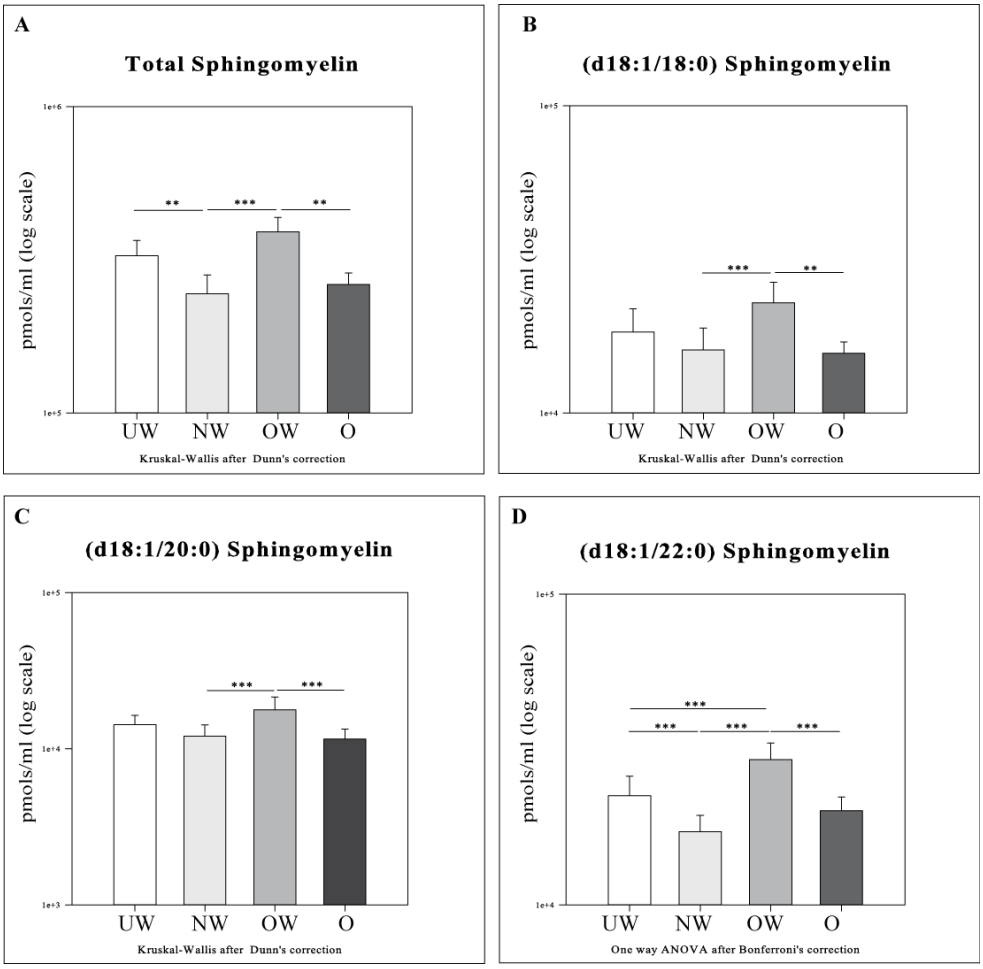

For total dhCers (Figure 9), the same tendency seen in Cers was observed. Higher levels of dhCers were seen in NW and O subjects when compared to the OW group (*p*-value < 0.001 in both comparisons). MRM analysis of S1P revealed a clear trend for decrement across different BMI percentiles in S1P levels. In this case, statistically significant differences were seen when comparing NW vs. O (*p*-value < 0.05), and UW vs. O (*p*-value < 0.05).

Glycosphingolipids: HexCer, diHexCer, and GM3 (Figure 9) showed a clear and characteristic pattern. NW patients had, in fact, higher levels of those SLs species compared to UW (*p*-value < 0.001). For total HexCer, NW subjects also showed a higher level when compared to OW and O (*p*-value < 0.05 and 0.001, respectively). Total diHexCer levels in O were lower if compared to NW (*p*-value < 0.001), while UW subjects had lower levels in the OW comparison (*p*-value < 0.05). At last, total GM3 was found to be higher in NW compared to OW (*p*-value < 0.01) and O (*p*-value < 0.05) subjects. GM3 was also higher in the OW and O vs. UW comparison (*p*-value < 0.05 in both comparisons).

Figure 9. UPLC-MS and MRM results for total dhCers **A**, S1P **B**, total HexCer **C**, total dihexCer **D**, and total GM3 **E**. Data are in pmol/mL in Log scale; *p* values are expressed as * *p*-value < 0.05, ** *p*-value < 0.01, and *** *p*-value < 0.001.

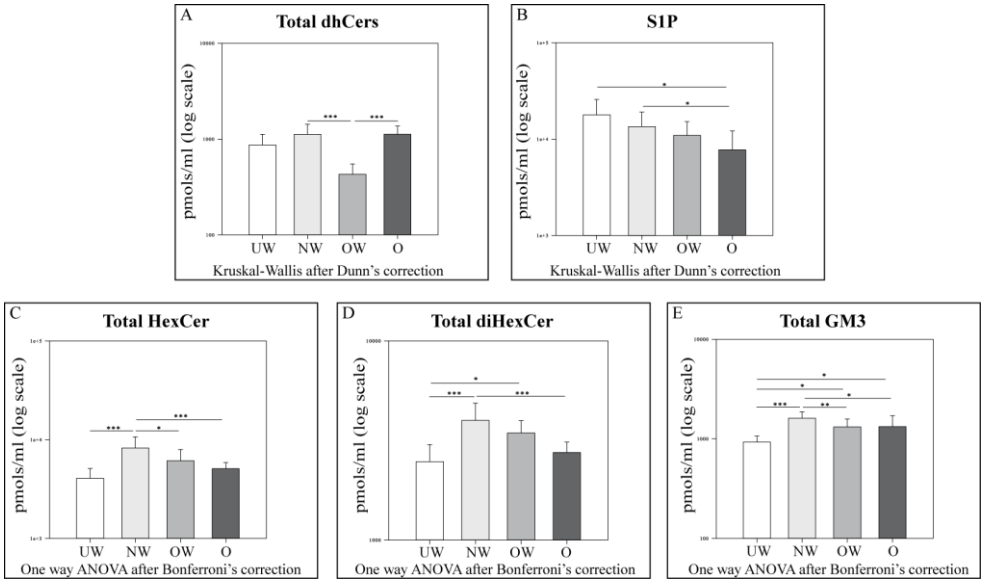

Figure 10 summarizes glyco/sphingolipid levels in the analyzed groups and highlights that UW and O subjects have similar glyco/sphingolipids levels, with S1P at variance, being high in UW and low in O subjects.

Figure 10. Summary of glyco/sphingolipid levels and altered ceramide-biosynthesis pathways in UW and O. Different size arrows indicate the different involvement of Cers biosynthetic pathways in UW and O. LC-MS and LC-MS/MS results for total Cers, total dhCers, total SMs, total HexCer, total dihexCer, and total GM3. Data are expressed as pmol/mL in Log scale; p values are expressed as * p-value < 0.05, ** p-value < 0.01, and *** p-value < 0.001.

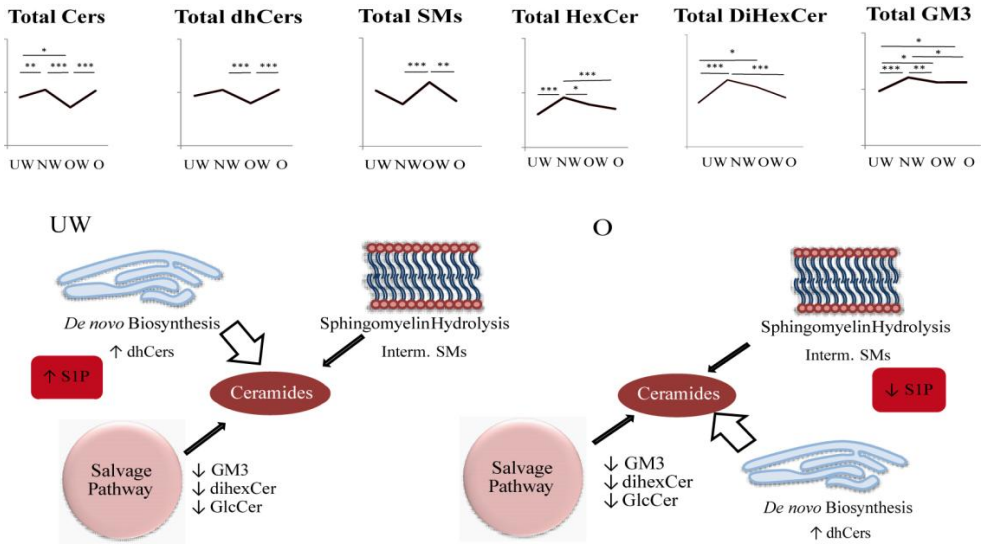

It can be hypothesized that Cers levels in the O and UW groups originate from *de novo* biosynthesis, as dhCers levels are comparable to NW group. The main discrepancy in SLs profiles between the four different groups relied on S1P levels that were high in UW and NW, whereas low in OW and O groups. Regarding S1P, a recent study from Sun *et al*. demonstrated that an increment in erythrocytes S1P levels, follows high altitude hypoxia exposure and that S1P stimulated the oxygen release capacity of erythrocytes by increasing cytoplasmatic 2,3-biphosphoglycerate [335], a specific glycolytic intermediate that facilitates O_2 release [336].

It is possible to speculate that UW and NW children showed a better metabolic adaptation to high altitude hypoxia due to their high constitutional levels of S1P that allow the activation of RBC glycolysis and a better release of O_2 from red blood cells to tissues reducing cell hypoxia and HIF1-α activation. The latter is known to be a lipogenic inducer, directly

inducing PPARγ and fatty-acid-binding proteins (FABP) [337–339]. Conversely, obese children with reduced levels of S1P were unable to adapt to oxygen lack due to their poor S1P-mediated O_2 release and they can undergo a constitutive activation of HIF1-α, causing accumulation of lipids, due to both HIF1-α induced lipogenesis/lipotoxicity and ceramide mediated lipotoxic effects [203,340,341].

UW and O children were also characterized by low levels of glycosphingolipid. The activation of Neuraminidase 3 sialidase (NEU3) in transgenic mice causes reduced tissue and circulating levels of GM3 [342]. From a previous study from our group performed on animal models exposed to prolonged severe hypoxia, NEU3 was increased [343]. In the present study, the decrease in GM3 levels could be associated with the activation of NEU3 sialidase, which has been recently described as a target of HIF2 alpha and thus regulated by hypoxia [344].

The restricted number of subjects and the lack of a verification study are the two major drawbacks of this study. The assessment of 2,3-BPG, pH, partial pressure of oxygen/carbon dioxide, and haemoglobin-O_2-saturation will, however, be undertaken in a separate study to determine the anomalous metabolism and consequent O_2 affinity in erythrocytes.

Not only parameters regarding hypoxia adaptation and O_2 affinity but also RNAs from peripheral blood mononuclear cells for the quantitative assessment of enzymes involved in SLs biosynthetic pathways and of circulating cytokines or adipokines will be collected and presented in a separate study.

7. CONCLUSIONS

The novelty introduced by our study on Saudi Arabian serum samples is the identification of specific Cers acyl chains associated with obesity and the impact of sexual dimorphism on circulating SLs independently from serum dyslipidemia and Vit. D status. Notably, recent results obtained in normal-weight subjects indicated that gender is associated with several plasma sphingolipids like Cers, SMs, and diHexCer, fostering our results [310].

Our study confirms previous observations, indicating that Cers levels are increased in ODL compared to NWNL [345]. Furthermore, our data highlighted that Cers are significantly higher not only in ODL but also in NWDL, indicating a direct association between dyslipidemia, Vit. D deficiency and Cers circulating levels. Results from Saudi Arabians, identified alterations in specific Cers, SMs, and dhSMs acyl chains, providing not only a signature for obesity, independently from dyslipidemia and Vit. D deficiency, but also an indication of the relevance of SLs' acyl chains variations rather than changes on "total SLs species", where information from single bioactive acyl moiety could be lost.

The study of Andean children, born and living at altitude, indicated the same dependency of Cers and SMs on Vit. D deficiency and dyslipidemia [346], supporting our previous results. Noteworthy, the correlation identified in Andean children between Cers, SMs, S1P and plasma lipid/Vit. D levels confirmed this association. Results indicate that UW and O Andean children, although a common dyslipidemic trait, are characterized by a common SLs profile with similar levels of dhCer, SMs, HexCer and diHexCer. Regarding S1P, UW and NW subjects compared to O showed a higher level of S1P not observed in the O group. It can be speculated that UW and NW children utilizing S1P can activate the same biochemical pathway promoting oxygen delivery to maintain energy production and

homeostasis, therefore resulting in a more fit phenotype. By contrast, O children, showing lower levels of S1P, display reduced O2 delivery to tissue, resulting in a less adapted phenotype prone to the activation of lipogenic and lipotoxic pathways. Further data based on 2,3-BPG, pH, partial pressure of carbon dioxide (PCO2), of oxygen (PO2), and haemoglobin-O2 saturation (SO2) will be necessary to determine the abnormal O2 affinity or altered metabolism of RBC. Studies in this direction are ongoing aimed to open new avenues in the complex field of hypoxia tolerance in high-altitude dwellers.

8. REFERENCES

1. Kelly, T.; Yang, W.; Chen, C.-S.; Reynolds, K.; He, J. Global burden of obesity in 2005 and projections to 2030. *Int. J. Obes.* **2008**, *32*, 1431–1437.
2. Pollack, A. A.M.A. Recognizes Obesity as a Disease - The New York Times Available online: https://www.nytimes.com/2013/06/19/business/ama-recognizes-obesity-as-a-disease.html?smid=pl-share.
3. Redinger, R.N. The pathophysiology of obesity and its clinical manifestations. *Gastroenterol. Hepatol. (N. Y).* **2007**, *3*, 856–63.
4. Hope, D.C.D.; Tan, T.M.M.; Bloom, S.R. No Guts, No Loss: Toward the Ideal Treatment for Obesity in the Twenty-First Century. *Front. Endocrinol. (Lausanne).* **2018**, *9*, 442.
5. Hu, M.; Yu, Z.; Luo, D.; Zhang, H.; Li, J.; Liang, F.; Chen, R. Association between -174G>C polymorphism in the IL-6 promoter region and the risk of obesity. *Medicine (Baltimore).* **2018**, *97*, e11773.
6. Vimaleswaran, K.S.; Berry, D.J.; Lu, C.; Tikkanen, E.; Pilz, S.; Hiraki, L.T.; Cooper, J.D.; Dastani, Z.; Li, R.; Houston, D.K.; et al. Causal Relationship between Obesity and Vitamin D Status: Bi-Directional Mendelian Randomization Analysis of Multiple Cohorts. *PLoS Med.* **2013**, *10*, e1001383.
7. Peterson, C.A.; Belenchia, A.M. Vitamin D deficiency & childhood obesity: a tale of two epidemics. *Mo. Med.* **2014**, *111*, 49–53.
8. Fairbrother, U.; Kidd, E.; Malagamuwa, T.; Walley, A. Genetics of Severe Obesity. *Curr. Diab. Rep.* **2018**, *18*, 85.
9. Nair, R.; Maseeh, A. Vitamin D: The "sunshine" vitamin. *J. Pharmacol. Pharmacother.* **2012**, *3*, 118–26.
10. Kang, S.-C.; Kim, B.-R.; Lee, S.-Y.; Park, T.-S. Sphingolipid Metabolism and Obesity-Induced Inflammation. *Front. Endocrinol. (Lausanne).* **2013**, *4*, 67.
11. Norris, G.H.; Blesso, C.N. Dietary and Endogenous Sphingolipid Metabolism in Chronic Inflammation. *Nutrients* **2017**, *9*, 1180.
12. Borodzicz, S.; Czarzasta, K.; Kuch, M.; Cudnoch-Jedrzejewska, A. Sphingolipids in cardiovascular diseases and metabolic disorders. *Lipids Health Dis.* **2015**, *14*, 55.
13. Meikle, P.J.; Summers, S.A. Sphingolipids and phospholipids in insulin resistance and related metabolic disorders. *Nat. Rev. Endocrinol.* **2017**, *13*, 79–91.
14. Régnier, M.; Polizzi, A.; Guillou, H.; Loiseau, N. Sphingolipid metabolism in non-alcoholic fatty liver diseases. *Biochimie* **2018**.

15. Kyle, T.K.; Dhurandhar, E.J.; Allison, D.B. Regarding Obesity as a Disease: Evolving Policies and Their Implications.
16. Clinical Guidelines on the Identification, Evaluation, and Treatment of Overweight and Obesity in Adults--The Evidence Report. National Institutes of Health. *Obes. Res.* **1998**, *6 Suppl 2*, 51S-209S.
17. WHO | Controlling the global obesity epidemic. *WHO* **2013**.
18. WHO *Obesity and overweight Fact sheet N°311*; 2016;
19. Etchison, W.C.; Bloodgood, E.A.; Minton, C.P.; Thompson, N.J.; Collins, M.A.; Hunter, S.C.; Dai, H. Body mass index and percentage of body fat as indicators for obesity in an adolescent athletic population. *Sports Health* **2011**, *3*, 249–52.
20. Chatterjee, S.; Chatterjee, P.; Bandyopadhyay, A. Skinfold thickness, body fat percentage and body mass index in obese and non-obese Indian boys. *Asia Pac. J. Clin. Nutr.* **2006**, *15*, 231–5.
21. Jacobsen, B.K.; Aars, N.A. Changes in waist circumference and the prevalence of abdominal obesity during 1994-2008 - cross-sectional and longitudinal results from two surveys: the Tromsø Study. *BMC Obes.* **2016**, *3*, 41.
22. Janssen, I.; Katzmarzyk, P.T.; Ross, R. Waist circumference and not body mass index explains obesity-related health risk. *Am. J. Clin. Nutr.* **2004**, *79*, 379–384.
23. Price, G.M.; Uauy, R.; Breeze, E.; Bulpitt, C.J.; Fletcher, A.E. Weight, shape, and mortality risk in older persons: elevated waist-hip ratio, not high body mass index, is associated with a greater risk of death1–3. *Am. J. Clin. Nutr.* **2006**, *84*, 449–460.
24. Cameron, A.J.; Magliano, D.J.; Söderberg, S. A systematic review of the impact of including both waist and hip circumference in risk models for cardiovascular diseases, diabetes and mortality. *Obes. Rev.* **2013**, *14*, 86–94.
25. Tataranni, P.A.; Ravussin, E. Use of dual-energy X-ray absorptiometry in obese individuals. *Am. J. Clin. Nutr.* **1995**, *62*, 730–734.
26. Han, T.S.; Sattar, N.; Lean, M. ABC of obesity. Assessment of obesity and its clinical implications. *BMJ* **2006**, *333*, 695–8.
27. for Disease Control, C. *CDC Vitalsigns - Adult Obesity: Obesity Rises Among Adults*;
28. WHO Expert Consultation Appropriate body-mass index for Asian populations and its implications for policy and intervention strategies. *Lancet* **2004**, *363*, 157–163.
29. Kuczmarski, R.J.; Ogden, C.L.; Guo, S.S.; Grummer-Strawn, L.M.; Flegal, K.M.; Mei, Z.; Wei, R.; Curtin, L.R.; Roche, A.F.; Johnson, C.L. 2000 CDC Growth Charts for the United States: methods and development. *Vital Health Stat. 11.* **2002**, 1–190.
30. Tobias, D.K.; Hu, F.B. The association between BMI and mortality:

implications for obesity prevention. *lancet. Diabetes Endocrinol.* **2018**, *6*, 916–917.
31. Bojanowska, E.; Ciosek, J. Can We Selectively Reduce Appetite for Energy-Dense Foods? An Overview of Pharmacological Strategies for Modification of Food Preference Behavior. *Curr. Neuropharmacol.* **2016**, *14*, 118–42.
32. Swinburn, B.A.; Caterson, I.; Seidell, J.C.; James, W. Diet, nutrition and the prevention of excess weight gain and obesity.
33. Smilowitz, J.T.; German, J.B.; Zivkovic, A.M. *Food Intake and Obesity: The Case of Fat*; CRC Press/Taylor & Francis, 2010; ISBN 9781420067750.
34. Steenhuis, I.; Poelman, M. Portion Size: Latest Developments and Interventions. **2017**.
35. Zlatevska, N.; Dubelaar, C.; Holden, S.S.; Holden is Associate Professor, S.S. Sizing Up the Effect of Portion Size on Consumption: A Meta-Analytic Review. *J. Mark.* **2014**, *78*, 140–154.
36. Centers for Disease Control Prevention (CDC) Trends in Intake of Energy and Macronutrients --- United States, 1971--2000 Available online: https://www.cdc.gov/mmwr/preview/mmwrhtml/mm5304a3.htm.
37. Hall, K.D.; Sacks, G.; Chandramohan, D.; Chow, C.C.; Wang, Y.C.; Gortmaker, S.L.; Swinburn, B.A. Quantification of the effect of energy imbalance on bodyweight. *Lancet (London, England)* **2011**, *378*, 826–37.
38. Vandevijvere, S.; Chow, C.C.; Hall, K.D.; Umali, E.; Swinburn, B.A. Increased food energy supply as a major driver of the obesity epidemic: a global analysis. *Bull World Heal. Organ* **2015**, *93*, 446–456.
39. Hall, K.D. Did the Food Environment Cause the Obesity Epidemic? *Obesity (Silver Spring).* **2018**, *26*, 11–13.
40. Church, T.; Martin, C.K. The Obesity Epidemic: A Consequence of Reduced Energy Expenditure and the Uncoupling of Energy Intake? *Obesity* **2018**, *26*, 14–16.
41. Hebebrand, J.; Friedel, S.; Schäuble, N.; Geller, F.; Hinney, A. Perspectives: molecular genetic research in human obesity. *Obes. Rev.* **2003**, *4*, 139–46.
42. Bell, C.G.; Walley, A.J.; Froguel, P. The genetics of human obesity. *Nat. Rev. Genet.* **2005**, *6*, 221–234.
43. Stunkard, A.J.; Sørensen, T.I.A.; Hanis, C.; Teasdale, T.W.; Chakraborty, R.; Schull, W.J.; Schulsinger, F. An Adoption Study of Human Obesity. *N. Engl. J. Med.* **1986**, *314*, 193–198.
44. Bray, M.S.; Loos, R.J.F.; McCaffery, J.M.; Ling, C.; Franks, P.W.; Weinstock, G.M.; Snyder, M.P.; Vassy, J.L.; Agurs-Collins, T.; Conference Working Group NIH working group report-using genomic

information to guide weight management: From universal to precision treatment. *Obesity* **2016**, *24*, 14–22.
45. Farooqi, I.S.; O'Rahilly, S. Mutations in ligands and receptors of the leptin–melanocortin pathway that lead to obesity. *Nat. Clin. Pract. Endocrinol. Metab.* **2008**, *4*, 569–577.
46. Clément, K.; Vaisse, C.; Lahlou, N.; Cabrol, S.; Pelloux, V.; Cassuto, D.; Gourmelen, M.; Dina, C.; Chambaz, J.; Lacorte, J.-M.; et al. A mutation in the human leptin receptor gene causes obesity and pituitary dysfunction. *Nature* **1998**, *392*, 398–401.
47. Austin, J.; Marks, D. Hormonal regulators of appetite. *Int. J. Pediatr. Endocrinol.* **2009**, *2009*, 141753.
48. Timper, K.; Brüning, J.C. Hypothalamic circuits regulating appetite and energy homeostasis: pathways to obesity. *Dis. Model. Mech.* **2017**, *10*, 679.
49. Fall, T.; Mendelson, M.; Speliotes, E.K. Recent Advances in Human Genetics and Epigenetics of Adiposity: Pathway to Precision Medicine? HHS Public Access. *Gastroenterology* **2017**, *152*, 1695–1706.
50. Pigeyre, M.; Yazdi, F.T.; Kaur, Y.; Meyre, D. Recent progress in genetics, epigenetics and metagenomics unveils the pathophysiology of human obesity. *Clin. Sci.* **2016**, *130*, 943–986.
51. Frayling, T.M.; Timpson, N.J.; Weedon, M.N.; Zeggini, E.; Freathy, R.M.; Lindgren, C.M.; Perry, J.R.B.; Elliott, K.S.; Lango, H.; Rayner, N.W.; et al. A Common Variant in the FTO Gene Is Associated with Body Mass Index and Predisposes to Childhood and Adult Obesity. *Science (80-.).* **2007**, *316*, 889–894.
52. Scuteri, A.; Sanna, S.; Chen, W.-M.; Uda, M.; Albai, G.; Strait, J.; Najjar, S.; Nagaraja, R.; Orrú, M.; Usala, G.; et al. Genome-Wide Association Scan Shows Genetic Variants in the FTO Gene Are Associated with Obesity-Related Traits. *PLoS Genet.* **2007**, *3*, e115.
53. Rinninella, E.; Raoul, P.; Cintoni, M.; Franceschi, F.; Abele, G.; Miggiano, D.; Gasbarrini, A.; Mele, M.C. microorganisms What is the Healthy Gut Microbiota Composition? A Changing Ecosystem across Age, Environment, Diet, and Diseases. **2019**, *7*, 14.
54. Wen, L.; Duffy, A. The Journal of Nutrition Supplement: Fourth Global Summit on the Health Effects of Yogurt. Yogurt and Type 2 Diabetes: Translating Evidence into Practice Factors Influencing the Gut Microbiota, Inflammation, and Type 2 Diabetes.
55. Dieterich, W.; Schink, M.; Zopf, Y. medical sciences Review Microbiota in the Gastrointestinal Tract.
56. Rowland, I.; Gibson, G.; Heinken, A.; Scott, K.; Swann, J.; Thiele, I.; Tuohy, K. Gut microbiota functions: metabolism of nutrients and other food components. *Eur. J. Nutr.* **2018**, *57*, 1–24.
57. Ubeda, C.; Djukovic, A.; Isaac, S. Roles of the intestinal microbiota in

pathogen protection. *Clin. Transl. Immunol.* **2017**, *6*, e128.
58. Cani, P.D. Human gut microbiome: hopes, threats and promises. *Gut* **2018**, *67*, 1716–1725.
59. Turnbaugh, P.J.; Ley, R.E.; Mahowald, M.A.; Magrini, V.; Mardis, E.R.; Gordon, J.I. An obesity-associated gut microbiome with increased capacity for energy harvest. *Nature* **2006**, *444*, 1027–1031.
60. Qin, J.; Li, R.; Raes, J.; Arumugam, M.; Burgdorf, K.S.; Manichanh, C.; Nielsen, T.; Pons, N.; Levenez, F.; Yamada, T.; et al. A human gut microbial gene catalogue established by metagenomic sequencing. *Nature* **2010**, *464*, 59–65.
61. Ley, R.E.; Turnbaugh, P.J.; Klein, S.; Gordon, J.I. Human gut microbes associated with obesity. *Nature* **2006**, *444*, 1022–1023.
62. Furet, J.-P.; Kong, L.-C.; Tap, J.; Poitou, C.; Basdevant, A.; Bouillot, J.-L.; Mariat, D.; Corthier, G.; Dore, J.; Henegar, C.; et al. Differential Adaptation of Human Gut Microbiota to Bariatric Surgery-Induced Weight Loss: Links With Metabolic and Low-Grade Inflammation Markers. *Diabetes* **2010**, *59*, 3049–3057.
63. Li, L.; Ma, L.; Fu, P. Gut microbiota–derived short-chain fatty acids and kidney diseases. *Drug Des. Devel. Ther.* **2017**, *Volume 11*, 3531–3542.
64. den Besten, G.; Lange, K.; Havinga, R.; van Dijk, T.H.; Gerding, A.; van Eunen, K.; Müller, M.; Groen, A.K.; Hooiveld, G.J.; Bakker, B.M.; et al. Gut-derived short-chain fatty acids are vividly assimilated into host carbohydrates and lipids. *Am. J. Physiol. Liver Physiol.* **2013**, *305*, G900–G910.
65. Velloso, L.A.; Folli, F.; Saad, M.J. TLR4 at the Crossroads of Nutrients, Gut Microbiota, and Metabolic Inflammation. *Endocr. Rev.* **2015**, *36*, 245–271.
66. Hug, H.; Mohajeri, M.H.; Fata, G. La Toll-Like Receptors: Regulators of the Immune Response in the Human Gut. *Nutrients* **2018**, *10*.
67. Sanyal, D.; Raychaudhuri, M. Hypothyroidism and obesity: An intriguing link. *Indian J. Endocrinol. Metab.* **2016**, *20*, 554–7.
68. Tiryakioglu, O.; Ugurlu, S.; Yalin, S.; Yirmibescik, S.; Caglar, E.; Yetkin, D.O.; Kadioglu, P. Screening for Cushing's syndrome in obese patients. *Clinics (Sao Paulo).* **2010**, *65*, 9–13.
69. Woo, Y.S.; Seo, H.-J.; McIntyre, R.S.; Bahk, W.-M. Obesity and Its Potential Effects on Antidepressant Treatment Outcomes in Patients with Depressive Disorders: A Literature Review. *Int. J. Mol. Sci.* **2016**, *17*.
70. Merritt, R.J.; Hack, S.L.; Kalsch, M.; Olson, D. Corticosteroid Therapy-induced Obesity in Children. *Clin. Pediatr. (Phila).* **1986**, *25*, 149–152.
71. Day, J.; Ternouth, A.; Collier, D.A. Eating disorders and obesity: two

sides of the same coin? *Epidemiol. Psichiatr. Soc. 18*, 96–100.
72. Chiang, C.; Ismaeel, A.; Griffis, R.B.; Weems, S. Effects of Vitamin D Supplementation on Muscle Strength in Athletes A Systematic Review. *J. Strength Cond. Res.* **2016**, 1.
73. Christakos, S.; Dhawan, P.; Porta, A.; Mady, L.J.; Seth, T. Vitamin D and intestinal calcium absorption. *Mol. Cell. Endocrinol.* **2011**, *347*, 25–9.
74. Fukumoto, S. Phosphate metabolism and vitamin D. *Bonekey Rep.* **2014**, *3*, 497.
75. Rusińska, A.; Płudowski, P.; Walczak, M.; Borszewska-Kornacka, M.K.; Bossowski, A.; Chlebna-Sokół, D.; Czech-Kowalska, J.; Dobrzańska, A.; Franek, E.; Helwich, E.; et al. Vitamin D Supplementation Guidelines for General Population and Groups at Risk of Vitamin D Deficiency in Poland—Recommendations of the Polish Society of Pediatric Endocrinology and Diabetes and the Expert Panel With Participation of National Specialist Consultants and Representatives of Scientific Societies—2018 Update. *Front. Endocrinol. (Lausanne).* **2018**, *9*, 246.
76. Lehmann, B.; Genehr, T.; Knuschke, P.; Meurer, M.; Pietzsch, J. UVB-Induced Conversion of 7-Dehydrocholesterol to 1α,25-Dihydroxyvitamin D3 in an In Vitro Human Skin Equivalent Model. *J. Invest. Dermatol.* **2001**, *117*, 1179–1185.
77. Kägi, L.; Bettoni, C.; Pastor-Arroyo, E.M.; Schnitzbauer, U.; Hernando, N.; Wagner, C.A. Regulation of vitamin D metabolizing enzymes in murine renal and extrarenal tissues by dietary phosphate, FGF23, and 1,25(OH) 2 D 3. **2018**.
78. Jones, G.; Prosser, D.E.; Kaufmann, M. 25-Hydroxyvitamin D-24-hydroxylase (CYP24A1): Its important role in the degradation of vitamin D. *Arch. Biochem. Biophys.* **2012**, *523*, 9–18.
79. Holick, M.F. Vitamin D Deficiency. *N. Engl. J. Med.* **2007**, *357*, 266–281.
80. Kato, S. The Function of Vitamin D Receptor in Vitamin D Action. *J. Biochem.* **2000**, *127*, 717–722.
81. Bettoun, D.J.; Burris, T.P.; Houck, K.A.; Buck, D.W.; Stayrook, K.R.; Khalifa, B.; Lu, J.; Chin, W.W.; Nagpal, S. Retinoid X Receptor Is a Nonsilent Major Contributor to Vitamin D Receptor-Mediated Transcriptional Activation. *Mol. Endocrinol.* **2003**, *17*, 2320–2328.
82. Veldurthy, V.; Wei, R.; Oz, L.; Dhawan, P.; Jeon, Y.H.; Christakos, S. Vitamin D, calcium homeostasis and aging. *Bone Res.* **2016**, *4*, 16041.
83. Bikle, D.D. Vitamin D and Bone. *Curr. Osteoporos. Rep.* **2012**, *10*, 151.
84. Dusso, A.S.; Brown, A.J.; Slatopolsky, E. Vitamin D. *Am. J. Physiol. Physiol.* **2005**, *289*, F8–F28.

85. Blaine, J.; Chonchol, M.; Levi, M. Renal control of calcium, phosphate, and magnesium homeostasis. *Clin. J. Am. Soc. Nephrol.* **2015**, *10*, 1257–72.
86. Sahay, M.; Sahay, R. Rickets–vitamin D deficiency and dependency. *Indian J. Endocrinol. Metab.* **2012**, *16*, 164.
87. Kearns, M.D.; Alvarez, J.A.; Seidel, N.; Tangpricha, V. Impact of vitamin D on infectious disease. *Am. J. Med. Sci.* **2015**, *349*, 245–62.
88. Azrielant, S.; Shoenfeld, Y. Vitamin D and Autoimmune Diseases. In; Humana Press, Cham, 2018; pp. 41–55.
89. Rita, M.; Young, I.; Xiong, Y. *Influence of vitamin D on cancer risk and treatment: Why the variability?*;
90. Danik, J.S.; Manson, J.E. Vitamin d and cardiovascular disease. *Curr. Treat. Options Cardiovasc. Med.* **2012**, *14*, 414–24.
91. Kirsty Pourshahidi, L.; Pourshahidi, L.K. Vitamin D and obesity: current perspectives and future directions. *Proc. Nutr. Soc.* **2014**, *74*, 18–20.
92. Parikh, S.J.; Edelman, M.; Uwaifo, G.I.; Freedman, R.J.; Semega-Janneh, M.; Reynolds, J.; Yanovski, J.A. The Relationship between Obesity and Serum 1,25-Dihydroxy Vitamin D Concentrations in Healthy Adults. *J. Clin. Endocrinol. Metab.* **2004**, *89*, 1196–1199.
93. Roth, D.E.; Abrams, S.A.; Aloia, J.; Bergeron, G.; Bourassa, M.W.; Brown, K.H.; Calvo, M.S.; Cashman, K.D.; Combs, G.; De‐Regil, L.M.; et al. Global prevalence and disease burden of vitamin D deficiency: a roadmap for action in low‐ and middle‐income countries. *Ann. N. Y. Acad. Sci.* **2018**, *1430*, 44–79.
94. Palacios, C.; Gonzalez, L. Is vitamin D deficiency a major global public health problem? *J. Steroid Biochem. Mol. Biol.* **2014**, *144 Pt A*, 138–45.
95. Elangovan, H.; Chahal, S.; Gunton, J.E. Vitamin D in liver disease: Current evidence and potential directions. *Biochim. Biophys. Acta - Mol. Basis Dis.* **2017**, *1863*, 907–916.
96. Franca Gois, P.H.; Wolley, M.; Ranganathan, D.; Seguro, A.C. Vitamin D Deficiency in Chronic Kidney Disease: Recent Evidence and Controversies. *Int. J. Environ. Res. Public Health* **2018**, *15*.
97. Walsh, J.S.; Bowles, S.; Evans, A.L. Vitamin D in obesity. *Curr. Opin. Endocrinol. Diabetes Obes.* **2017**, *24*, 389–394.
98. Peterson, C.A.; Belenchia, A.M. *SCIENCE OF MEDICINE*;
99. Ananthakrishnan, A.N. Vitamin D and Inflammatory Bowel Disease. *Gastroenterol. Hepatol. (N. Y).* **2016**, *12*, 513–515.
100. Pereira-Santos, M.; Costa, P.R.F.; Assis, A.M.O.; Santos, C.A.S.T.; Santos, D.B. Obesity and vitamin D deficiency: a systematic review and meta-analysis. *Obes. Rev.* **2015**, *16*, 341–349.
101. Turer, C.B.; Lin, H.; Flores, G. Prevalence of Vitamin D Deficiency Among Overweight and Obese US Children. *Pediatrics* **2013**, *131*,

e152–e161.
102. Durá-Travé, T.; Gallinas-Victoriano, F.; Chueca-Guindulain, M.J.; Berrade-Zubiri, S.; Urretavizcaya-Martinez, M.; Ahmed-Mohamed, L. Assessment of vitamin D status and parathyroid hormone during a combined intervention for the treatment of childhood obesity. *Nutr. Diabetes* **2019**, *9*, 18.
103. Shahwan, M.; Jairoun, A.A.; Khattab, M.H. Association of serum calcium level with body mass index among type 2 diabetes patients in Palestine. *Obes. Med.* **2019**, *15*, 100110.
104. Hetta, H.F.; Fahmy, E.M.; Mohamed, G.A.; Gaber, M.A.; Elkady, A.; Elbadr, M.M.; Al-Kadmy, I.M.S. Does vitamin D status correlate with insulin resistance in obese prediabetic patients? An Egyptian multicenter study. *Diabetes Metab. Syndr. Clin. Res. Rev.* **2019**, *13*, 2813–2817.
105. TEITELBAUM, S.L. Abnormalities of Circulating 25-OH Vitamin D after Jejunal-Ileal Bypass for Obesity. *Ann. Intern. Med.* **1977**, *86*, 289.
106. Compston, J.E.; Vedi, S.; Ledger, J.E.; Webb, A.; Gazet, J.-C.; Pilkington, T.R.E. *Vitamin D status and bone histomorphometry in gross obesity1-3*; 1981;
107. Bell, N.H.; Epstein, S.; Greene, A.; Shary, J.; Oexmann, M.J.; Shaw, S. Evidence for alteration of the vitamin D-endocrine system in obese subjects. *J. Clin. Invest.* **1985**, *76*, 370–373.
108. Liel, Y.; Ulmer, E.; Shary, J.; Hollis, B.W.; Bell, N.H. Low circulating vitamin D in obesity. *Calcif. Tissue Int.* **1988**, *43*, 199–201.
109. Herranz Antolín, S.; García Martínez, M. del C.; Álvarez De Frutos, V. Concentraciones deficientes de vitamina D en pacientes con obesidad mórbida. Estudio de caso-control. *Endocrinol. y Nutr.* **2010**, *57*, 256–261.
110. Kamycheva, E.; Sundsfjord, J.; Jorde, R. Serum parathyroid hormone level is associated with body mass index. The 5th Tromso study. *Eur. J. Endocrinol.* **2004**, *151*, 167–172.
111. Strucińska, M.; Rowicka, G.; Dyląg, H.; Riahi, A.; Bzikowska, A. Dietary intake of vitamin D in obese children aged 1-3 years. *Rocz. Panstw. Zakl. Hig.* **2015**, *66*, 353–60.
112. Dyląg, H.; Rowicka, G.; Strucińska, M.; Riahi, A. Assessment of vitamin D status in children aged 1-5 with simple obesity. *Rocz. Panstw. Zakl. Hig.* **2014**, *65*, 325–30.
113. Karlsson, T.; Andersson, L.; Hussain, A.; Bosaeus, M.; Jansson, N.; Osmancevic, A.; Hulthén, L.; Holmäng, A.; Larsson, I. Lower vitamin D status in obese compared with normal-weight women despite higher vitamin D intake in early pregnancy. *Clin. Nutr.* **2015**, *34*, 892–898.
114. Kull, M.; Kallikorm, R.; Lember, M. Body mass index determines

sunbathing habits: implications on vitamin D levels. *Intern. Med. J.* **2009**, *39*, 256–258.
115. Wortsman, J.; Matsuoka, L.Y.; Chen, T.C.; Lu, Z.; Holick, M.F. Decreased bioavailability of vitamin D in obesity. *Am. J. Clin. Nutr.* **2000**, *72*, 690–693.
116. Wamberg, L.; Christiansen, T.; Paulsen, S.K.; Fisker, S.; Rask, P.; Rejnmark, L.; Richelsen, B.; Pedersen, S.B. Expression of vitamin D-metabolizing enzymes in human adipose tissue—the effect of obesity and diet-induced weight loss. *Int. J. Obes.* **2013**, *37*, 651–657.
117. Ching, S.; Kashinkunti, S.; Niehaus, M.D.; Zinser, G.M. Mammary adipocytes bioactivate 25-hydroxyvitamin D3 and signal via vitamin D3 receptor, modulating mammary epithelial cell growth. *J. Cell. Biochem.* **2011**, *112*, 3393–3405.
118. Thode, J.; Nistrup Madsen, S.; Hey, H.; Lund, B.; Hey, H.; Lund, B.; Sørensen, O.H.; Christensen, M.S. VITAMIN D AND JEJUNOILEAL BYPASS. *Lancet* **1978**, *312*, 264–265.
119. Compston, J.; Laker, M.F.; Woodhead, J.S.; Gazet, J.-C.; Horton, L.W.L.; Ayers, A.B.; Bull, H.J.; Pilkington, T.R.E. BONE DISEASE AFTER JEJUNO-ILEAL BYPASS FOR OBESITY. *Lancet* **1978**, *312*, 1–4.
120. Sitrin, M. Vitamin D Deficiency and Bone Disease in Gastrointestinal Disorders. *Arch. Intern. Med.* **1978**, *138*, 886.
121. PARFITT, A.M. Metabolic Bone Disease After Intestinal Bypass for Treatment of Obesity. *Ann. Intern. Med.* **1978**, *89*, 193.
122. Rosenstreich, S.J.; Rich, C.; Volwiler, W. Deposition in and release of vitamin D3 from body fat: evidence for a storage site in the rat. *J. Clin. Invest.* **1971**, *50*, 679–87.
123. Blum, M.; Dolnikowski, G.; Seyoum, E.; Harris, S.S.; Booth, S.L.; Peterson, J.; Saltzman, E.; Dawson-Hughes, B. Vitamin D(3) in fat tissue. *Endocrine* **2008**, *33*, 90–4.
124. Drincic, A.T.; Armas, L.A.G.; Van Diest, E.E.; Heaney, R.P. Volumetric Dilution, Rather Than Sequestration Best Explains the Low Vitamin D Status of Obesity. *Obesity* **2012**, *20*, 1444–1448.
125. Feingold, K.R.; Grunfeld, C. *Obesity and Dyslipidemia*; MDText.com, Inc., 2000;
126. Vekic, J.; Zeljkovic, A.; Stefanovic, A.; Jelic-Ivanovic, Z.; Spasojevic-Kalimanovska, V. Obesity and dyslipidemia. *Metabolism* **2019**, *92*, 71–81.
127. Chaudhuri, J.R.; Mridula, K.R.; Anamika, A.; Boddu, D.B.; Misra, P.K.; Lingaiah, A.; Balaraju, B.; Bandaru, V.S. Deficiency of 25-hydroxyvitamin d and dyslipidemia in Indian subjects. *J. Lipids* **2013**, *2013*, 623420.
128. Ponda, M.P.; Huang, X.; Odeh, M.A.; Breslow, J.L.; Kaufman, H.W.

Vitamin D May Not Improve Lipid Levels. *Circulation* **2012**, *126*, 270–277.
129. Jiang, X.; Peng, M.; Chen, S.; Wu, S.; Zhang, W. Vitamin D deficiency is associated with dyslipidemia: a cross-sectional study in 3788 subjects. *Curr. Med. Res. Opin.* **2019**, *35*, 1059–1063.
130. Wang, Y.; Si, S.; Liu, J.; Wang, Z.; Jia, H.; Feng, K.; Sun, L.; Song, S.J. The Associations of Serum Lipids with Vitamin D Status. *PLoS One* **2016**, *11*, e0165157.
131. Sun, X.; Cao, Z.-B.; Tanisawa, K.; Oshima, S.; Higuchi, M. Serum 25-Hydroxyvitamin D Concentrations Are Inversely Correlated with Hepatic Lipid Content in Male Collegiate Football Athletes. *Nutrients* **2018**, *10*.
132. Lacour, B.; Basile, C.; Drüeke, T.; Funck-Brentano, J.L. Parathyroid function and lipid metabolism in the rat. *Miner. Electrolyte Metab.* **1982**, *7*, 157–65.
133. Barger-Lux, M.J.; Heaney, R.P.; Lanspa, S.J.; Healy, J.C.; DeLuca, H.F. An investigation of sources of variation in calcium absorption efficiency. *J. Clin. Endocrinol. Metab.* **1995**, *80*, 406–411.
134. Chiu, K.C.; Chu, A.; Go, V.L.W.; Saad, M.F. Hypovitaminosis D is associated with insulin resistance and β cell dysfunction. *Am. J. Clin. Nutr.* **2004**, *79*, 820–825.
135. Earthman, C.P.; Beckman, L.M.; Masodkar, K.; Sibley, S.D. The link between obesity and low circulating 25-hydroxyvitamin D concentrations: considerations and implications. *Int. J. Obes.* **2012**, *36*, 387–396.
136. Jorde, R.; Grimnes, G. Vitamin D and metabolic health with special reference to the effect of vitamin D on serum lipids. *Prog. Lipid Res.* **2011**, *50*, 303–312.
137. Jorde, R.; Figenschau, Y.; Hutchinson, M.; Emaus, N.; Grimnes, G. High serum 25-hydroxyvitamin D concentrations are associated with a favorable serum lipid profile. *Eur. J. Clin. Nutr.* **2010**, *64*, 1457–1464.
138. Zittermann, A.; F. Gummert, J.; Borgermann, J. The Role of Vitamin D in Dyslipidemia and Cardiovascular Disease. *Curr. Pharm. Des.* **2011**, *17*, 933–942.
139. Eich, C.; Manzo, C.; Keijzer, S. de; Bakker, G.-J.; Reinieren-Beeren, I.; García-Parajo, M.F.; Cambi, A. Changes in membrane sphingolipid composition modulate dynamics and adhesion of integrin nanoclusters. *Sci. Rep.* **2016**, *6*, 20693.
140. Wang, G.; Spassieva, S.D.; Bieberich, E. Ceramide and S1P Signaling in Embryonic Stem Cell Differentiation. *Methods Mol. Biol.* **2018**, *1697*, 153–171.
141. Bartke, N.; Hannun, Y.A. Bioactive sphingolipids: metabolism and function. *J. Lipid Res.* **2009**, *50 Suppl*, S91-6.

142. Ogretmen, B. Sphingolipid metabolism in cancer signalling and therapy. *Nat. Rev. Cancer* **2017**, *18*, 33–50.
143. Gault, C.R.; Obeid, L.M.; Hannun, Y.A. *An overview of sphingolipid metabolism: from synthesis to breakdown*;
144. Tidhar, R.; Futerman, A.H. The complexity of sphingolipid biosynthesis in the endoplasmic reticulum. *Biochim. Biophys. Acta - Mol. Cell Res.* **2013**, *1833*, 2511–2518.
145. Hanada, K. Serine palmitoyltransferase, a key enzyme of sphingolipid metabolism. *Biochim. Biophys. Acta - Mol. Cell Biol. Lipids* **2003**, *1632*, 16–30.
146. Mullen, T.D.; Hannun, Y.A.; Obeid, L.M.; Johnson, R.H. Ceramide synthases at the centre of sphingolipid metabolism and biology. **2012**.
147. Young, S.A.; Mina, J.G.; Denny, P.W.; Smith, T.K. Sphingolipid and Ceramide Homeostasis: Potential Therapeutic Targets. *Biochem. Res. Int.* **2012**, *2012*, 1–12.
148. Ichikawa, S.; Hirabayashi, Y. Glucosylceramide synthase and glycosphingolipid synthesis. *Trends Cell Biol.* **1998**, *8*, 198–202.
149. Shayman, J.A. Glucosylceramide and Galactosylceramide Synthase. In *Sphingolipid Biology*; Springer Japan: Tokyo, 2006; pp. 83–94.
150. Villani, M.; Subathra, M.; Im, Y.-B.; Choi, Y.; Signorelli, P.; Poeta, M. Del; Luberto, C. Sphingomyelin synthases regulate production of diacylglycerol at the Golgi. *Biochem. J.* **2008**, *414*, 31.
151. Angelo, G.D.'; Capasso, S.; Sticco, L.; Russo, D. Glycosphingolipids: synthesis and functions.
152. Goñi, F.M.; Alonso, A. Sphingomyelinases: enzymology and membrane activity. *FEBS Lett.* **2002**, *531*, 38–46.
153. MAO, C.; Obeid, L.M. Ceramidases: regulators of cellular responses mediated by ceramide, sphingosine, and sphingosine-1-phosphate. *Biochim. Biophys. Acta - Mol. Cell Biol. Lipids* **2008**, *1781*, 424–434.
154. Johnson, K.R.; Johnson, K.Y.; Becker, K.P.; Bielawski, J.; Mao, C.; Obeid, L.M. Role of Human Sphingosine-1-phosphate Phosphatase 1 in the Regulation of Intra-and Extracellular Sphingosine-1-phosphate Levels and Cell Viability*. **2003**.
155. Hla, T.; Dannenberg, A.J. Sphingolipid signaling in metabolic disorders. **2012**.
156. Young, M.M.; Wang, H.-G. Sphingolipids as Regulators of Autophagy and Endocytic Trafficking. *Adv. Cancer Res.* **2018**, *140*, 27–60.
157. Hidari KIPJ, K.I.-P.J.; Ichikawa, S.; Fujita, T.; Sakiyama, H.; Hirabayashi, Y. Complete removal of sphingolipids from the plasma membrane disrupts cell to substratum adhesion of mouse melanoma cells. *J. Biol. Chem.* **1996**, *271*, 14636–41.
158. van Echten-Deckert, G. Sphingolipid extraction and analysis by thin-

layer chromatography. *Methods Enzymol.* **2000**, *312*, 64–79.
159. Čačić, M.; Šoštarić, K.; Weber-Schürholz, S.; Müthing, J. Immunohistological analyses of neutral glycosphingolipids and gangliosides in normal mouse skeletal muscle and in mice with neuromuscular diseases. *Glycoconj. J.* **1995**, *12*, 721–728.
160. O'Connor, P.B.; Budnik, B.A.; Ivleva, V.B.; Kaur, P.; Moyer, S.C.; Pittman, J.L.; Costello, C.E. A high pressure matrix-assisted laser desorption ion source for Fourier transform mass spectrometry designed to accommodate large targets with diverse surfaces. *J. Am. Soc. Mass Spectrom.* **2004**, *15*, 128–132.
161. Houjou, T.; Yamatani, K.; Nakanishi, H.; Imagawa, M.; Shimizu, T.; Taguchi, R. Rapid and selective identification of molecular species in phosphatidylcholine and sphingomyelin by conditional neutral loss scanning and MS3. *Rapid Commun. Mass Spectrom.* **2004**, *18*, 3123–3130.
162. Sullards, M.C.; Allegood, J.C.; Kelly, S.; Wang, E.; Haynes, C.A.; Park, H.; Chen, Y.; Merrill, A.H. Structure- Specific, Quantitative Methods for Analysis of Sphingolipids by Liquid Chromatography–Tandem Mass Spectrometry: "Inside- Out" Sphingolipidomics. In *Methods in enzymology*; 2007; Vol. 432, pp. 83–115.
163. Kirsch, S.; Zarei, M.; Cindrić, M.; Müthing, J.; Bindila, L.; Peter-Katalinić, J. On-Line Nano-HPLC/ESI QTOF MS and Tandem MS for Separation, Detection, and Structural Elucidation of Human Erythrocytes Neutral Glycosphingolipid Mixture. *Anal. Chem.* **2008**, *80*, 4711–4722.
164. Pól, J.; Vidová, V.; Kruppa, G.; Kobliha, V.; Novák, P.; Lemr, K.; Kotiaho, T.; Kostiainen, R.; Havlíček, V.; Volný, M. Automated Ambient Desorption−Ionization Platform for Surface Imaging Integrated with a Commercial Fourier Transform Ion Cyclotron Resonance Mass Spectrometer. *Anal. Chem.* **2009**, *81*, 8479–8487.
165. Wucherpfennig, K.W. Structural Basis of Molecular Mimicry. *J. Autoimmun.* **2001**, *16*, 293–302.
166. Sommer, U.; Herscovitz, H.; Welty, F.K.; Costello, C.E. LC-MS-based method for the qualitative and quantitative analysis of complex lipid mixtures. *J. Lipid Res.* **2006**, *47*, 804–814.
167. Cacas, J.-L.; Melser, S.; Domergue, F.; Joubès, J.; Bourdenx, B.; Schmitter, J.-M.; Mongrand, S. Rapid nanoscale quantitative analysis of plant sphingolipid long-chain bases by GC-MS. *Anal. Bioanal. Chem.* **2012**, *403*, 2745–2755.
168. Luftmann, H. A simple device for the extraction of TLC spots: direct coupling with an electrospray mass spectrometer. *Anal. Bioanal. Chem.* **2004**, *378*, 964–968.
169. Peng, S.; Edler, M.; Ahlmann, N.; Hoffmann, T.; Franzke, J. A new interface to couple thin-layer chromatography with laser

desorption/atmospheric pressure chemical ionization mass spectrometry for plate scanning. *Rapid Commun. Mass Spectrom.* **2005**, *19*, 2789–2793.
170. Munoz-Garcia, A.; Ro, J.; Brown, J.C.; Williams, J.B. Cutaneous water loss and sphingolipids in the stratum corneum of house sparrows, Passer domesticus L., from desert and mesic environments as determined by reversed phase high-performance liquid chromatography coupled with atmospheric pressure photospray ionization mass spectrometry. *J. Exp. Biol.* **2008**, *211*, 447–458.
171. Tsugawa, H.; Ikeda, K.; Tanaka, W.; Senoo, Y.; Arita, M.; Arita, M. Comprehensive identification of sphingolipid species by in silico retention time and tandem mass spectral library. *J. Cheminform.* **2017**, *9*, 19.
172. Masood, M.A.; Rao, R.P.; Acharya, J.K.; Blonder, J.; Veenstra, T.D. Quantitation of Multiple Sphingolipid Classes Using Normal and Reversed-Phase LC–ESI–MS/MS: Comparative Profiling of Two Cell Lines. *Lipids* **2012**, *47*, 209–226.
173. Bobzin, S.C.; Yang, S.; Kasten, T.P. Application of liquid chromatography–nuclear magnetic resonance spectroscopy to the identification of natural products. *J. Chromatogr. B Biomed. Sci. Appl.* **2000**, *748*, 259–267.
174. Montealegre, C.; Verardo, V.; Luisa Marina, M.; Caboni, M.F. Analysis of glycerophospho- and sphingolipids by CE. *Electrophoresis* **2014**, *35*, 779–792.
175. Torretta, E.; Vasso, M.; Fania, C.; Capitanio, D.; Bergante, S.; Piccoli, M.; Tettamanti, G.; Anastasia, L.; Gelfi, C. Application of direct HPTLC-MALDI for the qualitative and quantitative profiling of neutral and acidic glycosphingolipids: The case of NEU3 overexpressing C2C12 murine myoblasts. *Electrophoresis* **2014**, *35*, 1319–1328.
176. Torretta, E.; Fania, C.; Vasso, M.; Gelfi, C. HPTLC-MALDI MS for (glyco)sphingolipid multiplexing in tissues and blood: A promising strategy for biomarker discovery and clinical applications. *Electrophoresis* **2016**, *37*, 2036–2049.
177. Salo, P.K.; Salomies, H.; Harju, K.; Ketola, R.A.; Kotiaho, T.; Yli-Kauhaluoma, J.; Kostiainen, R. Analysis of Small Molecules by Ultra Thin-Layer Chromatography-Atmospheric Pressure Matrix-Assisted Laser Desorption/Ionization Mass Spectrometry. *J. Am. Soc. Mass Spectrom.* **2005**, *16*, 906–915.
178. Tames, F.; Watson, I.D.; Morden, W.; Wilson, I.D. Detection and identification of morphine in urine extracts using thin-layer chromatography and tandem mass spectrometry. *J. Chromatogr. B. Biomed. Sci. Appl.* **1999**, *729*, 341–6.

179. Ellulu, M.S.; Patimah, I.; Khaza'ai, H.; Rahmat, A.; Abed, Y. Obesity and inflammation: the linking mechanism and the complications. *Arch. Med. Sci.* **2017**, *13*, 851.
180. Boden, G. Obesity and free fatty acids. *Endocrinol. Metab. Clin. North Am.* **2008**, *37*, 635–46, viii–ix.
181. Marseglia, L.; Manti, S.; D'angelo, G.; Nicotera, A.; Parisi, E.; Rosa, G. Di; Gitto, E.; Arrigo, T. Oxidative Stress in Obesity: A Critical Component in Human Diseases. *Int. J. Mol. Sci* **2015**, *16*, 378–400.
182. Engin, A.B. What Is Lipotoxicity? In *Advances in experimental medicine and biology*; 2017; Vol. 960, pp. 197–220.
183. Alkhouri, N.; Dixon, L.J.; Feldstein, A.E. Lipotoxicity in nonalcoholic fatty liver disease: not all lipids are created equal. *Expert Rev. Gastroenterol. Hepatol.* **2009**, *3*, 445–51.
184. Oh, Y.S.; Bae, G.D.; Baek, D.J.; Park, E.-Y.; Jun, H.-S. Fatty Acid-Induced Lipotoxicity in Pancreatic Beta-Cells During Development of Type 2 Diabetes. *Front. Endocrinol. (Lausanne).* **2018**, *9*, 384.
185. Unger, R.H.; Scherer, P.E. Gluttony, Sloth and the Metabolic Syndrome: A Roadmap to Lipotoxicity.
186. Iqbal, J.; Walsh, M.T.; Hammad, S.M.; Hussain, M.M. Sphingolipids and Lipoproteins in Health and Metabolic Disorders. *Trends Endocrinol. Metab.* **2017**, *28*, 506–518.
187. Holland, W.L.; Bikman, B.T.; Wang, L.-P.; Yuguang, G.; Sargent, K.M.; Bulchand, S.; Knotts, T.A.; Shui, G.; Clegg, D.J.; Wenk, M.R.; et al. Lipid-induced insulin resistance mediated by the proinflammatory receptor TLR4 requires saturated fatty acid–induced ceramide biosynthesis in mice. *J. Clin. Invest.* **2011**, *121*, 1858–1870.
188. Cuschieri, J.; Bulger, E.; Billgrin, J.; Garcia, I.; Maier, R. V. Acid Sphingomyelinase Is Required for Lipid Raft TLR4 Complex Formation. *Surg. Infect. (Larchmt).* **2007**, *8*, 91–106.
189. Samad, F.; Hester, K.D.; Yang, G.; Hannun, Y.A.; Bielawski, J. Altered Adipose and Plasma Sphingolipid Metabolism in Obesity. *Diabetes* **2006**, *55*, 2579–2587.
190. Amar, J.; Chabo, C.; Waget, A.; Klopp, P.; Vachoux, C.; Bermúdez-Humarán, L.G.; Smirnova, N.; Bergé, M.; Sulpice, T.; Lahtinen, S.; et al. Intestinal mucosal adherence and translocation of commensal bacteria at the early onset of type 2 diabetes: molecular mechanisms and probiotic treatment. *EMBO Mol. Med.* **2011**, *3*, 559.
191. Shi, H.; Kokoeva, M. V; Inouye, K.; Tzameli, I.; Yin, H.; Flier, J.S. TLR4 links innate immunity and fatty acid-induced insulin resistance. *J. Clin. Invest.* **2006**, *116*, 3015–25.
192. Surmi, B.K.; Hasty, A.H. Macrophage infiltration into adipose tissue: initiation, propagation and remodeling. *Futur. Lipidol* **2008**, *3*, 545–556.

193. Lee, Y.S.; Kim, J.; Osborne, O.; Oh, D.Y.; Sasik, R.; Schenk, S.; Chen, A.; Chung, H.; Murphy, A.; Watkins, S.M.; et al. Increased adipocyte O2 consumption triggers HIF-1α, causing inflammation and insulin resistance in obesity. *Cell* **2014**, *157*, 1339–52.
194. Rodríguez-Hernández, H.; Simental-Mendía, L.E.; Rodríguez-Ramírez, G.; Reyes-Romero, M.A. Obesity and inflammation: epidemiology, risk factors, and markers of inflammation. *Int. J. Endocrinol.* **2013**, *2013*, 678159.
195. Choi, S.; Snider, A.J. Sphingolipids in High Fat Diet and Obesity-Related Diseases. *Mediators Inflamm.* **2015**, *2015*, 1–12.
196. Hirosumi, J.; Tuncman, G.; Chang, L.; Görgün, C.Z.; Uysal, K.T.; Maeda, K.; Karin, M.; Hotamisligil, G.S. A central role for JNK in obesity and insulin resistance. *Nature* **2002**, *420*, 333–336.
197. Medzhitov, R. Toll-like receptors and innate immunity. *Nat. Rev. Immunol.* **2001**, *1*, 135–145.
198. Dressler, K.; Mathias, S.; Kolesnick, R. Tumor necrosis factor-alpha activates the sphingomyelin signal transduction pathway in a cell-free system. *Science (80-.).* **1992**, *255*, 1715–1718.
199. Schütze, S.; Wiegmann, K.; Machleidt, T.; Krönke, M. TNF-induced activation of NF-kappa B. *Immunobiology* **1995**, *193*, 193–203.
200. Teruel, T.; Hernandez, R.; Lorenzo, M. Ceramide mediates insulin resistance by tumor necrosis factor-alpha in brown adipocytes by maintaining Akt in an inactive dephosphorylated state. *Diabetes* **2001**, *50*, 2563–71.
201. Kolak, M.; Westerbacka, J.; Velagapudi, V.R.; Wågsäter, D.; Yetukuri, L.; Makkonen, J.; Rissanen, A.; Häkkinen, A.-M.; Lindell, M.; Bergholm, R.; et al. Adipose tissue inflammation and increased ceramide content characterize subjects with high liver fat content independent of obesity. *Diabetes* **2007**, *56*, 1960–8.
202. Hammad, S.M.; Pierce, J.S.; Soodavar, F.; Smith, K.J.; Al Gadban, M.M.; Rembiesa, B.; Klein, R.L.; Hannun, Y.A.; Bielawski, J.; Bielawska, A. Blood sphingolipidomics in healthy humans: impact of sample collection methodology. *J. Lipid Res.* **2010**, *51*, 3074–3087.
203. Chaurasia, B.; Summers, S.A. Ceramides – Lipotoxic Inducers of Metabolic Disorders. *Trends Endocrinol. Metab.* **2015**, *26*, 538–550.
204. Patwardhan, G.A.; Beverly, L.J.; Siskind, L.J. Sphingolipids and mitochondrial apoptosis.
205. Lipina, C.; Hundal, H.S. Sphingolipids: agents provocateurs in the pathogenesis of insulin resistance. *Diabetologia* **2011**, *54*, 1596–1607.
206. Cogolludo, A.; Villamor, E.; Perez-Vizcaino, F.; Moreno, L. Molecular Sciences Ceramide and Regulation of Vascular Tone.
207. Turinsky, J.; O'Sullivan, D.M.; Bayly, B.P. 1,2-Diacylglycerol and ceramide levels in insulin-resistant tissues of the rat in vivo. *J. Biol.*

Chem. **1990**, *265*, 16880–5.
208. Rothwell, N.J.; Stock, M.J. The development of obesity in animals: the role of dietary factors. *Clin. Endocrinol. Metab.* **1984**, *13*, 437–49.
209. Buettner, R.; Schölmerich, J.; Bollheimer, L.C. High-fat Diets: Modeling the Metabolic Disorders of Human Obesity in Rodents*. *Obesity* **2007**, *15*, 798–808.
210. Warwick, Z.S.; Schiffman, S.S. Role of dietary fat in calorie intake and weight gain. *Neurosci. Biobehav. Rev.* **1992**, *16*, 585–96.
211. Hu, W.; Bielawski, J.; Samad, F.; Merrill, A.H.; Cowart, L.A. Palmitate increases sphingosine-1-phosphate in C2C12 myotubes via upregulation of sphingosine kinase message and activity. *J. Lipid Res.* **2009**, *50*, 1852–1862.
212. Abildgaard, J.; Henstridge, D.C.; Pedersen, A.T.; Langley, K.G.; Scheele, C.; Pedersen, B.K.; Lindegaard, B.; Johannsen, D. In Vitro Palmitate Treatment of Myotubes from Postmenopausal Women Leads to Ceramide Accumulation, Inflammation and Affected Insulin Signaling. *PLoS One* **2014**, *9*, e101555.
213. Cinar, R.; Godlewski, G.; Liu, J.; Tam, J.; Jourdan, T.; Mukhopadhyay, B.; Harvey-White, J.; Kunos, G. Hepatic cannabinoid-1 receptors mediate diet-induced insulin resistance by increasing de novo synthesis of long-chain ceramides. *Hepatology* **2014**, *59*, 143–53.
214. Bruce, C.R.; Risis, S.; Babb, J.R.; Yang, C.; Kowalski, G.M.; Selathurai, A.; Lee-Young, R.S.; Weir, J.M.; Yoshioka, K.; Takuwa, Y.; et al. Overexpression of Sphingosine Kinase 1 Prevents Ceramide Accumulation and Ameliorates Muscle Insulin Resistance in High-Fat Diet-Fed Mice. *Diabetes* **2012**, *61*, 3148–3155.
215. Chocian, G.; Chabowski, A.; Żendzian-Piotrowska, M.; Harasim, E.; Łukaszuk, B.; Górski, J. High fat diet induces ceramide and sphingomyelin formation in rat's liver nuclei. *Mol. Cell. Biochem.* **2010**, *340*, 125–131.
216. Turner, N.; Kowalski, G.M.; Leslie, S.J.; Risis, S.; Yang, C.; Lee-Young, R.S.; Babb, J.R.; Meikle, P.J.; Lancaster, G.I.; Henstridge, D.C.; et al. Distinct patterns of tissue-specific lipid accumulation during the induction of insulin resistance in mice by high-fat feeding. *Diabetologia* **2013**, *56*, 1638–1648.
217. Shah, C.; Yang, G.; Lee, I.; Bielawski, J.; Hannun, Y.A.; Samad, F. Protection from High Fat Diet-induced Increase in Ceramide in Mice Lacking Plasminogen Activator Inhibitor 1. *J. Biol. Chem.* **2008**, *283*, 13538–13548.
218. Bikman, B.T.; Guan, Y.; Shui, G.; Siddique, M.M.; Holland, W.L.; Kim, J.Y.; Fabriàs, G.; Wenk, M.R.; Summers, S.A. Fenretinide Prevents Lipid-induced Insulin Resistance by Blocking Ceramide Biosynthesis. *J. Biol. Chem.* **2012**, *287*, 17426–17437.

219. Lanza, I.R.; Blachnio-Zabielska, A.; Johnson, M.L.; Schimke, J.M.; Jakaitis, D.R.; Lebrasseur, N.K.; Jensen, M.D.; Sreekumaran Nair, K.; Zabielski, P. Influence of fish oil on skeletal muscle mitochondrial energetics and lipid metabolites during high-fat diet. *Am. J. Physiol. Metab.* **2013**, *304*, E1391–E1403.
220. Liu, Y.; Turdi, S.; Park, T.; Morris, N.J.; Deshaies, Y.; Xu, A.; Sweeney, G. Adiponectin Corrects High-Fat Diet-Induced Disturbances in Muscle Metabolomic Profile and Whole-Body Glucose Homeostasis. *Diabetes* **2013**, *62*, 743–752.
221. Sankella, S.; Garg, A.; Agarwal, A.K. Activation of Sphingolipid Pathway in the Livers of Lipodystrophic Agpat2-/- Mice. *J. Endocr. Soc.* **2017**, *1*, 980–993.
222. Bruce, C.R.; Risis, S.; Babb, J.R.; Yang, C.; Lee-Young, R.S.; Henstridge, D.C.; Febbraio, M.A. The Sphingosine-1-Phosphate Analog FTY720 Reduces Muscle Ceramide Content and Improves Glucose Tolerance in High Fat-Fed Male Mice. *Endocrinology* **2013**, *154*, 65–76.
223. Turpin, S.M.; Nicholls, H.T.; Willmes, D.M.; Mourier, A.; Brodesser, S.; Wunderlich, C.M.; Mauer, J.; Xu, E.; Hammerschmidt, P.; Brönneke, H.S.; et al. Obesity-Induced CerS6-Dependent C16:0 Ceramide Production Promotes Weight Gain and Glucose Intolerance. *Cell Metab.* **2014**, *20*, 678–686.
224. Lyn-Cook, L.E.; Lawton, M.; Tong, M.; Silbermann, E.; Longato, L.; Jiao, P.; Mark, P.; Wands, J.R.; Xu, H.; de la Monte, S.M. Hepatic Ceramide May Mediate Brain Insulin Resistance and Neurodegeneration in Type 2 Diabetes and Non-alcoholic Steatohepatitis. *J. Alzheimer's Dis.* **2009**, *16*, 715–729.
225. Longato, L.; Tong, M.; Wands, J.R.; de la Monte, S.M. High fat diet induced hepatic steatosis and insulin resistance: Role of dysregulated ceramide metabolism. *Hepatol. Res.* **2012**, *42*, 412–427.
226. Ussher, J.R.; Koves, T.R.; Cadete, V.J.J.; Zhang, L.; Jaswal, J.S.; Swyrd, S.J.; Lopaschuk, D.G.; Proctor, S.D.; Keung, W.; Muoio, D.M.; et al. Inhibition of De Novo Ceramide Synthesis Reverses Diet-Induced Insulin Resistance and Enhances Whole-Body Oxygen Consumption. *Diabetes* **2010**, *59*, 2453–2464.
227. Dekker, M.J.; Baker, C.; Naples, M.; Samsoondar, J.; Zhang, R.; Qiu, W.; Sacco, J.; Adeli, K. Inhibition of sphingolipid synthesis improves dyslipidemia in the diet-induced hamster model of insulin resistance: Evidence for the role of sphingosine and sphinganine in hepatic VLDL-apoB100 overproduction. *Atherosclerosis* **2013**, *228*, 98–109.
228. Li, Z.; Zhang, H.; Liu, J.; Liang, C.-P.; Li, Y.; Li, Y.; Teitelman, G.; Beyer, T.; Bui, H.H.; Peake, D.A.; et al. Reducing Plasma Membrane Sphingomyelin Increases Insulin Sensitivity. *Mol. Cell. Biol.* **2011**, *31*,

4205–4218.
229. Kurek, K.; Piotrowska, D.M.; Wiesiołek-Kurek, P.; Łukaszuk, B.; Chabowski, A.; Górski, J.; Żendzian-Piotrowska, M. Inhibition of ceramide *de novo* synthesis reduces liver lipid accumulation in rats with nonalcoholic fatty liver disease. *Liver Int.* **2014**, *34*, 1074–1083.
230. Boini, K.M.; Zhang, C.; Xia, M.; Poklis, J.L.; Li, P.-L. Role of sphingolipid mediator ceramide in obesity and renal injury in mice fed a high-fat diet. *J. Pharmacol. Exp. Ther.* **2010**, *334*, 839–46.
231. Haus, J.M.; Kashyap, S.R.; Kasumov, T.; Zhang, R.; Kelly, K.R.; Defronzo, R.A.; Kirwan, J.P. Plasma Ceramides Are Elevated in Obese Subjects With Type 2 Diabetes and Correlate With the Severity of Insulin Resistance. *Diabetes* **2009**, *58*, 337–343.
232. Majumdar, I.; Mastrandrea, L.D. Serum sphingolipids and inflammatory mediators in adolescents at risk for metabolic syndrome. *Endocrine* **2012**, *41*, 442–449.
233. Raichur, S.; Brunner, B.; Bielohuby, M.; Hansen, G.; Pfenninger, A.; Wang, B.; Bruning, J.C.; Larsen, P.J.; Tennagels, N. The role of C16:0 ceramide in the development of obesity and type 2 diabetes: CerS6 inhibition as a novel therapeutic approach. *Mol. Metab.* **2019**, *21*, 36–50.
234. Turpin-Nolan, S.M.; Hammerschmidt, P.; Chen, W.; Jais, A.; Timper, K.; Awazawa, M.; Brodesser, S.; Brüning, J.C. CerS1-Derived C18:0 Ceramide in Skeletal Muscle Promotes Obesity-Induced Insulin Resistance. *Cell Rep.* **2019**, *26*, 1-10.e7.
235. Bielawska, A.; Crane, H.M.; Liotta, D.; Obeid, L.M.; Hannun, Y.A. Selectivity of ceramide-mediated biology. Lack of activity of erythro-dihydroceramide. *J. Biol. Chem.* **1993**, *268*, 26226–32.
236. Mitoma, J.; Ito, M.; Furuya, S.; Hirabayashi, Y. Bipotential roles of ceramide in the growth of hippocampal neurons: Promotion of cell survival and dendritic outgrowth in dose- and developmental stage-dependent manners. *J. Neurosci. Res.* **1998**, *51*, 712–722.
237. Summers, S.A.; Garza, L.A.; Zhou, H.; Birnbaum, M.J. Regulation of insulin-stimulated glucose transporter GLUT4 translocation and Akt kinase activity by ceramide. *Mol. Cell. Biol.* **1998**, *18*, 5457–64.
238. Zheng, W.; Kollmeyer, J.; Symolon, H.; Momin, A.; Munter, E.; Wang, E.; Kelly, S.; Allegood, J.C.; Liu, Y.; Peng, Q.; et al. Ceramides and other bioactive sphingolipid backbones in health and disease: Lipidomic analysis, metabolism and roles in membrane structure, dynamics, signaling and autophagy. **2006**, *1758*, 1864–1884.
239. Brozinick, J.T.; Hawkins, E.; Hoang Bui, H.; Kuo, M.-S.; Tan, B.; Kievit, P.; Grove, K. Plasma sphingolipids are biomarkers of metabolic syndrome in non-human primates maintained on a Western-style diet. *Int. J. Obes. (Lond).* **2013**, *37*, 1064–70.

240. Lopez, X.; Goldfine, A.B.; Holland, W.L.; Gordillo, R.; Scherer, P.E. Plasma ceramides are elevated in female children and adolescents with type 2 diabetes. *J. Pediatr. Endocrinol. Metab.* **2013**, *26*, 995–8.
241. Mamtani, M.; Meikle, P.J.; Kulkarni, H.; Weir, J.M.; Barlow, C.K.; Jowett, J.B.; Bellis, C.; Dyer, T.D.; Almasy, L.; Mahaney, M.C.; et al. Plasma dihydroceramide species associate with waist circumference in Mexican American families. *Obesity (Silver Spring).* **2014**, *22*, 950–6.
242. Bergman, B.C.; Brozinick, J.T.; Strauss, A.; Bacon, S.; Kerege, A.; Bui, H.H.; Sanders, P.; Siddall, P.; Kuo, M.S.; Perreault, L. Serum sphingolipids: relationships to insulin sensitivity and changes with exercise in humans. *Am. J. Physiol. - Endocrinol. Metab.* **2015**, *309*, E398.
243. Wigger, L.; Cruciani-Guglielmacci, C.; Nicolas, A.; Denom, J.; Fernandez, N.; Fumeron, F.; Marques-Vidal, P.; Ktorza, A.; Kramer, W.; Schulte, A.; et al. Plasma Dihydroceramides Are Diabetes Susceptibility Biomarker Candidates in Mice and Humans. *Cell Rep.* **2017**, *18*, 2269–2279.
244. Siddique, M.M.; Li, Y.; Chaurasia, B.; Kaddai, V.A.; Summers, S.A. Dihydroceramides: From Bit Players to Lead Actors. *J. Biol. Chem.* **2015**, *290*, 15371–9.
245. Holland, W.L.; Brozinick, J.T.; Wang, L.-P.; Hawkins, E.D.; Sargent, K.M.; Liu, Y.; Narra, K.; Hoehn, K.L.; Knotts, T.A.; Siesky, A.; et al. Inhibition of Ceramide Synthesis Ameliorates Glucocorticoid-, Saturated-Fat-, and Obesity-Induced Insulin Resistance. *Cell Metab.* **2007**, *5*, 167–179.
246. Zhang, Q.-J.; Holland, W.L.; Wilson, L.; Tanner, J.M.; Kearns, D.; Cahoon, J.M.; Pettey, D.; Losee, J.; Duncan, B.; Gale, D.; et al. Ceramide mediates vascular dysfunction in diet-induced obesity by PP2A-mediated dephosphorylation of the eNOS-Akt complex. *Diabetes* **2012**, *61*, 1848–59.
247. Barbarroja, N.; Rodriguez-Cuenca, S.; Nygren, H.; Camargo, A.; Pirraco, A.; Relat, J.; Cuadrado, I.; Pellegrinelli, V.; Medina-Gomez, G.; Lopez-Pedrera, C.; et al. Increased dihydroceramide/ceramide ratio mediated by defective expression of degs1 impairs adipocyte differentiation and function. *Diabetes* **2015**, *64*, 1180–92.
248. Jiang, X.-C.; Paultre, F.; Pearson, T.A.; Reed, R.G.; Francis, C.K.; Lin, M.; Berglund, L.; Tall, A.R. *Plasma Sphingomyelin Level as a Risk Factor for Coronary Artery Disease*; 2000;
249. Eisinger, K.; Liebisch, G.; Schmitz, G.; Aslanidis, C.; Krautbauer, S.; Buechler, C. Lipidomic analysis of serum from high fat diet induced obese mice. *Int. J. Mol. Sci.* **2014**, *15*, 2991–3002.
250. Norris, G.H.; Porter, C.M.; Jiang, C.; Millar, C.L.; Blesso, C.N. Dietary sphingomyelin attenuates hepatic steatosis and adipose

tissue inflammation in high-fat-diet-induced obese mice. *J. Nutr. Biochem.* **2017**, *40*, 36–43.
251. Mitsutake, S.; Zama, K.; Yokota, H.; Yoshida, T.; Tanaka, M.; Mitsui, M.; Ikawa, M.; Okabe, M.; Tanaka, Y.; Yamashita, T.; et al. Dynamic modification of sphingomyelin in lipid microdomains controls development of obesity, fatty liver, and type 2 diabetes. *J. Biol. Chem.* **2011**, *286*, 28544–55.
252. Hanamatsu, H.; Ohnishi, S.; Sakai, S.; Yuyama, K.; Mitsutake, S.; Takeda, H.; Hashino, S.; Igarashi, Y. Altered levels of serum sphingomyelin and ceramide containing distinct acyl chains in young obese adults. *Nutr. Diabetes* **2014**, *4*, e141.
253. Tulipani, S.; Palau-Rodriguez, M.; Miñarro Alonso, A.; Cardona, F.; Marco-Ramell, A.; Zonja, B.; Lopez de Alda, M.; Muñoz-Garach, A.; Sanchez-Pla, A.; Tinahones, F.J.; et al. Biomarkers of Morbid Obesity and Prediabetes by Metabolomic Profiling of Human Discordant Phenotypes. *Clin. Chim. Acta* **2016**, *463*, 53–61.
254. Bagheri, M.; Djazayery, A.; Farzadfar, F.; Qi, L.; Yekaninejad, M.S.; Aslibekyan, S.; Chamari, M.; Hassani, H.; Koletzko, B.; Uhl, O. Plasma metabolomic profiling of amino acids and polar lipids in Iranian obese adults. *Lipids Health Dis.* **2019**, *18*, 94.
255. Hellmuth, C.; Kirchberg, F.F.; Brandt, S.; Moß, A.; Walter, V.; Rothenbacher, D.; Brenner, H.; Grote, V.; Gruszfeld, D.; Socha, P.; et al. An individual participant data meta-analysis on metabolomics profiles for obesity and insulin resistance in European children. *Sci. Rep.* **2019**, *9*, 5053.
256. Im, S.-S.; Park, H.Y.; Shon, J.C.; Chung, I.-S.; Cho, H.C.; Liu, K.-H.; Song, D.-K. Plasma sphingomyelins increase in pre-diabetic Korean men with abdominal obesity. *PLoS One* **2019**, *14*, e0213285.
257. Knowles, C.J.; Cebova, M.; Pinz, I.M. Palmitate Diet-induced Loss of Cardiac Caveolin-3: A Novel Mechanism for Lipid-induced Contractile Dysfunction. *PLoS One* **2013**, *8*, e61369.
258. Kleuser, B. Divergent Role of Sphingosine 1-Phosphate in Liver Health and Disease. *Int. J. Mol. Sci.* **2018**, *19*, 722.
259. Danieli-Betto, D.; Peron, S.; Germinario, E.; Zanin, M.; Sorci, G.; Franzoso, S.; Sandonà, D.; Betto, R. Sphingosine 1-phosphate signaling is involved in skeletal muscle regeneration. *Am. J. Physiol. Physiol.* **2010**, *298*, C550–C558.
260. Thuy, A. V.; Reimann, C.-M.; Hemdan, N.Y.A.; Gräler, M.H. Sphingosine 1-Phosphate in Blood: Function, Metabolism, and Fate. *Cell. Physiol. Biochem.* **2014**, *34*, 158–171.
261. Wang, J.; Badeanlou, L.; Bielawski, J.; Ciaraldi, T.P.; Samad, F. Sphingosine kinase 1 regulates adipose proinflammatory responses and insulin resistance. *Am. J. Physiol. Endocrinol. Metab.* **2014**, *306*, E756-68.

262. Kowalski, G.M.; Carey, A.L.; Selathurai, A.; Kingwell, B.A.; Bruce, C.R. Plasma Sphingosine-1-Phosphate Is Elevated in Obesity. *PLoS One* **2013**, *8*, e72449.
263. Ito, S.; Iwaki, S.; Koike, K.; Yuda, Y.; Nagasaki, A.; Ohkawa, R.; Yatomi, Y.; Furumoto, T.; Tsutsui, H.; Sobel, B.E.; et al. Increased plasma sphingosine-1-phosphate in obese individuals and its capacity to increase the expression of plasminogen activator inhibitor-1 in adipocytes. *Coron. Artery Dis.* **2013**, *24*, 1.
264. Fayyaz, S.; Henkel, J.; Japtok, L.; Krämer, S.; Damm, G.; Seehofer, D.; Püschel, G.P.; Kleuser, B. Involvement of sphingosine 1-phosphate in palmitate-induced insulin resistance of hepatocytes via the S1P2 receptor subtype. *Diabetologia* **2014**, *57*, 373–382.
265. Japtok, L.; Schmitz, E.I.; Fayyaz, S.; Krämer, S.; Hsu, L.J.; Kleuser, B. Sphingosine 1-phosphate counteracts insulin signaling in pancreatic β-cells *via* the sphingosine 1-phosphate receptor subtype 2. *FASEB J.* **2015**, *29*, 3357–3369.
266. Moon, M.H.; Jeong, J.K.; Lee, J.H.; Park, Y.G.; Lee, Y.J.; Seol, J.W.; Park, S.Y. Antiobesity activity of a sphingosine 1-phosphate analogue FTY720 observed in adipocytes and obese mouse model. *Exp. Mol. Med.* **2012**, *44*, 603–14.
267. MOON, M.-H.; JEONG, J.-K.; LEE, Y.-J.; SEOL, J.-W.; PARK, S.-Y.; Lee, Y.-J.; Seol, J.-W.; Seol, J.-W.; Park, S.-Y.; Park, S.-Y. Sphingosine-1-phosphate inhibits the adipogenic differentiation of 3T3-L1 preadipocytes. *Int. J. Mol. Med.* **2014**, *34*, 1153–1158.
268. Jo, E.; Sanna, M.G.; Gonzalez-Cabrera, P.J.; Thangada, S.; Tigyi, G.; Osborne, D.A.; Hla, T.; Parrill, A.L.; Rosen, H. S1P1-Selective In Vivo-Active Agonists from High- Throughput Screening: Off-the-Shelf Chemical Probes of Receptor Interactions, Signaling, and Fate. *Chem. Biol.* **2005**, *12*, 703–715.
269. Silva, V.R.R.; Micheletti, T.O.; Pimentel, G.D.; Katashima, C.K.; Lenhare, L.; Morari, J.; Mendes, M.C.S.; Razolli, D.S.; Rocha, G.Z.; de Souza, C.T.; et al. Hypothalamic S1P/S1PR1 axis controls energy homeostasis. *Nat. Commun.* **2014**, *5*, 4859.
270. Ross, J.S.; Hu, W.; Rosen, B.; Snider, A.J.; Obeid, L.M.; Cowart, L.A. Sphingosine kinase 1 is regulated by peroxisome proliferator-activated receptor α in response to free fatty acids and is essential for skeletal muscle interleukin-6 production and signaling in diet-induced obesity. *J. Biol. Chem.* **2013**, *288*, 22193–206.
271. Nagahashi, M.; Yamada, A.; Katsuta, E.; Aoyagi, T.; Huang, W.-C.; Terracina, K.P.; Hait, N.C.; Allegood, J.C.; Tsuchida, J.; Yuza, K.; et al. Targeting the SphK1/S1P/S1PR1 Axis That Links Obesity, Chronic Inflammation, and Breast Cancer Metastasis. *Cancer Res.* **2018**, *78*, 1713–1725.
272. Ravichandran, S.; Finlin, B.S.; Kern, P.A.; Özcan, S. Sphk2−/− mice

are protected from obesity and insulin resistance. *Biochim. Biophys. Acta - Mol. Basis Dis.* **2019**, *1865*, 570–576.
273. Liang, J.; Nagahashi, M.; Kim, E.Y.; Harikumar, K.B.; Yamada, A.; Huang, W.-C.; Hait, N.C.; Allegood, J.C.; Price, M.M.; Avni, D.; et al. Sphingosine-1-phosphate links persistent STAT3 activation, chronic intestinal inflammation, and development of colitis-associated cancer. *Cancer Cell* **2013**, *23*, 107–20.
274. Kharel, Y.; Morris, E.A.; Congdon, M.D.; Thorpe, S.B.; Tomsig, J.L.; Santos, W.L.; Lynch, K.R. Sphingosine Kinase 2 Inhibition and Blood Sphingosine 1-Phosphate Levels. *J. Pharmacol. Exp. Ther.* **2015**, *355*, 23–31.
275. Kharel, Y.; Raje, M.; Gao, M.; Gellett, A.M.; Tomsig, J.L.; Lynch, K.R.; Santos, W.L. Sphingosine kinase type 2 inhibition elevates circulating sphingosine 1-phosphate. *Biochem. J.* **2012**, *447*, 149–157.
276. Obesity and overweight Available online: http://www.who.int/en/news-room/fact-sheets/detail/obesity-and-overweight (accessed on Sep 3, 2018).
277. Al-Daghri, N.M.; Torretta, E.; Capitanio, D.; Fania, C.; Guerini, F.R.; Sabico, S.B.; Clerici, M.; Gelfi, C. Intermediate and low abundant protein analysis of vitamin D deficient obese and non-obese subjects by MALDI-profiling. *Sci. Rep.* **2017**, *7*, 12633.
278. Al-Daghri, N.M.; Al-Attas, O.S.; Johnston, H.E.; Singhania, A.; Alokail, M.S.; Alkharfy, K.M.; Abd-Alrahman, S.H.; Sabico, S. l.; Roumeliotis, T.I.; Manousopoulou-Garbis, A.; et al. Whole Serum 3D LC-nESI-FTMS Quantitative Proteomics Reveals Sexual Dimorphism in the *Milieu Intérieur* of Overweight and Obese Adults. *J. Proteome Res.* **2014**, *13*, 5094–5105.
279. Jin, J.; Zhang, X.; Lu, Z.; Perry, D.M.; Li, Y.; Russo, S.B.; Cowart, L.A.; Hannun, Y.A.; Huang, Y. Acid sphingomyelinase plays a key role in palmitic acid-amplified inflammatory signaling triggered by lipopolysaccharide at low concentrations in macrophages. *Am. J. Physiol. Endocrinol. Metab.* **2013**, *305*, E853-67.
280. Memon, R.A.; Holleran, W.M.; Moser, A.H.; Seki, T.; Uchida, Y.; Fuller, J.; Shigenaga, J.K.; Grunfeld, C.; Feingold, K.R. Endotoxin and cytokines increase hepatic sphingolipid biosynthesis and produce lipoproteins enriched in ceramides and sphingomyelin. *Arterioscler. Thromb. Vasc. Biol.* **1998**, *18*, 1257–65.
281. Jiang, X.-C.; Goldberg, I.J.; Park, T.-S. Sphingolipids and Cardiovascular Diseases: Lipoprotein Metabolism, Atherosclerosis and Cardiomyopathy. In; Springer, New York, NY, 2011; pp. 19–39.
282. Al-Daghri, N.M.; Al-Saleh, Y.; Aljohani, N.; Alokail, M.; Al-Attas, O.; Alnaami, A.M.; Sabico, S.; Alsulaimani, M.; Al-Harbi, M.; Alfawaz, H.; et al. Vitamin D Deficiency and Cardiometabolic Risks: A

Juxtaposition of Arab Adolescents and Adults. *PLoS One* **2015**, *10*, e0131315.
283. Hirschler, V.; Gonzalez, C.; Maccallini, G.; Hidalgo, M.; Molinari, C. Comparison Between HDL-C Levels in Argentine Indigenous Children Living at High Altitudes and U.S. Children. *Diabetes Technol. Ther.* **2016**, *18*, 233–239.
284. Cingolani, F.; Casasampere, M.; Sanllehí, P.; Casas, J.; Bujons, J.; Fabrias, G. Inhibition of dihydroceramide desaturase activity by the sphingosine kinase inhibitor SKI II. *J. Lipid Res.* **2014**, *55*, 1711–1720.
285. Karp, N.A.; Lilley, K.S. Design and Analysis Issues in Quantitative Proteomics Studies. **2007**, 42–50.
286. Karp, N.A.; Spencer, M.; Lindsay, H.; O'Dell, K.; Lilley, K.S. Impact of Replicate Types on Proteomic Expression Analysis. *J. Proteome Res.* **2005**, *4*, 1867–1871.
287. Kramer, C.Y. Extension of Multiple Range Tests to Group Means with Unequal Numbers of Replications. *Biometrics* **1956**, *12*, 307.
288. *World Health Organization. 2009.*; 2009;
289. Al-Nozha, M.M.; Al-Mazrou, Y.Y.; Al-Maatouq, M.A.; Arafah, M.R.; Khalil, M.Z.; Khan, N.B.; Al-Marzouki, K.; Abdullah, M.A.; Al-Khadra, A.H.; Al-Harthi, S.S.; et al. Obesity in Saudi Arabia. *Saudi Med. J.* **2005**, *26*, 824–9.
290. Al-Kadi, A.; Malik, A.M.; Mansour, A.E. Rising incidence of obesity in Saudi residents. A threatening challenge for the surgeons. *Int. J. Health Sci. (Qassim).* **2018**, *12*, 45–49.
291. Al-Nozha, M.M.; Arafah, M.R.; Al-Maatouq, M.A.; Khalil, M.Z.; Khan, N.B.; Al-Marzouki, K.; Al-Mazrou, Y.Y.; Abdullah, M.; Al-Khadra, A.; Al-Harthi, S.S.; et al. Hyperlipidemia in Saudi Arabia. *Saudi Med. J.* **2008**, *29*, 282–7.
292. Hamam, F. Dyslipidemia and Related Risk Factors in a Saudi University Community. *Food Nutr. Sci.* **2017**, *8*, 56–69.
293. F. Al-Kaabba, A.; A. Al-Hamdan, N.; El Tahir, A.; M. Abdalla, A.; A. Saeed, A.; A. Hamza, M.; Al-Kaabba, A.F.; Al-Hamdan, N.A.; Tahir, A. El; Abdalla, A.M.; et al. Prevalence and Correlates of Dyslipidemia among Adults in Saudi Arabia: Results from a National Survey. *Open J. Endocr. Metab. Dis.* **2012**, *02*, 89–97.
294. Al-Alyani, H.; Al-Turki, H.A.; Al-Essa, O.N.; Alani, F.M.; Sadat-Ali, M. Vitamin D deficiency in Saudi Arabians: A reality or simply hype: A meta-analysis (2008-2015). *J. Family Community Med.* **2018**, *25*, 1–4.
295. Alamoudi, L.H.; Almuteeri, R.Z.; Al-Otaibi, M.E.; Alshaer, D.A.; Fatani, S.K.; Alghamdi, M.M.; Safdar, O.Y. Awareness of Vitamin D Deficiency among the General Population in Jeddah, Saudi Arabia. *J. Nutr. Metab.* **2019**, *2019*, 1–7.

296. *High Blood Cholesterol ATP III Guidelines At-A-Glance Quick Desk Reference*;
297. 2018 Guideline on the Management of Blood Cholesterol GUIDELINES MADE SIMPLE.
298. Bischoff-Ferrari, H.A.; Giovannucci, E.; Willett, W.C.; Dietrich, T.; Dawson-Hughes, B. Estimation of optimal serum concentrations of 25-hydroxyvitamin D for multiple health outcomes. *Am. J. Clin. Nutr.* **2006**, *84*, 18–28.
299. Watt, M.J.; Barnett, A.C.; Bruce, C.R.; Schenk, S.; Horowitz, J.F.; Hoy, A.J. Regulation of plasma ceramide levels with fatty acid oversupply: evidence that the liver detects and secretes de novo synthesised ceramide. *Diabetologia* **2012**, *55*, 2741–2746.
300. Hotamisligil, G.S.; Arner, P.; Caro, J.F.; Atkinson, R.L.; Spiegelman, B.M. Increased adipose tissue expression of tumor necrosis factor-alpha in human obesity and insulin resistance. *J. Clin. Invest.* **1995**, *95*, 2409–2415.
301. Aburasayn, H.; Al Batran, R.; Ussher, J.R. Targeting ceramide metabolism in obesity. *Am. J. Physiol. Metab.* **2016**, *311*, E423–E435.
302. Adams, J.M.; Pratipanawatr, T.; Berria, R.; Wang, E.; DeFronzo, R.A.; Sullards, M.C.; Mandarino, L.J. Ceramide content is increased in skeletal muscle from obese insulin-resistant humans. *Diabetes* **2004**, *53*, 25–31.
303. Maynard, L.M.; Wisemandle, W.; Roche, A.F.; Chumlea, W.C.; Guo, S.S.; Siervogel, R.M. Childhood Body Composition in Relation to Body Mass Index. *Pediatrics* **2001**, *107*, 344–350.
304. Hernandez, T.L.; Kittelson, J.M.; Law, C.K.; Ketch, L.L.; Stob, N.R.; Lindstrom, R.C.; Scherzinger, A.; Stamm, E.R.; Eckel, R.H. Fat Redistribution Following Suction Lipectomy: Defense of Body Fat and Patterns of Restoration. *Obesity* **2011**, *19*, 1388–1395.
305. Karastergiou, K.; Smith, S.R.; Greenberg, A.S.; Fried, S.K. Sex differences in human adipose tissues – the biology of pear shape. *Biol. Sex Differ.* **2012**, *3*, 13.
306. Wells, J.C.; Treleaven, P.; Cole, T.J. BMI compared with 3-dimensional body shape: the UK National Sizing Survey. *Am. J. Clin. Nutr.* **2007**, *85*, 419–425.
307. Muir, L.A.; Neeley, C.K.; Meyer, K.A.; Baker, N.A.; Brosius, A.M.; Washabaugh, A.R.; Varban, O.A.; Finks, J.F.; Zamarron, B.F.; Flesher, C.G.; et al. Adipose tissue fibrosis, hypertrophy, and hyperplasia: Correlations with diabetes in human obesity. *Obesity (Silver Spring).* **2016**, *24*, 597–605.
308. Blüher, M. Adipose Tissue Dysfunction in Obesity. *Exp. Clin. Endocrinol. Diabetes* **2009**, *117*, 241–250.
309. Gruzdeva, O.; Borodkina, D.; Uchasova, E.; Dyleva, Y.; Barbarash,

O. Localization of fat depots and cardiovascular risk. *Lipids Health Dis.* **2018**, *17*, 218.
310. Weir, J.M.; Wong, G.; Barlow, C.K.; Greeve, M.A.; Kowalczyk, A.; Almasy, L.; Comuzzie, A.G.; Mahaney, M.C.; Jowett, J.B.M.M.; Shaw, J.; et al. Plasma lipid profiling in a large population-based cohort. *J. Lipid Res.* **2013**, *54*, 2898–2908.
311. Mittelstrass, K.; Ried, J.S.; Yu, Z.; Krumsiek, J.; Gieger, C.; Prehn, C.; Roemisch-Margl, W.; Polonikov, A.; Peters, A.; Theis, F.J.; et al. Discovery of sexual dimorphisms in metabolic and genetic biomarkers. *PLoS Genet.* **2011**, *7*, e1002215.
312. Carlsson, E.R.; Grundtvig, J.L.G.; Madsbad, S.; Fenger, M. Changes in Serum Sphingomyelin After Roux-en-Y Gastric Bypass Surgery Are Related to Diabetes Status. *Front. Endocrinol. (Lausanne).* **2018**, *9*.
313. Nikkilä, J.; Sysi-Aho, M.; Ermolov, A.; Seppänen-Laakso, T.; Simell, O.; Kaski, S.; Oresic, M. Gender-dependent progression of systemic metabolic states in early childhood. *Mol. Syst. Biol.* **2008**, *4*, 197.
314. Chavez, J.A.; Siddique, M.M.; Wang, S.T.; Ching, J.; Shayman, J.A.; Summers, S.A. Ceramides and glucosylceramides are independent antagonists of insulin signaling. *J. Biol. Chem.* **2014**, *289*, 723–34.
315. Edsfeldt, A.; Dunér, P.; Ståhlman, M.; Mollet, I.G.; Asciutto, G.; Grufman, H.; Nitulescu, M.; Persson, A.F.; Fisher, R.M.; Melander, O.; et al. Sphingolipids Contribute to Human Atherosclerotic Plaque Inflammation. *Arterioscler. Thromb. Vasc. Biol.* **2016**, *36*, 1132–1140.
316. Johanna von Gerichten, A.; Schlosser, K.; Lamprecht, D.; Morace, I.; Eckhardt, M.; Wachten, D.; Jennemann, R.; Gröne, H.-J.; Mack, M.; Sandhoff, R. *Diastereomer-specific Quantification of Bioactive Hexosylceramides from Bacteria and Mammals*;
317. Mousa, A.; Naderpoor, N.; Mellett, N.; Wilson, K.; Plebanski, M.; Meikle, P.J.; de Courten, B. Lipidomic profiling reveals early-stage metabolic dysfunction in overweight or obese humans. *Biochim. Biophys. Acta - Mol. Cell Biol. Lipids* **2019**, *1864*, 335–343.
318. Meikle, P.J.; Wong, G.; Barlow, C.K.; Weir, J.M.; Greeve, M.A.; MacIntosh, G.L.; Almasy, L.; Comuzzie, A.G.; Mahaney, M.C.; Kowalczyk, A.; et al. Plasma lipid profiling shows similar associations with prediabetes and type 2 diabetes. *PLoS One* **2013**, *8*, e74341.
319. Berdyshev, E. V.; Gorshkova, I.A.; Usatyuk, P.; Zhao, Y.; Saatian, B.; Hubbard, W.; Natarajan, V. De novo biosynthesis of dihydrosphingosine-1-phosphate by sphingosine kinase 1 in mammalian cells. *Cell. Signal.* **2006**, *18*, 1779–1792.
320. Hirschler, V.; Martin, M.; Molinari, C.; Botta, E.; Tetzlaff, W.F.; Brites, F. Activity of Lipoprotein-Associated Enzymes in Indigenous Children Living at Different Altitudes. *Arch. Med. Res.* **2019**, *50*, 98–104.

321. Hirschler, V.; Maccallini, G.; Aranda, C.; Molinari, C.; San Antonio de los Cobres Study Group Dyslipidemia without Obesity in Indigenous Argentinean Children Living at High Altitude. *J. Pediatr.* **2012**, *161*, 646-651.e1.
322. Epidemiological Condition of Obesity in Argentina.
323. Mohanna, S.; Baracco, R.; Seclén, S. Lipid Profile, Waist Circumference, and Body Mass Index in a High Altitude Population. *High Alt. Med. Biol.* **2006**, *7*, 245–255.
324. Ferrero, M.E.; Villalba, R. Interannual and Long-Term Precipitation Variability Along the Subtropical Mountains and Adjacent Chaco (22–29° S) in Argentina. *Front. Earth Sci.* **2019**, *7*, 148.
325. Hirschler, V.; Molinari, C.; Maccallini, G.; Intersimone, P.; Gonzalez, C.D. Vitamin D Levels and Cardiometabolic Markers in Indigenous Argentinean Children Living at Different Altitudes. *Glob. Pediatr. Heal.* **2019**, *6*, 2333794X1882194.
326. Hirschler, V.; Maccallini, G.; Molinari, C.; Aranda, C. Low vitamin D concentrations among indigenous Argentinean children living at high altitudes. *Pediatr. Diabetes* **2012**, *14*, n/a-n/a.
327. Hirschler, V.; Maccallini, G.; Sanchez, M.S.; Castaño, L.; Molinari, C. Improvement in High-Density Lipoprotein Cholesterol Levels in Argentine Indian School Children after Vitamin D Supplementation. *Horm. Res. Paediatr.* **2013**, *80*, 335–342.
328. National Cholesterol Education Program (NCEP): highlights of the report of the Expert Panel on Blood Cholesterol Levels in Children and Adolescents. *Pediatrics* **1992**, *89*, 495–501.
329. *Expert Panel on Integrated Guidelines for Cardiovascular Health and Risk Reduction in Children and Adolescents SUMMARY REPORT Expert Panel on Integrated Guidelines for Cardiovascular Health and Risk Reduction in Children and Adolescents SUMMARY RepoRt National Heart, Lung, and Blood Institute*; 2012;
330. Zalloua, P.; Kadar, H.; Hariri, E.; Abi Farraj, L.; Brial, F.; Hedjazi, L.; Le Lay, A.; Colleu, A.; Dubus, J.; Touboul, D.; et al. Untargeted Mass Spectrometry Lipidomics identifies correlation between serum sphingomyelins and plasma cholesterol. *Lipids Health Dis.* **2019**, *18*, 38.
331. Martínez-Beamonte, R.; Lou-Bonafonte, J.M.; Martínez-Gracia, M. V; Osada, J. Sphingomyelin in high-density lipoproteins: structural role and biological function. *Int. J. Mol. Sci.* **2013**, *14*, 7716–41.
332. Swaney, J.B. Membrane cholesterol uptake by recombinant lipoproteins. *Chem. Phys. Lipids* **1985**, *37*, 317–327.
333. Yuwei Zhao, ‡; Daniel L. Sparks, ‡,§ and; Yves L. Marcel*, ‡,§ Effect of the Apolipoprotein A-I and Surface Lipid Composition of Reconstituted Discoidal HDL on Cholesterol Efflux from Cultured Fibroblasts†. **1996**.

334. Boslem, E.; Meikle, P.J.; Biden, T.J. Roles of ceramide and sphingolipids in pancreatic β-cell function and dysfunction. *Islets* **2012**, *4*, 177–87.
335. Sun, K.; Zhang, Y.; D'alessandro, A.; Nemkov, T.; Song, A.; Wu, H.; Liu, H.; Adebiyi, M.; Huang, A.; Wen, Y.E.; et al. ARTICLE Sphingosine-1-phosphate promotes erythrocyte glycolysis and oxygen release for adaptation to high-altitude hypoxia. *Nat. Publ. Gr.* **2016**, *7*.
336. MacDonald, R. Red cell 2,3-diphosphoglycerate and oxygen affinity. *Anaesthesia* **1977**, *32*, 544–53.
337. Mylonis, I.; Simos, G.; Paraskeva, E. Hypoxia-Inducible Factors and the Regulation of Lipid Metabolism. *Cells* **2019**, *8*.
338. Krishnan, J.; Suter, M.; Windak, R.; Krebs, T.; Felley, A.; Montessuit, C.; Tokarska-Schlattner, M.; Aasum, E.; Bogdanova, A.; Perriard, E.; et al. Activation of a HIF1α-PPARγ Axis Underlies the Integration of Glycolytic and Lipid Anabolic Pathways in Pathologic Cardiac Hypertrophy. *Cell Metab.* **2009**, *9*, 512–524.
339. Bensaad, K.; Favaro, E.; Lewis, C.A.; Peck, B.; Lord, S.; Collins, J.M.; Pinnick, K.E.; Wigfield, S.; Buffa, F.M.; Li, J.-L.; et al. Fatty Acid Uptake and Lipid Storage Induced by HIF-1α Contribute to Cell Growth and Survival after Hypoxia-Reoxygenation. *Cell Rep.* **2014**, *9*, 349–365.
340. Sanders, F.W.B.; Griffin, J.L. De novo lipogenesis in the liver in health and disease: more than just a shunting yard for glucose. *Biol. Rev. Camb. Philos. Soc.* **2016**, *91*, 452.
341. SUMMERS, S. Ceramides in insulin resistance and lipotoxicity. *Prog. Lipid Res.* **2006**, *45*, 42–72.
342. Yoshizumi, S.; Suzuki, S.; Hirai, M.; Hinokio, Y.; Yamada, T.; Yamada, T.; Tsunoda, U.; Aburatani, H.; Yamaguchi, K.; Miyagi, T.; et al. Increased hepatic expression of ganglioside-specific sialidase, NEU3, improves insulin sensitivity and glucose tolerance in mice. *Metabolism* **2007**, *56*, 420–429.
343. Capitanio, D.; Fania, C.; Torretta, E.; Viganò, A.; Moriggi, M.; Bravatà, V.; Caretti, A.; Levett, D.Z.H.; Grocott, M.P.W.; Samaja, M.; et al. TCA cycle rewiring fosters metabolic adaptation to oxygen restriction in skeletal muscle from rodents and humans. *Sci. Rep.* **2017**, *7*, 9723.
344. Xie, C.; Yagai, T.; Luo, Y.; Liang, X.; Chen, T.; Wang, Q.; Sun, D.; Zhao, J.; Ramakrishnan, S.K.; Sun, L.; et al. Activation of intestinal hypoxia-inducible factor 2α during obesity contributes to hepatic steatosis. *Nat. Med.* **2017**, *23*, 1298–1308.
345. Boon, J.; Hoy, A.J.; Stark, R.; Brown, R.D.; Meex, R.C.; Henstridge, D.C.; Schenk, S.; Meikle, P.J.; Horowitz, J.F.; Kingwell, B.A.; et al. Ceramides Contained in LDL Are Elevated in Type 2 Diabetes and

Promote Inflammation and Skeletal Muscle Insulin Resistance.
346. Barbacini, P.; Casas, J.; Torretta, E.; Capitanio, D.; Maccallini, G.; Hirschler, V.; Gelfi, C.; Barbacini, P.; Casas, J.; Torretta, E.; et al. Regulation of Serum Sphingolipids in Andean Children Born and Living at High Altitude (3775 m). *Int. J. Mol. Sci.* **2019**, *20*, 2835.

9. SUPPLEMENTARY MATERIAL

Supplementary File 1:

Sphingolipid identified and quantified in Saudi Arabian subjects.

All SLs species cited in this file were identified and precisely quantified. For statistical analyses, single lipid species quantities were summed to obtain total class levels.
Total Cer was obtained as the sum of Cer (d18:1/14:0), Cer (d18:1/16:0), Cer (d18:1/18:0), Cer (d18:1/18:1), Cer (d18:1/20:0), Cer (d18:1/20:1), Cer (d18:1/22:0), Cer (d18:1/22:1), Cer (d18:1/24:0), Cer (d18:1/24:1) and Cer (d18:1/24:2). Total dhCer was obtained as the sum of dhCer (d18:0/16:0), dhCer (d18:0/18:0), dhCer (d18:0/22:0) and dhCer (d18:0/24:0). Total sphingomyelin was obtained as the sum of SM (d18:1/14:0), SM (d18:1/14:1), SM (d18:1/16:0), SM (d18:1/16:1), SM (d18:1/18:0), SM (d18:1/18:1), SM (d18:1/20:0), SM (d18:1/20:1), SM (d18:1/22:0), SM (d18:1/22:1), SM (d18:1/24:0), SM (d18:1/24:1), SM (d18:1/24:2) and SM (d18:1/24:3). Total dhSm was obtained as the sum of dhSM (d18:0/14:0), dhSM (d18:0/16:0), dhSM (d18:0/18:0), dhSM (d18:0/20:0), dhSM (d18:0/22:0) and dhSM (d18:0/24:0). Total hexCer was obtained as the sum of HexCer (d18:1/16:0), HexCer (d18:1/22:0), HexCer (d18:1/24:0) and HexCer (d18:1/24:1). Total dihexCer was obtained as CDH (d18:1/14:0), CDH (d18:1/16:0), CDH (d18:1/18:0), CDH (d18:1/22:0), CDH (d18:1/24:0) and CDH (d18:1/24:1).

Sphingolipid identified and quantified in Andean subjects.

All SLs species cited in this file were identified and precisely quantified. For statistical analyses, single lipid species quantities were summed to obtain total class levels.
Total Cer was obtained as the sum of Cer (d18:1/14:0), Cer (d18:1/16:0), Cer (d18:1/18:0), Cer (d18:1/18:1), Cer (d18:1/20:0), Cer (d18:1/20:1), Cer (d18:1/22:0), Cer (d18:1/22:1), Cer (d18:1/24:0), Cer (d18:1/24:1) and Cer (d18:1/24:2). Total dhCer was obtained as the sum of dhCer (d18:0/16:0), dhCer (d18:0/22:0), dhCer (d18:0/24:0) and dhCer (d18:0/24:1). Total sphingomyelin was obtained as the sum of SM (d18:1/14:0), SM (d18:1/14:1), SM (d18:1/16:0), SM (d18:1/16:1), SM (d18:1/18:0), SM (d18:1/18:1), SM (d18:1/20:0), SM (d18:1/20:1), SM (d18:1/22:0), SM (d18:1/22:1), SM (d18:1/24:0), SM (d18:1/24:1), SM (d18:1/24:2) and SM (d18:1/24:3). Total dhSm was obtained as the sum of dhSM (d18:0/14:0), dhSM (d18:0/16:0), dhSM (d18:0/18:0), dhSM (d18:0/20:0), dhSM (d18:0/22:0) and dhSM (d18:0/24:0). Total hexCer was obtained as the sum of HexCer (d18:1/16:0), HexCer (d18:1/22:0), HexCer (d18:1/24:0) and HexCer (d18:1/24:1). Total dihexCer was obtained as CDH (d18:1/14:0), CDH (d18:1/16:0), CDH (d18:1/18:0), CDH (d18:1/22:0), CDH (d18:1/24:0) and CDH (d18:1/24:1). Total GM3 was obtained as the sum of GM3 (d18:1/16:0), GM3 (d18:1/18:0), GM3 (d18:1/20:0), GM3 (d18:1/22:0), GM3 (d18:1/24:0) and GM3 (d18:1/24:1).

Supplementary Table 1: p-values from One-way ANOVA comparison after Bonferroni's correction (bold) or after Dunn's correction (regular).

	NWNL vs. NWDL	NWNL vs. ODL	NWDL vs. ODL
	p-value	p-value	p-value
Age	0.6294	0.9108	>0.9999
Weight (Kg)	**0.7646**	**<0.0001**	**<0.0001**
Height (Cm)	**<0.0001**	**<0.0001**	**0.2506**
BMI	**0.0659**	**<0.0001**	**<0.0001**
TC (mg/dL)	**0.0007**	**0.0026**	**>0.9999**
HDL-C (mg/dL)	<0.0001	<0.0001	0.3893
LDL-C (mg/dL)	<0.0001	0.0027	0.0009
TG (mg/dL)	<0.0001	<0.0001	0.0519

Supplementary Figure 1. (A) calibration curve of Cer (d18:1/16:0) resulting from 3 different HPTLC separation performed in three different days. (B) calibration curve of LacCer (d18:1/17:0) resulting from 3 different HPTLC separation performed in three different days. (C) limit of detection (LOD) were set at 44 pmol for Cer (d18:1/16:0) and at 18 pmol for LacCer (d18:1/17:0) (D).

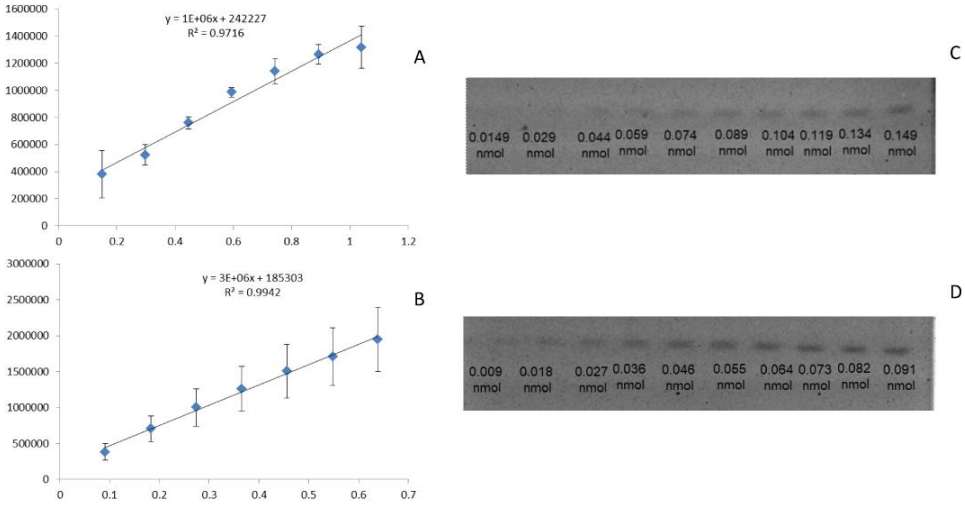

Supplementary Figure 2. Non statistically significant results from Cers (C20-24) and SMs (C20-24) by HPTLC-Primuline profiling.

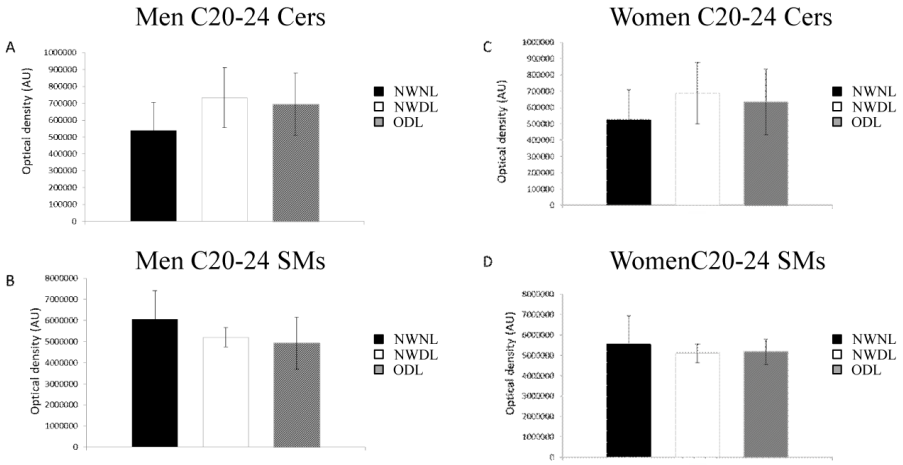

Supplementary Figure 3. UPLC-MS analysis of Cers, dhCers, SMs and dhSMs, acyl chains from NWNL, NWNL and ODL men (A, C, E and G) and from NWNL; NWDL and ODL women (B; D; F; H).

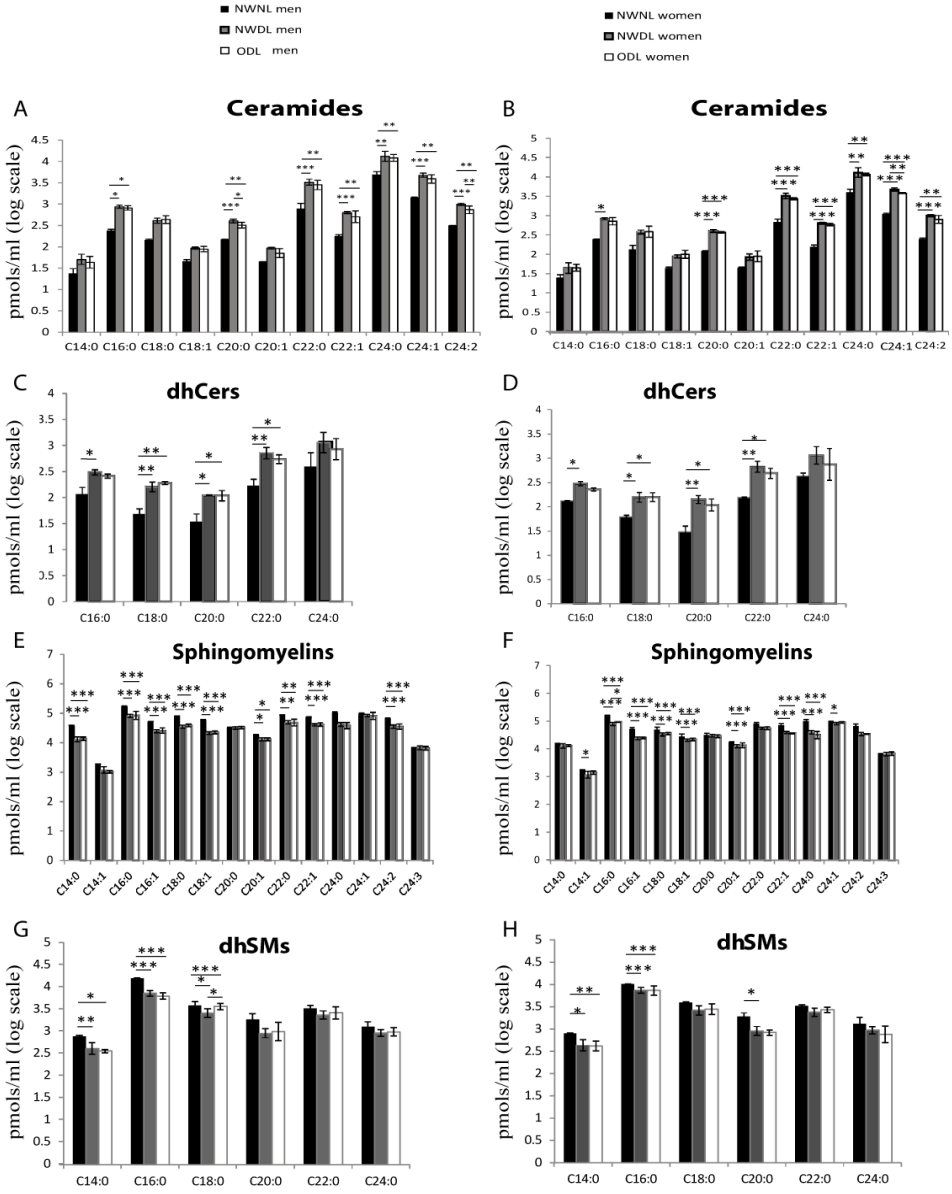

Supplementary Figure 4. Non statistically significant results from UPLC-MS analysis of Cers, dhCers, SMs, dhSMs, HexCer and dihexCers acyl chains from NWNL, NWDL and ODL men and women. Non statistically significant results from MRM analysis of Sph, S1P and dhS1P from NWNL, NWDL and ODL men and women.

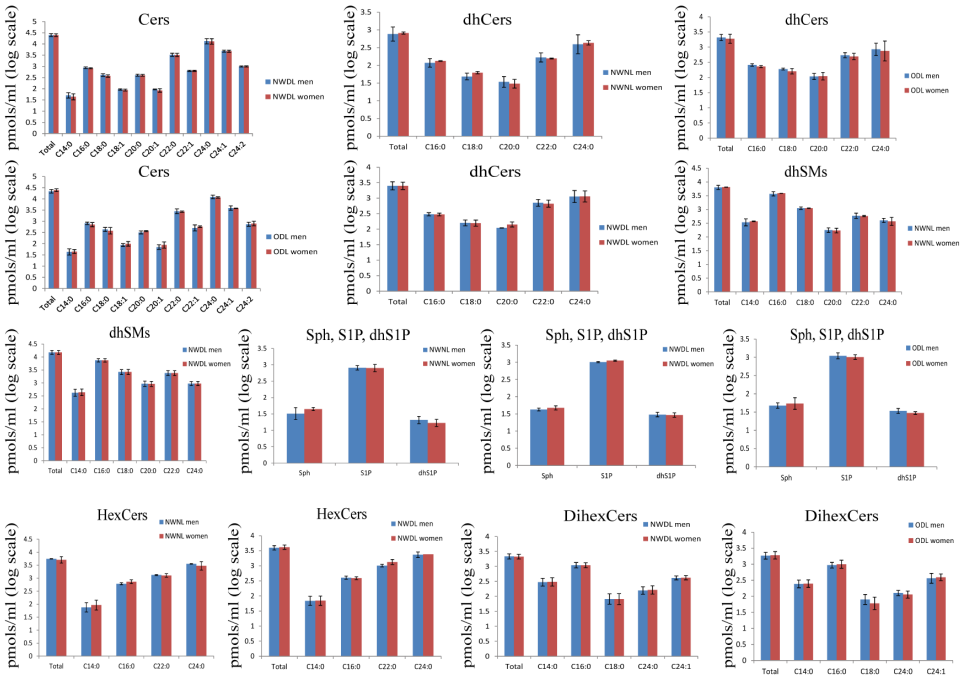

Supplementary Table 2. P-values from One-Way ANOVA comparison after Bonferroni's correction (regular) or after Dunn's correction (bold)

	UW vs. NW	UW vs. OW	UW vs. O	NW vs. OW	NW vs. O	OW vs. O
Age	**>0,999**	**>0,999**	**>0,999**	**>0,999**	**>0,999**	**0,354**
Weight	>0,999	<0,0001	0,001	<0,0001	0,002	>0,999
Height	>0,999	0,436	>0,999	0,096	>0,999	0,164
BMI	**0,092**	**<0,001**	**<0,001**	**0,001**	**<0,001**	**>0,999**
TC	0,052	>0,999	0,106	0,154	>0,999	0,326
HDL-C	0,433	>0,999	>0,999	0,057	0,002	>0,999
TC/HDL-C	**>0,999**	**>0,999**	**0,018**	**>0,999**	**0,006**	**0,291**
LDL-C	0,490	>0,999	>0,999	0,822	>0,999	>0,999
Vit.D	0,586	>0,999	>0,999	>0,999	>0,999	>0,999
Glycaemia	>0,999	>0,999	>0,999	>0,999	>0,999	>0,999
HOMA-IR	>0,999	>0,999	0,316	0,032	0,004	>0,999
Insulin	>0,999	0,673	0,152	0,013	0,002	>0,999
TG	>0,999	>0,999	0,296	>0,999	0,284	>0,999

Supplementary Table 3. P-values from two-tailed test, r-values from Pearson's correlation (regular), or Spearman's correlation (bold).

	Total Cholesterol		HDL-C		CT/HDL		LDL-C		Vit. D		Glycemia		HOMA-IR		Insulin		TG	
	r	p	r	p	r	p	r	p	r	p	r	p	r	p	r	p	r	p
UW Total Cers	-0.303	0.509	0.066	0.888	-0.373	0.411	-0.440	0.323	-0.292	0.526	-0.393	0.383	-0.320	0.485	-0.310	0.498	-0.026	0.957
NW Total Cers	0.091	0.632	-0.238	0.206	0.319	0.085	0.107	0.574	-0.400	0.028	0.035	0.852	0.389	0.036	0.418	0.021	0.379	0.039
OW Total Cers	0.721	0.005	**0.335**	0.263	0.280	0.355	0.619	0.024	-0.312	0.299	0.028	0.928	-0.097	0.753	-0.109	0.723	0.359	0.228
O Total Cers	0.440	0.237	-0.321	0.399	**0.544**	0.135	-0.268	0.486	-0.035	0.929	0.683	0.043	0.477	0.195	0.420	0.260	0.3285	0.4269
UW Total SMs	0.478	0.278	0.854	0.015	-0.368	0.417	0.311	0.497	-0.052	0.912	0.167	0.721	-0.267	0.564	-0.281	0.541	-0.176	0.706
NW Total SMs	-0.093	0.624	-0.049	0.798	0.024	0.901	-0.029	0.880	-0.091	0.634	-0.095	0.616	-0.257	0.171	-0.240	0.202	-0.040	0.834
OW Total SMs	0.721	0.005	0.603	0.029	0.027	0.931	0.655	0.015	-0.064	0.834	0.055	0.859	0.189	0.537	0.188	0.538	-0.010	0.975
O Total SMs	0.225	0.560	0.264	0.492	**-0.259**	0.498	0.183	0.637	0.425	0.254	0.152	0.696	-0.152	0.696	-0.203	0.601	-0.018	0.975
UW Total S1P	0.384	0.396	0.400	0.374	0.006	0.990	0.385	0.394	0.557	0.194	-0.386	0.392	-0.512	0.241	-0.459	0.301	-0.166	0.723
NW Total S1P	-0.183	0.333	-0.375	0.041	0.350	0.058	0.052	0.786	0.015	0.936	-0.010	0.957	0.049	0.798	0.014	0.941	0.205	0.278
OW Total S1P	**-0.528**	0.067	-0.176	0.566	-0.376	0.205	-0.691	0.011	0.077	0.806	0.271	0.368	0.187	0.539	0.132	0.669	0.344	0.249
O Total S1P	-0.348	0.358	-0.491	0.180	**-0.008**	0.988	-0.464	0.208	0.637	0.065	0.410	0.273	0.458	0.215	0.451	0.224	**0.360**	0.339

10. SCIENTIFIC PRODUCTION

1. Regulation of Serum Sphingolipids in Andean Children Born and Living at High Altitude (3775 m). Int J Mol Sci. 2019;20(11):2835. doi:10.3390/ijms20112835. Barbacini P, Casas J, Torretta E, et al.doi:10.3390/ijms20112835. Barbacini P, Casas J, Torretta E, et al.

2. Particular CSF sphingolipid patterns identify iNPH and AD patients. Sci Rep. 2018;8(1):13639. doi:10.1038/s41598-018-31756-0. Torretta E, Arosio B, Barbacini P, et al.

3. 6-10/05/2019: Poster session at: FEBS special Meeting 2019. Sphingolipid Biology: Sphingolipids in physiology and pathology. Cascais, Portugal.

4. 16-18/10/2017: Poster session at: 49° Congresso nazionale SIBIOC-Medicina di laboratorio e clinica: tra presente e futuro. Firenze, Italia.

11. ACKNOWLEDGMENTS

I would like to thank Prof.ssa Cecilia Gelfi for the fundamental scientific guidance, for the valuable and stimulating discussion and for the support and time dedicated to me.

I would also like to thank my colleagues Daniele Capitanio, Manuela Moriggi, and Enrica Torretta, for their constant support and their precious tips during these years.

I want to thank the Ph.D. School of Molecular and Translational Medicine of Milan Study University.

This study was partially supported by the Italian Space Agency (ASI), project: DC-VUM-2016-068.

This thesis was evaluated by two independent reviewers which I really want to thank for the excellent feedback and the valuable help: Professor Josefina Casas, Spanish National Research Council (CSIC), Research Unit on BioActive Molecules, Dept. of Biological Chemistry (IQAC-CSIC), e-mail: fina.casas@iqac.csic.es and Professor Valeria Hirschler, Department of Nutrition and Diabetes Durand Hospital, e-mail: vhirschler@intramed.net.